Filipe Miguel Sobreira Rodrigues

Bachelor of Science in Biomedical Engineering

Establishing a Framework for the development of Multimodal Virtual Reality Interfaces with Applicability in Education and Clinical Practice

Dissertation submitted in partial fulfillment
of the requirements for the degree of
Master in **Biomedical Engineering**

Adviser: Hugo Alexandre Ferreira, Assistant Professor,
Instituto de Biofísica e Engenharia Biomédica,
Faculdade de Ciências da Universidade de Lisboa

Examination Committee

Chairperson:
Raporteurs:
Members:

FACULDADE DE CIÊNCIAS E TECNOLOGIA
UNIVERSIDADE NOVA DE LISBOA

October, 2015

Establishing a Framework for the development of Multimodal Virtual Reality Interfaces with Applicability in Education and Clinical Practice

This document was created unsing the (pdf)LaTeX processor, based in the "unlthesis" template[1], developed at the Dep. Informática of FCT-NOVA [2]. [1] https://github.com/joaomlourenco/unlthesis [2] http://www.di.fct.unl.pt

Acknowledgements

First and foremost, I would like to thank my adviser and mentor Hugo Alexandre Ferreira, for welcoming me into *Instituto de Biofísica e Engenharia Biomédica* (IBEB) and tirelessly accompanying me throughout this past academic year. Besides behooving my way of thinking in an almost uncanny way, his somewhat less than orthodox approach towards research and science in general greatly broadened my horizons and incited me to enroll in similar pursuits.

It cannot be left unsaid that this project would not have been the same without the financial aid that ensued from the partnership between IBEB and the Luso-Illyrian Institute for Human Development (iLIDH) in the Museum of Universal Values (MUV) project, for which I am much obliged.

I would also like to take the opportunity to express my gratitude to Professor Hugo Gamboa, who was my co-adviser on all accounts but the official one. His readiness to help me with both resources and guidance did not go unnoticed.

On the same train of thought, I am also obligated to acknowledge Professors Hugo Silva, Pedro Vieira and Ivo Costa, who collectively lent me their time, expertise and advice. If not for them, my previously virtually non-existent soldering skills would have seeped into this project and undermined it immensely.

My sincere appreciation for Filipe Silvestre, João Melo Costa and Rachel Freire who respectively aided me with all my 3D printing, textile design and pattern cutting needs.

A huge thank you goes out to Kip Bunyea, Alex Colgan, Kate Mitchell and the whole of Leap Motion©'s team for all the support and coverage.

Last but definitely not least, I have to end by thanking all my friends and family for putting up with me even as I receded into a thesis-writing hermit. At this point I have pretty much used up all the fancy words in my vocabulary so I will just name you randomly: Mom (sorry about turning the living-room into a cellphone graveyard), Dad, Duarte Folgado, Miguel Aragão, João Valverde, Vasco Valverde, Gonçalo Sousa, José Maria Tanqueiro, Teresa Serradas Duarte, Renato Gomes, Pedro Rodrigues, Tiago Rodrigues, Cátia Cepeda, Marta Telhada, Carolina Ramalho, João Pedro Freitas, José Maria Freire, Francisco Dias Lopes and Nuno Torres.

And Joana, whatever sanity I have left, I owe it to you.

"Research is what I'm doing when I don't know what I'm doing."

Wernher von Braun

Abstract

The development of Virtual Reality (VR) and Augmented Reality (AR) content with multiple sources of both input and output has led to countless contributions in a great many number of fields, among which medicine and education.

Nevertheless, the actual process of integrating the existing VR/AR media and subsequently setting it to purpose is yet a highly scattered and esoteric undertaking. Moreover, seldom do the architectures that derive from such ventures comprise haptic feedback in their implementation, which in turn deprives users from relying on one of the paramount aspects of human interaction, their sense of touch.

Determined to circumvent these issues, the present dissertation proposes a centralized albeit modularized framework that thus enables the conception of multimodal VR/AR applications in a novel and straightforward manner.

In order to accomplish this, the aforesaid framework makes use of a stereoscopic VR Head Mounted Display (HMD) from Oculus Rift©, a hand tracking controller from Leap Motion©, a custom-made VR mount that allows for the assemblage of the two preceding peripherals and a wearable device of our own design. The latter is a glove that encompasses two core modules in its innings, one that is able to convey haptic feedback to its wearer and another that deals with the non-intrusive acquisition, processing and registering of his/her Electrocardiogram (ECG), Electromyogram (EMG) and Electrodermal Activity (EDA). The software elements of the aforementioned features were all interfaced through Unity3D©, a powerful game engine whose popularity in academic and scientific endeavors is evermore increasing.

Upon completion of our system, it was time to substantiate our initial claim with thoroughly developed experiences that would attest to its worth. With this premise in mind, we devised a comprehensive repository of interfaces, amid which three merit special consideration: Brain Connectivity Leap (BCL), Ode to Passive Haptic Learning (PHL) and a Surgical Simulator.

Keywords: Framework, Virtual Reality, Motion Capture, Haptic Feedback, Electrophysiology, Connectome.

Resumo

A inclusão de múltiplas fontes de *input* e *output* no desenvolvimento de conteúdo para Realidades Virtual (VR) e Aumentada (AR) tem culminado em inúmeras e valorosas contribuições em diversas áreas, entre as quais medicina e educação.

Não obstante, os processos envolvidos tanto no processo de integração dos meios de VR/AR actualmente existentes como no da sua subsequente aplicação, permanece uma tarefa algo dispersa e ainda esotérica. Ademais, a grande maioria das interfaces que resultam destes procedimentos continua a não incorporar uma componente de *feedback* háptico na sua arquitectura, impossibilitando por conseguinte que os seus utilizadores possam fazer recurso daquele que é um dos aspectos preponderantes do esquema de interacção humana, o sentido do toque.

Com vista a lograr estas lacunas, a presente dissertação propõe uma plataforma centralizada e ainda assim modularizada que possibilita a concepção de interfaces de VR/AR multimodais, naquela que na nossa óptica é uma abordagem inovadora e focalizada. Para o conseguir, a plataforma supra-referida emprega os óculos de VR Oculus Rift©, ao qual um controlador de captura de movimento da Leap Motion© se associa por intermédio de um suporte personalizado. Complementarmente, um equipamento *wearable* por nós concebido está também incluído no sistema idealizado. Este último consiste numa luva que não só é capaz de transmitir *feedback* táctil ao seu utilizador como ainda está apta a adquirir, processar e registar os seus sinais Electrocardiográficos (ECG), Electromiográficos (EMG) e de Actividade Electrodérmica (EDA) de forma não invasiva. Os elementos anteriormente referidos foram interfaceados com recurso ao motor de videojogos Unity3D ©, cuja utilização em iniciativas académicas e científicas se tem vindo a popularizar.

Aquando da sua finalização, havia chegado a altura de despender a plataforma reunida de forma a substanciar a nossa alegação inicial. Decorrente desta predisposição, construímos um repositório considerável de interfaces, no qual se podem destacar: *Brain Connectivity Leap* (BCL), *Ode to Passive Haptic Learning* e *Surgical Simulator*.

Palavras-chave: Plataforma, Realidade Virtual, Captura de Movimento, *Feedback* Háptico, Electrofisiologia, Conectoma.

Contents

List of Figures

List of Tables

Glossary

.DICOM Digital Imaging and COmmunication in Medicine.

.FBX Filmbox.

.NIFTI Neuroimaging Informatics Technology Initiative.

.OBJ wavefront Object.

.STL Stereolithography.

.trk Track.

.txt Text.

2D Two-Dimensional.

3D Three-Dimensional.

AC Alternating Current.

AI Artificial Intelligence.

API Application Programming Interface.

AR Augmented Reality.

AV Atrioventricular.

BCL Brain Connectivity Leap.

BIH Brain Informatics & Health.

BVP Blood Volume Pulse.

CT Computed Tomography.

DC Direct Current.

DK Development Kit.

DOFs Degrees of Freedom.

DTI Diffusion Tensor Imaging.

ECG Electrocardiogram.

EDA Electrodermal Activity.

EEG Electroencephalography.

EMG Electromyogram.

ERM Eccentric Rotating Mass.

fMRI functional Magnetic Resonance Imaging.

FOV Field Of View.

FPS Frames Per Second.

HCI Human-Computer Interaction.

HMB Haptic Mitt Bit.

HMD Head Mounted Display.

I/O Input/Output.

IBEB *Instituto de Biofísica e Engenharia Biomédica*.

IDE Integrated Development Environment.

IICISGP *II Congresso Internacional da Saúde Gaia-Porto*.

iLIDH Luso-Illyrian Institute for Human Development.

IMUs Inertial Measurement Units.

IR Infrared.

LED Light Emitting Diode.

LRA Linear Resonance Actuator.

LxMLS Lisbon Machine Learning School.

MEMSs Micro Electro-Mechanical Systems.

MIBCA Multimodal Imaging Brain Connectivity Analysis.

MRI Magnetic Resonance Imaging.

MU Motor Unit.

MUAPs Motor Unit Action Potentials.

MUV Museum of Universal Values.

PCB Printed Circuit Board.

PET Positron Emission Tomography.

PHL Passive Haptic Learning.

PVA Piezoelectric Vibration Actuator.

PWM Pulse Width Modulation.

RAM Random-Access Memory.

RF Radio Frequency.

RGB Red-Green-Blue.

ROIs Regions Of Interest.

RPM Revolutions Per Minute.

SA Sinoatrial.

SCL Skin Conductance Level.

SCRs Skin Conductance Responses.

SDK Software Development Kit.

SI *Système Internationale* or International System.

SMA Shape Memory Alloy.

SNR Signal-to-Noise Ratio.

TOF Time of Flight.

UI User Interface.

USB Universal Serial Bus.

VR Virtual Reality.

Chapter 1

Introduction

1.1 Context & Motivation

With the exponential growth in technology, connectivity and automation of the late XX and beginning of XXI centuries, a want for interfacing the digital and real worlds emerged and soon matured into a need, leading to the development of Virtual Reality (VR) and Augmented Reality (AR) interfaces - technologies that provide a link between the user and a computer-generated synthetic environment. The more fluid and seamless the transition between the two domains, the less detached the user feels about the interaction and the more intuitive it becomes [57].

With that in mind, one should only stand to gain from an approach with multisensory integration when designing such an interface [95]. Endowing a VR/AR application with a stereoscopic Head Mounted Display (HMD), a stereophonic sound system and the ability to atleast partially exploit the human haptic sense, would only enhance its functionality and benefit the end-user's state of immersion. The latter sense deserves special consideration given that unlike the visual and auditory systems, their haptic counterpart is capable of both perceiving and acting on the environment [95]. A realization that in and of itself opens up a wide array of possibilities for software and hardware developers alike.

Adding a layer of physiological computing to said interface, enables the subject's Electrocardiogram (ECG), Electromyogram (EMG) and Electrodermal Activity (EDA) to be acquired in a non-invasive fashion and processed at run time. These biosignals and the features they entail, can subsequently be used to dynamically affect and modulate the constructed landscape, effectively laying down the foundations for biofeedback to be construed. It's establishment depends solely on the user's state of awareness regarding the causes that brought about the shifts in his/her surroundings, *i.e.*, on the paradigm of the experience, and like so poses no extra encumbrance on the programmer's end [1].

Couple these features with a reliable hand motion tracking mechanism, and not only is the interactivity of the system taken to new heights but the aforementioned immersion is accentuated even further. This would allow users to rely on their proprioception to control their movements and better understand depth, ideally up to a point where the "mind's eye" is fooled and true enthrallment is achieved [57].

In few other health related disciplines is attaining such levels of realism and captivation more crucial than it is so in rehabilitation. However, the branch does not stand alone in such regard. Accurately designing task-driven, engaging and motivational experiences can be determining not only when dealing with the innate lethargy that often ails therapy patients but also in educational, diagnostic and surgery settings [42, 90]. Moreover, having access to both real-time and offline electrophysiological data provides overseers with valuable insights to aid in their clinical and/or evaluation assessments [26].

Thus, the present dissertation was prompted. It proposes an innovative approach towards the development of wholesome VR/AR applications by integrating existing state of the art media and complementing them with a novel wearable device. A glove capable of not only conveying tactile feedback to its wearer but also acquiring electrophysiological data at run time, hence bringing physiology into the VR/AR scene.

1.2 Objectives

The core focuses of this thesis are then to, first and foremost, create the necessary tools for the development of cohesive multimodal VR/AR interfaces with educational and clinical applicability. And last but not least, to employ and showcase them in the conception of a set of applications that fall into the aforesaid categories. In order to reach these marks, the following milestones were set:

- Design and materialization of a physical VR mount with which to attach the hand tracking controller from Leap Motion© onto the HMD from Oculus Rift©;
- Design and confection of the glove's textile elements;
- Design and assembly of the haptic feedback module using a microcontroller-based prototyping platform from Arduino©;
- Design and soldering of the device's electrophysiology component resorting to the Bitalino© Freestyle Kit;
- Building the glove's Software Development Kit (SDK), in which a haptic stimuli library, a signal processing toolkit and gesture recognition algorithms are included;
- Integration of the final wearable device with the HMD from Oculus Rift© and the Leap Motion© controller in Unity3D© (chosen development platform);
- Development of VR/AR applications featuring the devised multimodality.

1.3 Dissertation Overview

The present chapter consists of a brief preface to the proposed thesis and as such, focuses mainly on its scope, motivations and goals. From this point onward, its structure is organized as follows:

- **Chapter 2** sheds some light on pertinent, and otherwise unfamiliar to most, theoretical notions that were deemed fundamental to the understanding of this dissertation. These will be addressed in a thorough albeit comprehensive manner;
- **Chapter 3** accounts for an exhaustive review of the literature pertaining to the current state of the art in the fields related to this project. To accomplish this, concrete examples of technologies, methodologies and designs of relevance are presented according to the category in which they insert themselves.
- **Chapter 4** performs a step-by-step chronological scrutiny of the resources and methods that were deployed in order to meet the requirements set by the appointed objectives;
- **Chapter 5** summarizes this dissertation's key results by disclosing our final framework, its principal constituents along with the applications that derived from them;
- **Chapter 6** states the overall conclusions of our campaign, the limitations that were encountered during its course, a concise synopsis of what we have planned for the future and lastly, the contributions that stemmed from it.

Chapter 2

Theoretical Concepts

2.1 Virtual Reality

The term *Virtual Reality* is credited to Jaron Lanier, who first coined it in the 1980's to differentiate between traditional computer simulations and those that involved multiple users in a shared environment. Since then, and given the span of its embrace, its meaning has been continuously tweaked by generations of academics, software developers and researchers who delved into the realm.

In accordance with today's definition, it can be thought of as a visceral form of digital display, through which one can be transported into an evermore Three-Dimensional (3D) synthetic form of real or imagined worlds [68].

As expected, development in VR frequently goes hand in hand with concepts such as immersion, interactivity and involvement, and more often than not, these end up serving as benchmarks to label the resulting interfaces. Depending on the pondered criteria, VR experiences can then be classified as either passive, exploratory or interactive (or any combination of these) [12, 24].

Given its stature as an emerging medium, VR still stands as a fairly esoteric and specialized discipline. Because of this, certain aspects pertaining the best practices for content creation in the field are yet unstudied to a point where authoritative statements cannot be made. That being said, observational theories do exist as to prevent the development of poorly conceived interfaces, which once combined with sub-optimal hardware generally increase the odds of triggering Simulation Sickness[1] [57, 68]. To circumvent this issue, extensive user testing remains an absolute necessity and a crucial step towards designing comfortable *in silico* experiences.

[1] Combination of symptoms clustered around eyestrain, disorientation, and nausea that arise from conflicting sensory inputs (*i.e.* inner ear, visual field and bodily position).

2.2 Augmented Reality

The underlying notion of *Augmented Reality* can be considered as a subcategory of a more encompassing albeit less disseminated concept called Mediated Reality, in which the user's perception of the physical world is not necessarily augmented, but can conversely be diminished.

AR contrasts with VR mainly in the composition of their simulation spaces. Whereas the latter are entirely computer-fabricated, the former raise the system's complexity by superimposing a layer of virtual elements on a view of the real world[2], ergo, augmenting it. Even the slightest misalignment in the integration process is enough to compromise immersion and incite disengagement, which is why it comes as no surprise that object recognition and other image processing algorithms play a big role in AR [12, 39].

Up until the insurgence of smartphones and tablets, AR was mostly restricted to large-scale scientific or military projects. However, recent developments in mobile technologies have significantly widen its audience and boosted independent research. Thereafter, AR data visualization applications related to navigation, advertising, art, education, tourism, entertainment, medicine (an example can be seen in figure 2.1) and so on are beginning to see the light of day [29].

Figure 2.1: VeinViewer© is an AR medical application that uses IR reflection to compute patterns of superficial veins. These are then projected them onto the patient's skin.

[2]Not necessarily visual and typically used as a reference frame.

2.3 Haptics

When debating *Haptics*, some ambiguity is bound to arise. One may be referring to the human haptic system or to the technologies that hope to either probe, emulate or interact with it. By elaborating on both of these topics, we hope to clear the veil of confusion that often clouds the definition of haptics.

2.3.1 Haptic Sense

More commonly dubbed as our sense of touch, or tact, the *Haptic Sense* is a key player in the overall spectrum of human exploratory procedures [37, 92]. As section 2.3.3 will shortly adress, it is closely related to muscle memory and therefore cannot be dissociated from the process by which motor skills are apprehended [75]. Roughly speaking, it can be broken down into two submodalities that differ mainly on the type of sensory information that is dealt with by them [10, 95].

- **Tactile** (or cutaneous) information is usually associated with texture, temperature and vibration. That first sense of contact whenever we touch an object's surface, happens when this kind of information is captured by specialized thermal and mechanical skin receptors which then send it through a fferent neural pathways to be processed by the parietal lobe in the cerebral cortex [11, 84];
- **Kinesthetic** (or proprioceptive) information on the other hand, has to do with the pressures, forces and motions that we perceive when interacting with the physical world. It is how we can discern the weight of an object just by holding it. Some of the object's features are not sensed directly though, but rather extrapolated from the relative positions and movements of the intervenient body parts [10, 95];

Notwithstanding their simultaneity and the fact that their separation is far from physiologically established, for the purpose of this dissertation, whenever the term "haptic sense" is invoked from this point onward, it shall be referencing its tactile component (unless explicitly saying otherwise) [10].

2.3.2 Haptic Technology

From a technological point of view, haptics tries to entice the supra referred senses of touch and kinesthesia to convey pertinent information - Haptic Feedback.

Although it might seem like a foreign notion at first glance, it is something we have been unknowingly familiarizing ourselves with ever since we first felt the buzzing of a silent-mode cellphone in our pockets [92]. Besides the obvious, fairly unambitious and already in place applications in the gaming and mobile industries, haptic devices have slowly but surely been seeping their way into other areas in recent years, such as medicine, military training, communications and education [24, 92, 95].

In fact, *Haptic Technology* now stands as a candidate in tackling one of the defining problems of our age: Information Overload, a direct consequence of an unprecedented unrelenting contact with the digital world through electronic devices that bombard us with visual and, to a lesser extent, auditory stimuli. In the words of Professor Karon MacLean, "People are not biologically equipped to handle the assault of information that all comes through one channel" [47].

Nevertheless, high production costs associated with a lack of a standard Application Programming Interface (API) and established User Interface (UI) conventions have somewhat limited a widespread market acceptance for haptic appliances [92]. This does not necessarily constitute a deterrent to venturing on the field but can on the contrary, be construed as an opportunity.

Historically speaking, the pioneer haptic devices that fell into the tactile category, were inspired by matrix pin-printers resembling those used in braille systems for the blind [10]. Today however, they have evolved into relying mostly on localized vibration actuators, known as Tactors [92]. These vary with respect to their response times, capacity to generate different waveform patterns, power requirements and functioning principle [5]. As such, vibrotactile actuators can be divided into different tiers. In light of their importance to this project and presence in applications of biomedical importance, the following four shall be given special emphasis:

- Eccentric Rotating Mass (ERM);
- Linear Resonance Actuator (LRA);
- Piezoelectric Vibration Actuator (PVA);
- Shape Memory Alloy (SMA);

To better understand each of the above variations, comprehensive albeit thorough explanations will be presented in the upcoming sections.

2.3.2.1 Eccentric Rotating Mass Motors

An ERM vibration actuator is, in its essence, an electromagnetic Direct Current (DC) motor with an off-centered mass attached to a shaft (represented in figure 2.2). As said asymmetrical mass rotates, it generates a non-null net centripetal force that ensues in the motor's displacement.

The shaft's rotation is achieved by applying a current to its armature windings. As these are inside a permanent magnetic field, Lorentz law dictates that a torque be applied on the shaft. To ensure the direction of rotation is maintained, the current in the windings has to be regularly reversed. This can be accomplished through the use of static metal brushes at the ERM's terminals that intermittently contact the different segments of a rotating commutator [52].

With a sufficiently high count of Revolutions Per Minute (RPM), the motor is constantly being moved in the plane perpendicular to the shaft's axis. The resulting rapid and repeated displacement is what is perceived as vibration [54].

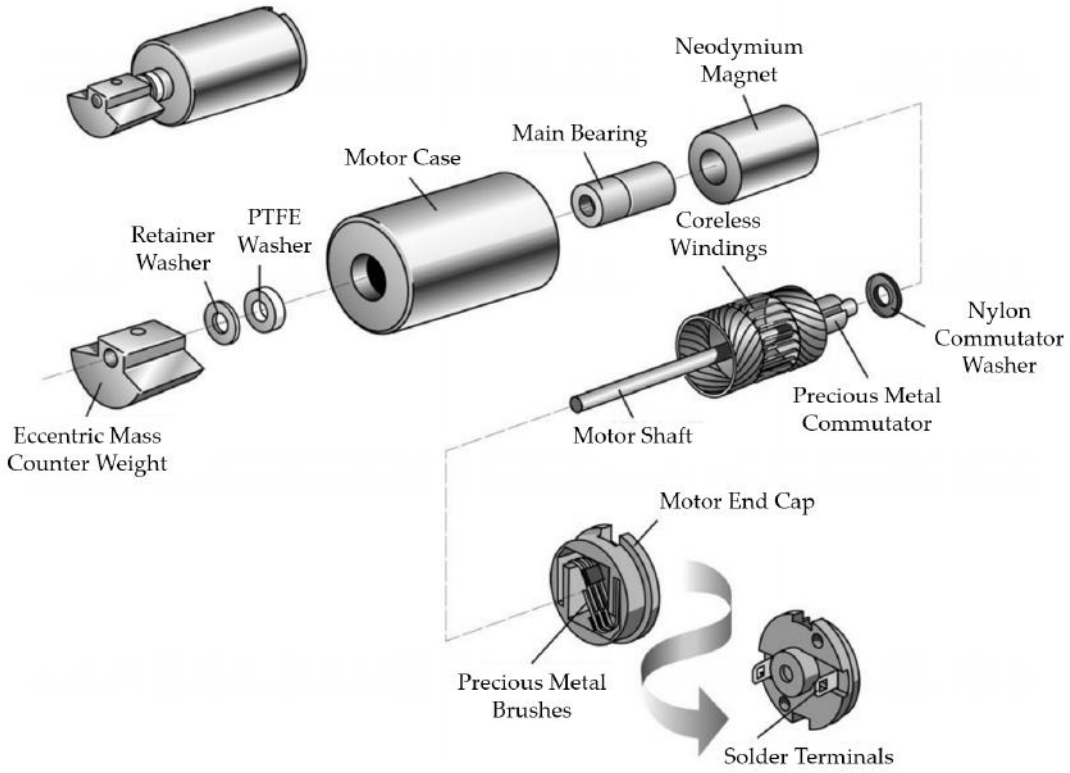

Figure 2.2: Exploded cylindrical ERM vibration motor. Coin-shaped ERMs also exist, and are typically more suited for haptic applications since they require no external moving parts. Adapted from [54].

This effect is generally unwanted in engineering pursuits, since it is often associated with noise, excessive wear and fatigue. Consequently, most literature on the matter focuses on minimizing vibration in mechanical systems rather than having it maximized.

To evaluate ERM performance, two metrics of vibration are commonly quoted:

- **Vibration Frequency** is the frequency at which the tactor oscillates and is fairly simple to derive since it depends exclusively on the motor's rotation speed (formalized in expression 2.1);

$$\nu = \frac{\nu_{RPM}}{60} \tag{2.1}$$

$\nu \rightarrow$ vibration frequency $[Hz]$;
$\nu_{RPM} \rightarrow$ motor speed $[RPM]$;

- **Vibration Amplitude** on the other hand, has a bit more complexity to it. As shown in equation 2.2, the centripetal force generated by the motor depends on the mass of the off-centered load, on the motor's eccentricity[3] and on its angular velocity. However, this does not tell the whole story. The total vibration amplitude also depends on the mass of the object to which the ERM is attached. If the total mass of the system is known, its acceleration can be calculated by applying Newton's second law of motion (also represented in equation 2.2). From there, it is a simple matter of multiplying it by the the earth's gravitational acceleration to obtain the vibration amplitude of the system in its standard unit (not *Système Internationale* or International System (SI)). In order to facilitate comparison among different ERM models, a typical normalized amplitude of vibration is cataloged. This pragmatic measurement expresses the level of vibration that the ERM in question produces when driven at its rated DC voltage in a system weighting 0.1 kg [54];

$$F_{ctp} = m_e r\omega^2 = Ma = (m_e + m_o)a \equiv A_g = \frac{F_{ctp}}{(m_e + m_o)G} \tag{2.2}$$

$F_{ctp} \rightarrow$ centripetal force $[N]$;
$m_e \rightarrow$ eccentric load's mass $[Kg]$;
$r \rightarrow$ eccentricity radius $[m]$;
$\omega \rightarrow$ angular velocity $[rad.s^{-1}]$;
$M \rightarrow$ total mass of the system $[Kg]$;
$m_o \rightarrow$ attached object's mass $[Kg]$;
$a \rightarrow$ acceleration of the system $[m.s^{-2}]$;
$A_g \rightarrow$ vibration amplitude $[G]$;
$G \rightarrow$ earth's gravitational acceleration $[m.s^{-2}]$;

To sum up, we have established that varying the input DC voltage of a system powered by an ERM, changes the centripetal force produced by it which by extension affects the system's frequency as well as its amplitude of oscillation. Thus deeming impossible their independent manipulation.

[3] Defined as the distance between the mass's center of gravity and the motor shaft.

2.3.2.2 Linear Resonance Actuators

While still in the gamma of electromagnetic tactors and despite operating on a similar basis (where a moving mass creates an unbalanced force that repeatedly displaces the mechanical system), LRAs differ greatly from their ERM counterparts. Unlike the latter, linear resonance motors use an internal magnetic mass attached to a spring to create motion. An Alternating Current (AC) through the LRA's coils (visible in figure 2.3) generates a fluctuating magnetic field that drives the inner mass back and forth in its direction, resulting in a force that causes displacement [52, 53].

The described system depicts a basic example of a driven harmonic oscillator, in the sense that when disturbed by an external force, it experiences a restoring one (exacted by the spring) that moves it towards its equilibrium position. This means that the device vibrates with greater amplitude when driven at particular frequencies - Resonance. Considering that the electromagnetic force that is felt by the mass's permanent magnet only acts in a single axis (perpendicular to the wider surface of the LRA's casing), it follows that its movement is also restricted to it. This "Linear Resonant" behavior is where the actuator gets its name [53, 54].

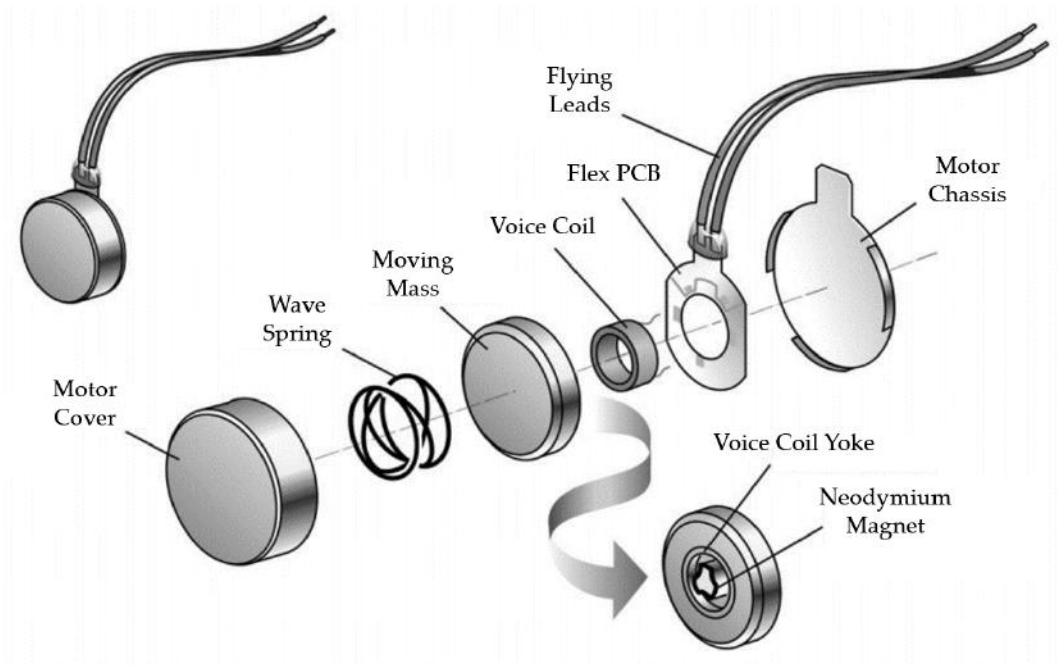

Figure 2.3: Exploded coin-shaped LRA vibration motor. Adapted from [52].

Being that they focus on efficiency, these vibrotactile actuators are usually associated with narrow bandwidths of operation, meaning that they will only vibrate when excited by an AC signal with a frequency that falls within a few Hz of their quoted resonant frequencies. Because of this, integrating a LRA into an application can be a hazardous task without resorting to dedicated driver chips, making them a slightly less viable choice when prototyping.

On the other hand, they do offer a couple of pivotal benefits that might render them the better option for finished products, specially when it comes to implementing haptic feedback. To name a few of these, we can highlight the fact that when compared to ERMs, LRAs have lower response times, meaning they can start to vibrate more quickly and stop equally as fast. This leads to a more realistic haptic response. Furthermore, having no electromechanical commutation and being effectively brushless[4] translates into less mechanical wear and thereby, much longer lifespans. Even the driving requirements that might make them less appealing at early stages of development, grant them an additional edge for final applications. This holds true because most LRA driver chips offer a wide range of specialized utility features that optimize overall performance (such as automatically detecting resonant frequencies and providing waveform libraries) [53, 82]. Lastly, relying on resonance to operate implies that there is no direct correlation between the input's amplitude and its nearly invariant frequency. This allows for the use of more complex excitation waveforms which in turn, result in a richer haptic experience for the user [51].

[4]The bottleneck of a DC motor is usually its precious metal brush.

2.3.2.3 Piezoelectric Vibration Actuators

These non-magnetic vibrotactile displays function on the premise that when strained, piezoelectric materials store charge. Conversely, when a DC voltage is applied to them, their shape is altered. If an AC input is used instead, multiple and successive deformations occur, *i.e.*, vibration [77] (this effect is portrayed in figure 2.4).

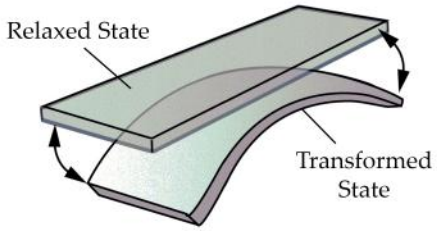

Figure 2.4: Abridged representation of a PVA, showing its relaxed and bent states [78].

This seamless conversion between mechanical and electrical energies award PVAs with a certain duality in regard to their purpose. Provided that the system's architecture adapts to their circumstantial role, they can be used not only as actuators but also as sensors. Adding to this feature, there are several others to be pointed out, that presumably give these tactors a competitive advantage over their electromagnetic cousins:

- **Static Deflection** refers to the capability to maintain a static DC driven curvature. Besides allowing for the illusion of height in certain UI elements of Two-Dimensional (2D) displays, this can be used to constrain certain movements in wearable applications - Kinesthetic Feedback;
- **Independent Frequency, Amplitude and Phase** manipulation adds a layer of customization to the feedback that is produced. As we have discussed in sections 2.3.2.1 and 2.3.2.2, such level of control simply cannot be attained with ERMs, and only partially can it be so with LRAs;
- **High Frequency** accredits these actuators with the ability to comply with high paced excitation impulses such as square waves and step functions;
- **No Magnetic Signature** means that piezo actuators can be used near magnetism-sensitive devices, *e.g.* compasses, Random-Access Memory (RAM), Radio Frequency (RF) antennas and even Magnetic Resonance Imaging (MRI) machines;
- **Low Current** needs make PVAs an asset in wearable electronics, where low gage, *i.e.* thin, fabric-embedded and high-flex wiring is required;

Despite all these bonuses, piezo actuators yet present some downsides. The most noticeable of which probably being their price, which greatly surpasses that of the previously mentioned vibromotors.

2.3.2.4 Shape Memory Alloys

Smart metals and muscle wires are just a couple of the colloquial aliases given to SMAs. The reason being that when heated above a characteristic threshold, these composites are able revert any existing deformation and return to their predefined original shapes, as if they "remembered" them. This phenomenon can be observed even with unusually large amounts of strain - Superelasticity.

In other words, SMAs can exist in two different phases, Austenite and Martensite. Transition between the two is diffusionless, *i.e.* time-independent, and dictated solely by the material's temperature and stress. While at its martensitic state, a SMA can be molded into any arbitrary shape. Said deformation is then maintained until the alloy is heated up beyond its A_s temperature (refer to figure 2.5 for this and any other subsequent variable allusions regardind the shape-memory effect), at which point it starts to regress into its austenitic shape. Once the temperature reaches the value of A_f, the transformation is complete [89, 91]. Analogously, we could enforce the same rationale to explain how the cooling process unfolds.

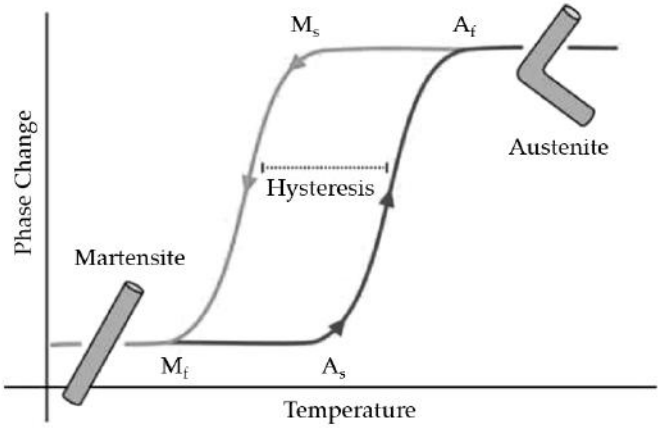

Figure 2.5: Representation of shape-memory physics. The differences between the cooling and heating transitions are an evidence of hysteresis, meaning that the effect is not without some inherent energy loss [89].

$A_s \rightarrow$ start temperature for martensite to austenite transitions;
$A_f \rightarrow$ temperature of completion for martensite to austenite transitions;
$M_s \rightarrow$ start temperature for austenite to martensite transitions;
$M_f \rightarrow$ temperature of completion for austenite to martensite transitions;

Since these reversible shifts can be driven by the resistive heating that an electric current flowing through a shape-memory wire creates, adopting this technology to haptic actuation becomes a matter of choosing the appropriate thermo-mechanical configuration [94]. However excellent the power-to-weight ratio and intrinsically high stiffness of SMAs, these are hindered by their relatively low rate of deformation, hence limiting their use as vibrotactile actuators [91].

2.3.3 Passive Haptic Learning

Krugman and Hartley eloquently define passive learning as "typically effortless, responsive to animated stimuli, amenable to artificial aid to relaxation and characterized by absence of resistance to what is learned" [41]. *Passive Haptic Learning* (PHL) embodies these traits to facilitate the apprehension of motor skills through haptic stimulation while little to no attention is dedicated to the process [75]. In fact, this mechanism has proven its effectiveness even when the subject is actively engaged in distraction tasks (*e.g.* completing a standardized test, watching a movie, walking a path) [40].

Most literature on the topic refers to its application in the process of learning and rehearsing relatively simple one-handed piano passages (*i.e.* sequences of 10-15 notes), through usage of haptic gloves with embedded vibration motors (in a configuration that resembles the one illustrated in figure 2.6) [40, 48]. However, recent studies have also proven its adequacy when it comes to acquiring and honing more challenging skills such as typing and reading Braille or playing two-handed chorded piano melodies [74, 75].

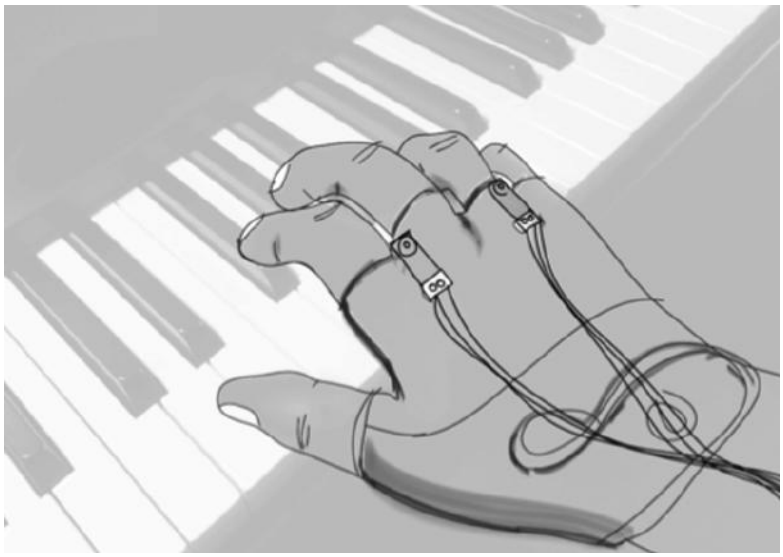

Figure 2.6: Typical configuration of PHL applied to musical retention [34].

Considering the limited amount of free time the typical adult has at his/her disposal, devoting a portion of it to actively learn high maintenance competences like playing an instrument can be a cumbersome and frustrating struggle. Specially considering that learning to play any given song once is insufficient. As soon as it is learned, forgetting begins [40]. PHL's appeal in this matter is irrevocable, as it provides a means to repeatedly reinforce motor skills while requiring no perceived attention from the user. Not only is this true for the average person trying to learn a new recreational expertise, but also for rehabilitation patients with impaired upper limb mobility, whose compliance is so often drained by repetitive and monotonous tasks. Researchers have supported this claim with promising results after using PHL with individuals with tetraplegia (resulting from incomplete Spinal Cord Injury) [48].

2.4 Electrophysiology

Electrical signaling is one among the fast communication channels of cells and tissues within living organisms. *Electrophysiology* is the branch of physiology that concerns itself with the acquisition, processing and analysis of these ionic currents [31, 64].

Its resolution envelops measurements on a wide variety of scales, ranging from single ion channel proteins to whole organs. Given this thesis's context, we will focus more towards the latter.

2.4.1 Electrocardiography

Heartbeats are triggered by low amplitude electrical impulses, generated by a specialized aggregate of fibers - the Sinoatrial (SA) node[5] [61]. These cardiomyocytes have the characteristic ability to spontaneously and periodically depolarize. Considering that in cardiac tissue, neighboring myocites are electrically coupled via low-resistance channels, *i.e.* gap junctions, and that these allow for direct ion exchanges between adjacent pairs, it follows that a single action potential can initiate a cascade of intercellular currents [31]. When that is the case, the exciting potential propagates throughout the cardiac conduction system (depicted in figure 2.7) and ultimately leads to a contraction, a beat.

Although they do not stand alone in such regard, meaning that there are other fibers in the heart capable of prompting contractions, the SA cells are normally the ones to set the pace, simply because they have a higher frequency of depolarization. For this reason, the SA node is commonly termed as the heart's natural pacemaker.

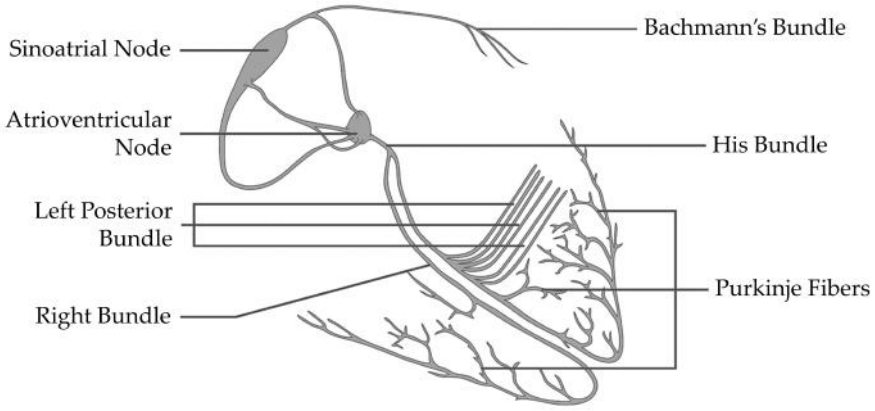

Figure 2.7: Isolated heart conduction system. Adapted from [18]

Electrocardiography (ECG) is the process by which the aforestated electrical activity is detected, translated into numerical values and then recorded over a period of time [61]. To do this, electrodes are placed in contact with the subject's skin, where the myocardium's depolarization potential yet reverberates with a measurable intensity.

[5] Positioned in the right atrial myocardium, just internally to the epicardium.

The resulting electrocardiogram tracings (exemplified in figure 2.8), greatly depend on the used electrode configuration. In a conventional 12 lead ECG, 4 are distributed over the patient's limbs and 6 are placed on his/her chest surface. What is then measured, is the heart's overall electrical potential from 12 different angles, ergo "12 lead ECG". Although this approach produces valuable information that can help diagnosing and monitoring underlying medical conditions, simpler ones exist for applications with less demanding purposes. Examples of these are a configuration in which 1 electrode is placed at each hand and another where 3 electrodes are placed at the chest [61].

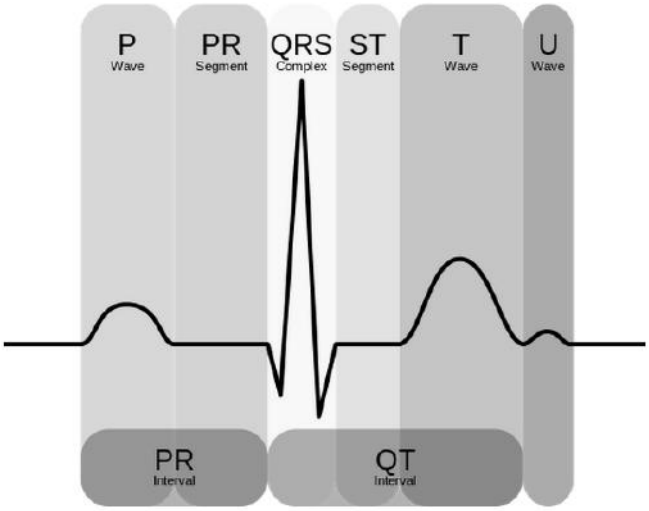

Figure 2.8: Simplified representation of a normal ECG and its typical waveforms. To a trained clinician, these tracings convey a large amount of structural and functional information about the heart and its conduction system. Authored by Hank Diskussion.

P wave → Indicates atrial depolarization, which leads to the contraction of the atria. For reasons listed above, the right atrium depolarizes slightly earlier than the right one;
PR interval → Period between the onsets of atrial and ventricular depolarizations. Correlates to the transmission delay imposed by the Atrioventricular (AV) node;
PR segment → Flat isoelectric section that reflects the depolarized state of the atria;
QRS complex → Announces ventricular depolarization, which coincides with and therefore obscures atrial repolarization. Given its amplitude, it is usually the marker used for peak detection and heart rate calculations;
QT interval → Period between the depolarization and repolarization of the ventricles;
ST segment → Flat isoelectric section that reflects the depolarized state of the ventricular chambers;
T wave → Marks the repolarization of the ventricles;
U wave → Not always seen due to its low amplitude, this waveform is thought to represent the repolarization of the Purkinje fibers;

It is important to note that intervals differ from segments, in the sense that the former are analyzed in terms of their duration while the latter denote fluctuations, *i.e.*, elevations or depressions with respect to the isoelectric basal line.

2.4.2 Electromyography

Electromyography (EMG) is a technique that focuses on acquiring and evaluating the electrical activity that precedes muscular contraction in skeletal muscles. This electromyographic signal (instantiated in figure 2.9) is essentially a collective of superimposed action potentials from bands of neurologically or artificially stimulated muscle fibers - Motor Unit Action Potentials (MUAPs) [19, 21]. These waveforms provide relevant insights about the anatomy and physiology of the Motor Unit (MU), and thereupon about the muscle these insert themselves in.

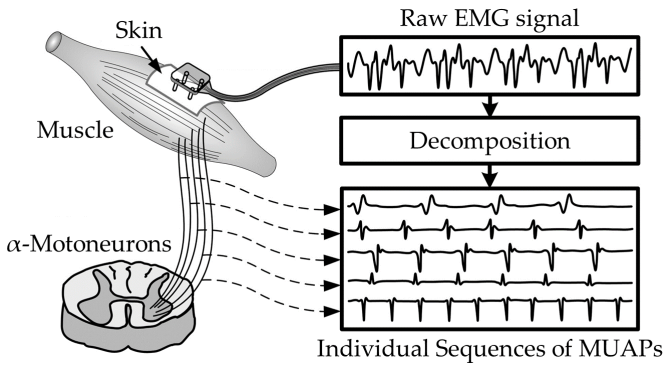

Figure 2.9: Pictorial outline of the decomposition of a raw surface EMG recording into its MUAP constituents. Adaptation from [21].

Concerning instrumentation, methodology and produced results, two detection approaches can be distinguished:

- **Surface EMG** assesses muscle function in a non intrusive manner by measuring the potential difference between one or more pairs of surface sensors placed on the skin above the muscle (as seen in figure 2.9). This bipolar configuration is ideal for high Signal-to-Noise Ratio (SNR) in the acquired data [63]. However, the method is not without its drawbacks. Reliably discriminating between discharges of adjoining muscles is unfeasible. Moreover, these recordings are restricted to superficial muscles and as such, are influenced by the depth of the subcutaneous tissue in the vicinity of the detection sites, which in turn is highly variable both inter- as well as intra-patients;
- **Intramuscular EMG** is performed either with needle or fine wire sensors placed within the muscle/s of interest [21]. Although it requires skin penetration and can only monitor smaller areas of said muscle, this method attenuates the significance of some of the limitations that affect surface EMG [59];

Raw EMG tracings are usually contaminated by noises and various artifacts inherent to the acquisition process. To compensate for this, numerous features can be extracted from the original amalgam of electrical activity and used in its stead as input for Human-Computer Interaction (HCI) and/or medical applications [19, 63].

2.4.3 Electrodermal Activity

Autonomic changes in the electrical properties of the skin are comprised by the notion of *Electrodermal Activity* (EDA). Said variations are modulated by the secretion levels of eccrine sweat glands, found virtually in all skin albeit with a considerable higher density in the palmar and plantar regions (hands and feet, respectively). Their high susceptibility to psychologically significant stimuli gives EDA its stature as an invaluable index of change in sympathetic alertness and arousal, which in turn is tractable to emotional and cognitive states [17, 62].

The most widely studied property of the EDA complex is skin conductance, which can be quantified by applying a potential difference between two points in the skin surface and measuring the current that flows between them. The resulting measurements include a background tonic component - Skin Conductance Level (SCL) - as well as rapid phasic events - Skin Conductance Responses (SCRs). An instance of the latter and its typically analyzed features can be seen in figure 2.10 [17].

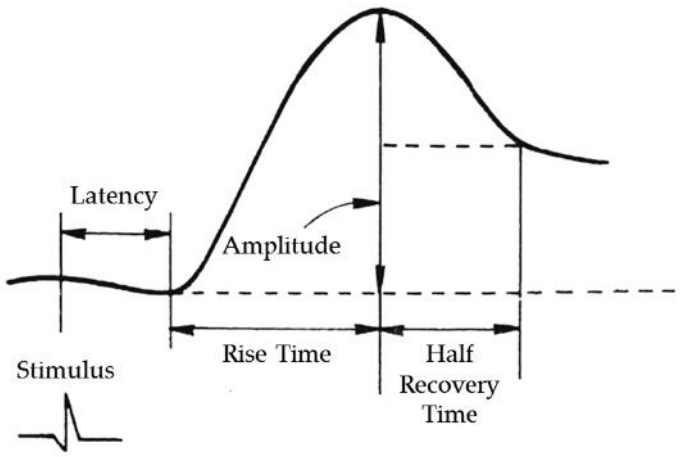

Figure 2.10: Graphical representation of an ideal SCR. Adapted from [17].

Fluctuations in psychological homeostasis in response to internal or external stimuli are loosely described in terms of "stress" [16]. From an evolutionary point of view, short term stress reactions are beneficial to the organism in the sense that they help it adapt to the stressor, *i.e.*, the stimulus that elicited the response. However, long term exposure to stressful situations and environments may lead to adverse effects, *e.g.* decreased productivity, distress, illness and mental breakdown [76].

For this and other reasons, having robust psychophysiological metrics for stress monitoring would be advantageous not only in applications focused on preventive medicine but also in those oriented towards rehabilitation and productivity maximization. Being that, as we previously stated, EDA is a marker for purely sympathetic responses, it stands a viable candidate for the role, specially when coupled with ECG or Blood Volume Pulse (BVP) readings for heart rate assessments [76].

2.5 Biofeedback

Biofeedback is an emerging yet increasingly credited technology in the field of alternative medicine. It can be summed up as a method for conscious manipulation of one self's physiological activity with the finality of improving health, well being and overall performance [1, 6].

Although it is not mandatory, the process can be reinforced through visualization of some of physiology's signature markers, *e.g.*, heart function, brainwaves, breathing and skin properties (both thermal and electrical). These traits can be quantified by biomedical equipment and then shown, or "fed back", to the user. Through practice and study, the subject can learn how to purposefully alter these signals and in the process, effectively affect his/her health. Over time, this skill can be mastered, eventually up to a point wherein continued use of auxiliary instruments is no longer necessary.

This deployable but affordable technique has proven its legitimacy as a complementary clinical and therapeutic tool in the treatment of over 100 illnesses, producing particularly positive outcomes in those where motivation and progress awareness are key agents of recuperation [1, 6].

As we have hinted in the previous section (2.4), any approach to biofeedback that could potentially stem from the framework assembled in this thesis would have to be centered mostly around the user's ECG, EMG and EDA signals[6]. In spite of not having developed any applications that exploit these phenomena ourselves, we reckoned it still merited a mention in the present chapter.

[6]Motion tracking can also play a part in its implementation.

2.6 Motion Tracking

The systematical study of animal locomotion, *i.e.*, gait analysis, has been an active research topic in biomechanics ever since the 1980's [6]. Interest has not dwindled in recent years, particularly in the case of human *Motion Tracking*, a submodality within the field that is given special focus in light of its potential in clinical and commercial applications [96].

Researchers are continuously trying to develop dynamic systems that can provide real-time data that is representative of changes in body poses while minimizing monetary costs and procedural intrusiveness. When evaluating the overall performance of these motion capture systems, several other aspects must be taken into consideration [70]:

- **Temporal Resolution** is dictated by the system's sampling rate, which translates the frequency at which information is read;
- **Spatial Resolution** indicates the smallest motion that the sensors can register;
- **Latency** is the delay between the actual motion and its detection by the sensors;
- **Accuracy** accounts for the amount of error in the performed measurements;
- **Robustness** reflects adaptability to different environmental settings;
- **Range** delimits the optimal tracking distance between the sensors and the target;
- **Degrees of Freedom (DOFs)** relate to the number of independent variables that the tracker uses to quantify motion;
- **Reference** can either be absolute, in the sense that motion is measured against a fixed coordinate system, or relative to previous measurements. It is important to note that the latter frame can lead to cumulative errors - Drift;
- **Mobility** rates the system in terms of portability. Logically, this cannot be dissociated from its weight, size and wired/wireless nature;

The parameters listed above can be heavily conditioned by the functioning principle of the sensing technology in focus. Because of this, the impending sections will address each of the presently listed types of existing systems individually:

- Acoustic Systems;
- Mechanical Systems;
- Magnetic Systems;
- Inertial Systems;
- Optical Systems.

2.6.1 Acoustic Systems

Typically, *Acoustic Systems* rely on several sound emitters and atleast three receivers to triangulate position. The emitting markers (*e.g.* microphones) are placed at strategic locations of the body that is being tracked, while the receptors (*e.g.* loudspeakers) are arranged in an orthogonal configuration at the capture site. Since the traveling speed of sound is known, tri-axial distances can then be extrapolated from the measured time intervals between emissions and receptions - Time of Flight (TOF) method (formalized in equation 2.3). To differentiate tracers from one another, they are can either be activated in a sequential manner or they can each have their own signature frequency [58].

Although it should not come as a surprise that the roles of emitters and receivers are interchangeable, the described setup is usually favored. Additionally, a fourth receiver can be fixed in order to dynamically measure the speed of sound and therefore minimize errors due to changes in humidity and temperature.

$$D_{ij} = \Delta t_{ij} v_s = (t_j - t_i) v_s \tag{2.3}$$

$D_{ij} \rightarrow$ distance between emitter i and receiver j $[m]$;
$\Delta t_{ij} \rightarrow$ time of flight between emitter i and receiver j $[s]$;
$v_s \rightarrow$ speed of sound $[m.s^{-1}]$;
$t_i \rightarrow$ instant of emission $[s]$;
$t_j \rightarrow$ instant of reception $[s]$;

The fact that this technology uses lightweight, low-cost and high resolution sensors, is often counter-weighted by issues related with robustness, range, wiring and reflections.

2.6.2 Mechanical Systems

Mechanical methods for capturing body motion require some form of rigidly articulated external structures, *i.e.*, exoskeletons (see figure 2.11). Positions of interest in Cartesian space are inferred from the joint angles of these kinematic chains - Forward Kinematics.

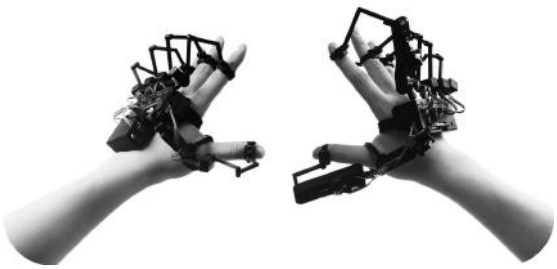

Figure 2.11: Finger tracking exoskeletons from Dexta Robotics© [69].

Despite being rather resilient, having noticeably high resolutions and being immune to field fluctuations and reflections, these structure-like*Mechanical Systems* are generally associated with high costs, limited mobility and higher assembly times.

2.6.3 Magnetic Systems

Much like acoustical and the majority of optical setups, *Magnetic Systems* use emitters and receivers to perceive motion, each composed by three perpendicular coils. Applying an AC signal on the source's coils generates an oscillating magnetic field that in turn flows trough the sensor's coils, inducing currents. Their relative intensity is what allows for the calculation of each transducer's position and orientation (six DOFs) [58].

These relatively cheap workstations are characterized by very small sensors with medium-high sampling rates and do not suffer from regular occlusion. In spite of this, being short-ranged, highly tethered and susceptible to interference caused by ferromagnetic metals and/or electronic devices limits their application [6, 96].

2.6.4 Inertial Systems

Inertial Systems fuse sensors such as accelerometers and gyroscopes (see figure 2.12) into Inertial Measurement Units (IMUs). Whereas the former provide information about the proper acceleration of the system, *i.e.*, relative to free-fall, the later exploit the Coriolis effect to sense angular motion. These are examples of Micro Electro-Mechanical Systems (MEMSs), which are able to translate mechanical phenomena into analog signals, usually by encoding information into the sensing circuit's capacitance [6, 96].

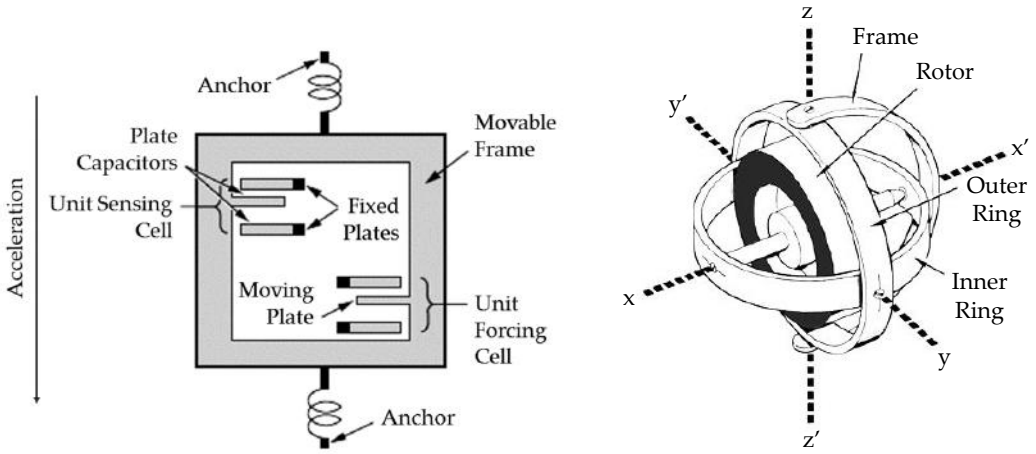

(a) Accelerometer (b) Gyroscope

Figure 2.12: Illustrations of typical inertial sensors. Adapted from [25, 86].

Besides their cost-efficiency and ease of use, high sensitivity, large capture areas and potentially wireless nature have made inertial sensors a frequent and trending choice in motion tracking, particularly when it comes to monitoring full-body poses and movements [6]. However, these systems' incorrect angle and position determinations due to offset fluctuation and acquisition noise may lead to integration drift, which compounds over time. Therefore, designing drift-free inertial trackers has been the core focus of current research in the field [96].

2.6.5 Optical Systems

Analogously to what happens with acoustic and electromagnetic motion capture configurations, most *Optical Systems* utilize markers, either passive or active, in conjunction with cameras to triangulate positions in 3D space. Nevertheless, modern sensors employing range imaging technology, have proven themselves capable of generating accurate data by dynamically tracking surface features (of the object of interest), hence bypassing the need for markers [6].

- **Passive Marker** setups rely on the reflective character of their coating material to determine positions. IR light sources surround the lens of each camera and illuminate the markers in an intermittent and sequential fashion. The pulses of reflected light are captured by each non-obscured camera, resulting in that many 2D images. These are subsequently combined by the system to compute each tracer's 3D position [96]. Despite having large and highly configurable capture volumes and not needing any wiring on the markers' end, these systems require several cameras (anywhere from 2 to hundreds) to minimize marker slippage, line-of-sight occlusion and bad volume calibration, which adds up to their cost. Even so, they remain the most widely used architectures in today's large-scale 3D motion analysis;

- **Active Marker** systems operate on the same basic principle, but replace the array of IR illuminators near each camera's lens with an embedded IR Light Emitting Diode (LED) on each marker. The fact that these emitters can be activated in a multiplexed, selective and sequential manner constitutes a crucial advantage over their passive counterparts, since this enables the system to discern between different markers [96]. Resolution- and accuracy-wise, these systems fare similarly to passive marker ones, but are arguably less versatile in terms of mobility and ease of assembly, as they require some sort of instrumentation on the markers' end;

- **Range Imaging** motion capture can be achieved by a variety of different marker-free techniques, such as sheet of light and stereo triangulation, the previously addressed TOF method (report to equation 2.3) and interferometry, among others. Most of these technologies produce either partial or complete 3D depth maps, or point clouds, of the tracked scene relative to the point of observation. The systems that collect this kind of images consist of IR sensors, traditionally called range, or depth cameras, and IR LEDs that emit light with a wavelength centered around 850 nm (outside the visible light spectrum) [56]. Low resolution, sensitivity and robustness are the most noticeable limitations of current depth cameras, but have nonetheless been improving in recent years. Moreover, given that the actual tracking is mostly done via software, physical constraints are replaced with computational ones, which usually translates into higher affordability, mobility and ease of use [58].

2.7 Game Development

Visualization is a fundamental mechanism in the process of learning. As David Marr puts it, to see is "to know what is where by looking" [49]. But it goes far beyond that, it allows for deductions about the physical properties of what is seen, which in turn promote inferences about its likely pasts and futures. With this premise in mind, for years now engineers have been modeling observable and hypothesized phenomena *in silico*, in hopes of better understanding, testing and explaining them.

Enter *Game Development*, a practice that comprises over 20 years of evolution when resorting to a combination of physics, audio, scripting, Artificial Intelligence (AI), animation and rendering engines in an evermore holistic and straightforward manner - Game Engines (report to figure 2.13 for a simplified representation) [93]. Adding to the value of enabling the creation of realistic, reliable and responsive multiplatform content, having extensive documentation and an active community makes for more friendly learning curves and expedites development in these platforms. Ergo, their use in education and scientific research has become all but logical, specially when considering that many of these frameworks now offer open-source and/or free to use editions [36, 44].

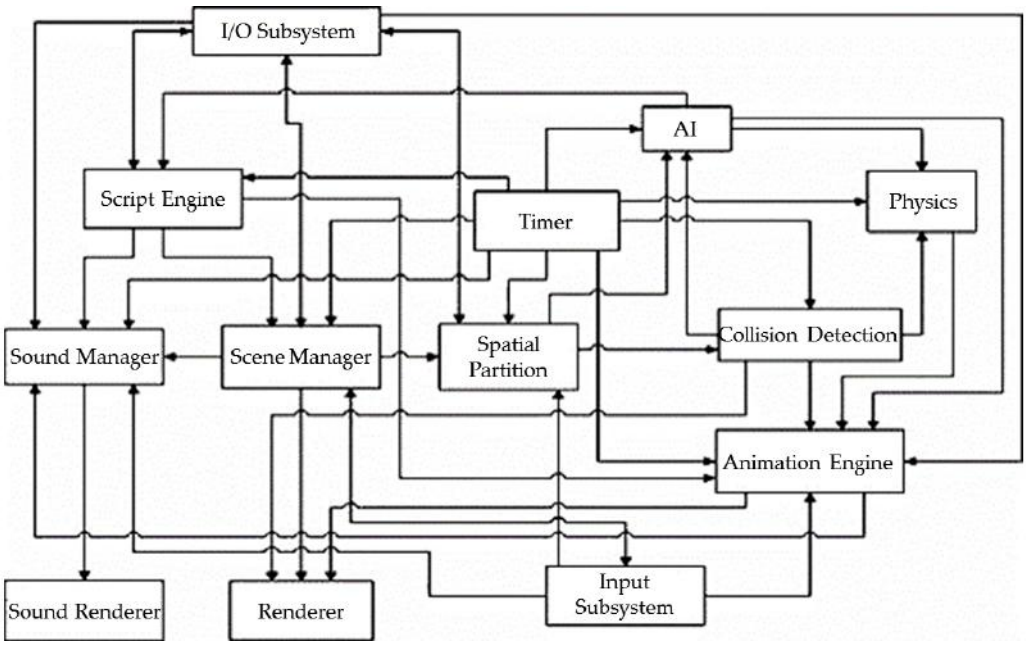

Figure 2.13: Block diagram of a modern 3D game engine. Adapted from [36].

Corroborating this claim, psychologists at the Massachusetts Institute of Technology have recently built a video game-based model that validated their proposition: all humans exhibit roughly the same patterns when attempting to comprehend the physical world [8]. The prime difference being that we run our hypothetical scenarios and prognostics in our brains, rather than in computer simulations [32]. This is just one among many studies that evidentiate the "gamification" of hypothesis-driven science [44].

2.8 3D Modeling

In computer graphics, *3D Modeling* is the process through which volumetric objects are digitally represented, either as a solid or more commonly as an aggregate of 2D polygons - Surface Mesh. Depending on its intended purpose, the resulting 3D model can then be rendered, meaning that it can be displayed as a 2D image, rigged, in the sense that it is bound to an articulated skeleton, animated or even physically printed.

When done "manually", the task of creating a mesh resembles that of sculpting, and is thus an artistically demanding one. Notwithstanding, automatic alternatives do exist, typically involving scanning technologies and/or algorithmic reconstructions.

Whichever the case, 3D modeling extends its reach far beyond the plastic arts and is in fact a highly valued trade in a wide variety of fields, ranging from architecture, gaming and medical sciences to industrial design, films and education.

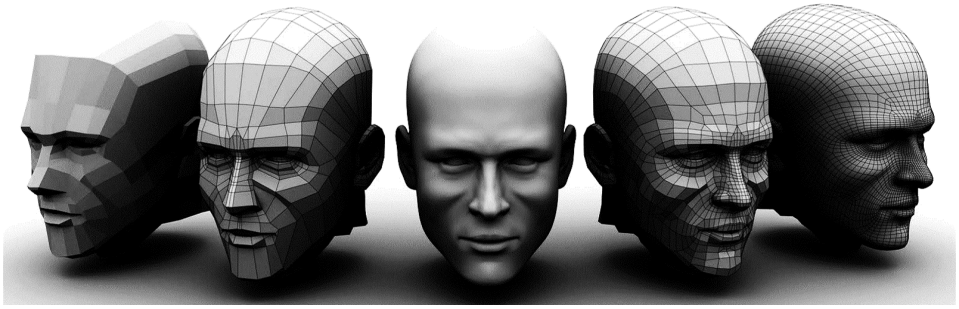

Figure 2.14: 3D polygonal modeling of a male human head. Poly-count increases from left to right (excluding the middle instance, which illustrates the final outcome).

Three main techniques of 3D modeling can be distinguished:

- **Polygonal Modeling** refers to the creation and rendering of wireframes, which consist of multiple vertices, connected by edges, typically forming a network of triangles or quads. One such a mesh can be seen in figure 2.14, wherein instances with different resolution levels, *i.e.*, poly-counts, are displayed. This showcases one of the main design issues associated this approach, which is that polygons are by definition, planar. Consequently, the illusion of curvature can only be achieved with high poly-counts. Ultimately, it comes down to a trade-off between resolution and performance, conditioned by the system's computational power;
- **Curve Modeling** defines surfaces with curves. These are influenced by weighed anchor points, which guide them through 3D space. Increasing the weight of any given point pulls the curve towards it, eventually forcing it to interpolate it;
- **Digital Sculpting** is a novel modeling technique, that even so, has found a significant embrace ever since its appearance. As it falls somewhat outside of the scope of this dissertation, suffice it to say that it offers tools to pull, smooth, grab, pinch or otherwise manipulate digital surfaces as if they were made of palpable substances.

2.8.1 3D Medical Imaging

Following the advent of MRI and Computed Tomography (CT) scanners in the early seventies, volume data became an integral and ubiquitous part of medical practice. Coupled with the continuous increase in both number and quality of imaging modalities (*e.g.* ultrasonography and functional Magnetic Resonance Imaging (fMRI)) that ensued in recent decades, it is now possible to acquire much more complex and relevant data sets. Their visualization in 3D remains a challenging feat, though a rewarding one as well, as it can provide valuable insights that are applicable to diagnosis (*e.g.* virtual endoscopy), intervention (*e.g.* surgical planning) and medical research (*e.g.* visualizing Diffusion Tensor Imaging (DTI) data) [15].

Figure 2.15: 3D reconstruction of the heart and aorta, based on CT images [7].

3D Medical Imaging is the field that concerns itself with this issue. Despite its youth, it has revolutionized modern medicine, and continues to do so in a pace mostly set contemporary computational power. Existing pipelines allow for such fast acquisitions that 3D videos of beating hearts (one frame is visible in figure 2.15) or DTI estimated tractographies can be created. Anatomical and functional visualizations of these and other structures have greatly aided practitioners and prompted critical scientific breakthroughs, particularly in the fields of neuroscience, genetics and biomechanics [55].

2.8.2 3D Printing

In the late 1980's, additive manufacturing was first introduced to help circumvent the hazardous and time-consuming process of prototyping. It accomplished this by providing either life-sized or more frequently miniaturized replicas of the designed model.

3D Printing employs this technology, by fusing and subsequently laying down successive layers of thermoplastic materials, as per specified in the model containing file (commonly in Stereolithography (.STL) or wavefront Object (.OBJ) formats). The considerable upsurge in the availability and quality of 3D printers in the last couple of years has led to its integration in the most varied of disciplines. Prototyping circuit casings, designing prosthetics and overall product development are a few of its applications [46].

2.9 Connectomics

Though it is not the core focus of this dissertation, *Connectomics* remains a paramount concept to its understanding, as it was the central theme of the most thoroughly developed application with the created framework. Thence, we shall refrain from digressing into the depths of neuroscience, and instead present some of the key dichotomies that frame current brain connectivity analysis in both a practical and a conceptual sense [27].

Thinking of the nervous system as an intricate network of interconnected parcels is a school of thought with a vast and illustrious history in brain science, and one that has yielded an extraordinary amount of information [80]. This can be partially attributed to the technological advances in histological techniques and noninvasive neuroimaging modalities[7], which begun paving the way for the mapping of structural connections (depicted in figure 2.16), *i.e.*, those based on axonal fiber tracts, functional ones, *i.e.*, correlations between time series of distinct regions, and effective, or causal relationships. Individual alterations in these may relate to individual variations in behavioral and/or cognitive states, but should not be interpreted in isolation, as brain function is believed to arise from the topology of the network as a whole, a Connectome [9, 33].

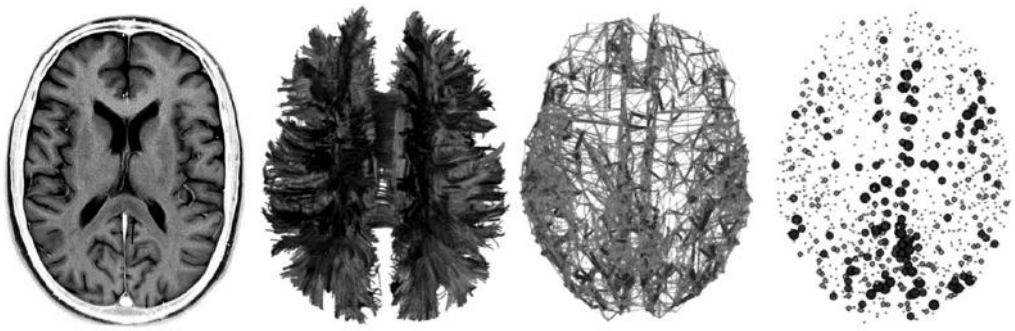

Figure 2.16: Structural analysis of brain connectivity metrics. From left to right: axial MRI slice; tractography streamlines; a network diagram of nodes and weighted graphs; representation of nodal centrality, a measure of network influence; Adapted from [80].

Prior to worrying about the intricacies of connectivity itself, the brain substrate has to be segregated into meaningful Regions Of Interest (ROIs). Among the existing segmentation atlases, those pertinent to the understanding of this thesis are presently listed:

Acronym	Name	# ROIs
AAL	Automated Anatomical Labeling	116
HOA	Harvard-Oxford Atlas (Cortical | Subcortical)	48 | 21
DKCA	Desikan Killiany Cortical Atlas	70
DCA	Destrieux Cortical Atlas	150

Table 2.1: Implemented brain parcellation atlases [14, 22, 23, 85].

[7] Such as fMRI, MRI, Positron Emission Tomography (PET) and DTI.

Chapter 3

State of the Art

3.1 Head Mounted Displays

Current VR and AR technologies tend to favor binocular stereoscopic *Head Mounted Displays* (HMDs) in detriment of their planar and monocular counterparts (*e.g.* screens or projections), primarily because the former allow for richer depth perception, which ensues from the disparity between the eyes' viewpoints when these are overlapped at the occipital lobe - *Stereopsis*. That being said, monocular depth cues such as the ones listed below remain a crucial component when conveying three-dimensionality [68]:

- **Motion Parallax** results from motion, as the name implies, and consists in the speed differences of the objects that are inside the line of sight. Closer ones seem to move faster while those that are farther away appear almost as static;
- **Curvilinear Perspective** refers to the convergence of straight lines as they extend into the distance;
- **Aerial Perspective** ensues from the refractive properties of the atmosphere, that cause distant objects to look fainter that those that are nearby;
- **Relative Scale** ensures that distant objects look smaller than their close-by cohorts;
- **Occlusion** has to do with the way closer opaque objects block our view of those that are far away;
- **Texture Gradients** conveys depth by increasing the density of repeating patterns as they move away from our eyes;
- **Lighting** helps us perceive shape, position and orientation with highlights and shadows.

3.1.1 Oculus Rift©

Modern VR/AR content development platforms like game engines, which will be addressed shortly (section 3.5), already provide the software tools to leverage a lot of the aforementioned depth cues. Nevertheless, some of them can only be achieved with a symbiotic confluence of specialized hardware and software.

An example of this, is the HMD from Oculus VR© - the *Oculus Rift*©, a Kickstarter© success story (whose chronology is portrayed in figure 3.1) that became "the" reference in VR/AR technology. Hardware specifications of its Development Kit (DK) prototypes and those of the yet to be released commercial version, can be seen in the following table:

	DK1	**DK2**	**Rift**
Screen Resolution	1200 x 800	1820 x 1080	2160 x 1200
Pixel Layout	Red-Green-Blue (RGB)	Pentile	-
Organic LED Displays	No	Yes	Yes
Screen Size	17.8 cm	14.5 cm	-
Latency	50 – 60 ms	20 – 40 ms	-
Low Persistence	No	Yes	Yes
Rotational Tracking (Inertial)	Yes	Yes	Yes
Positional Tracking (Optical)	No	Yes	Yes
Field Of View (FOV)	110°	100°	110°
Weight	380 g	440 g	-
Refresh Rate	60 Hz	90 Hz	90 Hz
Stereophonic Headphones	No	No	Yes

Table 3.1: Technical comparison between Oculus's HMD versions. Since the Rift has not been released yet, some of its specs remain unknown at this time (marked with a "-") [13].

Software-wise, Oculus provides a proprietary SDK for content creation, that can be integrated with today's most popular game engines with little to no effort on the programmer's end. This means that understanding VR-specific code is not a requirement for developers who are familiar with these environments [68].

Figure 3.1: Evolution of the HMD Oculus Rift© from 2012 to 2016. DK1 on the left, DK2 on the right and the Rift (commercial version) in the middle. Though not depicted, an external IR camera is needed in order for positional tracking to be enabled (does not apply to the DK1).

3.1.2 Project Morpheus©

Project Morpheus© is the code-name for the upcoming VR headset from Sony Computer Entertainment© (illustrated in figure 3.2). Although a specific date has not yet been announced, its release is due in 2016. Despite rivaling other VR HMDs in terms of specifications (report to table 3.2), the facts that it will only operate in conjunction with the PlayStation© 4 console and is reliant on external hardware, somewhat limits its application outside of the gaming industry, and discourages independent development [79].

	Project Morpheus
Screen Resolution	1920 x 1080
Pixel Layout	RGB
Organic LED Displays	Yes
Screen Size	14.5 cm
Latency	< 18 ms
Low Persistence	Yes
Rotational Tracking (Inertial)	Yes
Positional Tracking (Optical)	Yes
FOV	100°
Weight	-
Refresh Rate	120 Hz
Stereophonic Headphones	No

Table 3.2: Technical specs of the Project Morpheus© HMD. Again, uncharted parameters are marked with a "-" [79].

The main reason why we still felt it warranted a mention in this chapter has to do with the potential impact that comes with having a corporation as massive as Sony© enter the VR scene. It might just be the nudge this yet esoteric field has been begging for, and lead to evermore meaningful and varied contributions on its part.

Figure 3.2: Sony©'s HMD, Project Morpheus© (in the middle). Much like Oculus's DK2 and Rift models, it is not a standalone product and requires the PlayStation Eye© (on the left) and PlayStation Move© (on the right) to operate at its full capacity.

3.1.3 HTC Vive©

Yet another contestant in the race for the VR HMD monopoly, *HTC Vive*© already has a development edition for sale (visible in figure 3.3), though only available for select developers. Its release is scheduled for December 2015 and will undoubtedly bring a lot of new and more polished content to the industry [35].

	HTC Vive
Screen Resolution	2160 x 1200
Pixel Layout	-
Organic LED Displays	Yes
Screen Size	-
Latency	-
Low Persistence	-
Rotational Tracking (Inertial)	Yes
Positional Tracking (Optical)	Yes
FOV	-
Weight	-
Refresh Rate	90 Hz
Stereophonic Headphones	No

Table 3.3: Technical aspects of the HTC Vive© HMD. Once more, undisclosed specifications are indicated with a "-" [35].

An important distinction from its counterparts lies in the way the user's position is detected. Rather than embedding IR LEDs in the headset and using external IR sensors, *i.e.*, cameras to track them, the HTC Vive© uses a system that not only tracks position in an elegant manner but also maps the room. Besides what this means for AR applications, the fact that it allows for the creation of virtual representations of the physical boundaries of a room (*e.g.* walls and tables) prevents the user from bumping into them while submersed in the experience. Hence its name - the Lighthouse Chaperone. It works by attaching IR receptors to target objects (including the HMD) and using an external station with a bank of IR LEDs and two sweeping line IR lasers (one vertical and one horizontal). An initial flash of the LEDs starts a timer on the receptor's end. Then, based on the time it takes for the two out-of-phase lasers to be detected, x and y coordinates can be computed [35].

Figure 3.3: Developer edition of the HMD HTC© Vive©.

3.1.4 Gear VR©

As a direct consequence of Moore's law and the marketability of mobile devices, smartphones are becoming increasingly more so, and are in fact close to being on par with state-of-the art computers and displays. For this and other reasons, Samsung © saw it fit to invest in a smartphone-based VR/AR HMD, in a collaborative effort with Oculus Rift© that ultimately led to the conception of the *Gear VR*©.

The final consumer version is on track to being released until the end of 2015 but in the meantime, a developers version, called the Innovators edition (visible in figure 3.4), is already available for purchase. For the time being, it is shipped with a custom controller for VR/AR navigation and is compatible solely with Samsung©'s Galaxy S6/S6 Edge [72].

	Gear VR
Screen Resolution	2560 x 1440
Pixel Layout	-
Organic LED Displays	Yes
Screen Size	14.5 cm
Latency	< 20 ms
Low Persistence	-
Rotational Tracking (Inertial)	Yes
Positional Tracking (Optical)	No
FOV	96°
Weight	-
Refresh Rate	60 Hz
Stereophonic Headphones	No

Table 3.4: Technical specifications for Samsung©'s Innovator edition HMD, Gear VR©. As before, unknown specifications are marked with a "-" [73].

A paramount differentiation regarding the headsets examined thus far, are the prospects of mobility and AR development, granted by the fact that besides relying only on an already mobile device that integrates high-end cameras, the Gear VR stands as the only wireless HMD in the industry. However, being an untethered standalone device does not come without its drawbacks, as it is, for the moment, incompatible with positional tracking and confined to less demanding content. This is mainly due to having less processing capacity, which has also been known to cause some overheating issues.

Figure 3.4: Innovator edition of the Gear VR© headset.

3.2 Wearable Haptic Devices

Wearable technology encompasses any piece of clothing that is embedded with programmable electronics. These devices are usually associated with activity monitoring and as such, stand as a testament to the "Internet of Things", through which inanimate objects are able to acquire and exchange data without active human supervision.

A subcategory of this, are *Wearable Haptic Devices*, that by adding a layer of tactile and/or kinesthetic feedback to HCI-based applications are able to open new and somewhat unexplored paths of communication with their users. Seeing as the hands are the most sensitive and dexterous parts of the human body, logic dictates that the majority of these devices be gloves [45].

3.2.1 Gloveone©

The VR/AR media we have examined so far are concurring to be at the forefront of the industry, but they all seem to focus almost exclusively on the sense of sight, and to a lesser degree, on the auditory sense. NeuroDigital©'s *Gloveone*©, another brand fostered by the Kickstarter© campaign, hopes to take advantage of the opportunity and become the haptics reference in the field. Now in its latent prototyping phase, the company has already released a developers edition (see figure 3.5) that includes a SDK and some preliminary demos. Some of the hardware's disclosed features are:

- **Independent Finger Tracking** with 6 IMUs (3-axis);
- **Hand Rotational Tracking** with 1 IMU (9-axis);
- **800 mAh LiPo Battery** with 4 hours of autonomy;
- **Bluetooth 4.0** wireless low latency connection;
- **Universal Serial Bus (USB) 2.0** tethered connection with ultra low latency;
- **10 Independent LRAs** for tactile feedback;
- **4 Conductive Contact Areas** for unambiguous gesture recognition;

The glove itself does not provide positional tracking, and like so relies on auxiliary technologies like the Lighthouse Chaperone system (discussed in section 3.1.3) and other devices, specially designed to capture hand motion (these will be addressed in the upcoming section 3.4) [30].

Figure 3.5: NeuroDigital©'s tactile feedback device, the Gloveone©.

3.2.2 HandsOmni

Though not quite at the same development stage as that of the Goveone© team, a group of mechanical engineering students from Rice University is being sponsored by Virtuix© to develop a haptic glove. Not much has been disclosed about the technology behind it, except that their approach neglects traditional vibrotactile actuators (examined in detail in section 2.3.2) and instead relies on inflatable air bladders, placed at the fingertips and palm of the hand. These can expand or contract independently and on command, resulting in localized pressure variations that are perceived by the wearer as tactile feedback.

The current prototype of the *HandsOmni* glove weights close to 350 g which according to the authors, is light enough to not be noticeable by the user, even after extended utilization. Although the device is mainly intended as a VR/AR gaming peripheral, it can be easily adapted to other fields of research [38].

3.2.3 InerTouchHand

The *InerTouchHand* is an instrumented hand worn device that was developed in 2013 by a team of Portuguese researchers, at the University of Coimbra. Its working principle resembles that of the Gloveone© but instead of LRAs it utilizes ERM vibration motors coupled with minute IMUs distributed throughout the hand to not only compute its relative orientation but also convey haptic feedback [43].

The study reveals that the glove-like device was designed with VR/HCI applications in mind and presented some insightful and interesting plans for future implementations, such as gesture recognition and kinetic energy harvest, but seems to have stagnated in the meantime.

3.2.4 Mobile Music Touch

Standing as the reason to why we decided to delve into PHL in this dissertation, the *Mobile Music Touch* is a system that has been proven to allow its users to learn and reproduce simple piano passages, even when simultaneously engaging in distraction tasks [40, 48].

Basically, it consists of a fingerless glove equipped with a microcontroller unit and 5 Precision Microdrives™'s 310-101 ERMs (one on each knuckle) that communicates with a mobile computing device via Bluetooth.

As the wearer listens to each note of a melody to be learned, the vibration motor that is located at the finger he/she would have to use in order to play said note on a piano keyboard, is triggered. By doing this repeatedly and periodically (biweekly sessions nearing on 30 minutes each), able-bodied users were able to learn and retain the sequence in which the notes were played without actively devoting attention to the process [40].

Given how hand rehabilitation often involves partaking in repetitive and monotonous exercises, it should come as no surprise that this glove showed promising results in a pilot study with incomplete Spinal Chord Injury-derived tetraplegic patients [48].

3.3 Microcontroller-based Prototyping Platforms

Microcontrollers are integrated circuits that can be thought of as small computers, containing a processor core, some memory and programmable Input/Output (I/O) peripherals. *Microcontroller-based Prototyping Platforms* are development tools that conciliate versatility with affordability, by providing plug and play hardware with matching software, often in an open-source format. Because of this, they are widely used in early development stages and/or in simple embedded applications.

3.3.1 Arduino©

Arduino© is one such a platform, and arguably the most disseminated throughout the engineering and tinkering communities. The company produces easy to use prototyping boards that are able to read analog and digital inputs (*e.g.* sensor and button respectively) and produce digital outputs (*e.g.* activating an LED or a DC motor). Additionally, a high-level Integrated Development Environment (IDE) is provided in order to facilitate the process of programming the instructions that control the board's I/O pins.

	UNO Rev3	**LilyPad**
Microcontroller	ATmega328P	ATmega168V or ATmega328V
Operating Voltage	5 V	2.7 – 5.5 V
Input Voltage	7 – 12 V	2.7 – 5.5 V
# Digital I/O Pins	14	14
# PWM Digital I/O Pins	6	6
# Analog Input Pins	6	6
DC per I/O Pin	20 – 40 A	40 A
DC for 3.3 V Pin	50 A	N/A
Flash Memory RAM	32 kB	16 kB
Static RAM	2 kB	1 kB
Clock Speed	16 MHz	8 MHz
Size	68.6 x 53.4 mm	50 x 50 mm

Table 3.5: Technical specs of the UNO Rev3 and LilyPad prototyping boards [2, 3].

Among their range of available boards lies the Arduino UNO Rev3, which stands as the most used and documented of the Arduino© family. Also worth mentioning is the LilyPad board, seeing as it was designed to be sewn to fabric in wearable and e-textile applications. Table 3.5 and figure 3.6 offer more details about these devices [2, 3].

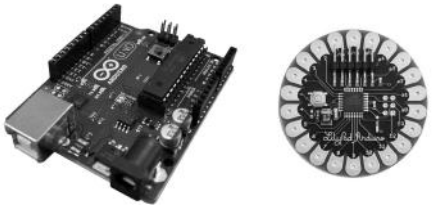

Figure 3.6: Arduino©'s UNO Rev3 (on the left) and LilyPad (on the right) boards [2, 3].

3.3.2 Bitalino©

Yet another do-it-yourself development platform that bridges the analog and digital worlds - Physical Computing - is Plux©'s *Bitalino©*, a low-cost toolkit that specializes in electrophysiological acquisitions. An implication of this is that it needs to implement stricter measures when it comes to maximizing SNR and specifying sampling rates. Bitalino© does so and more, by complementing its hardware (shown in figure 3.7) with OpenSignals, a cross-platform software that allows for data recording, visualization and analysis, thus making these biosignals readily available for research [60].

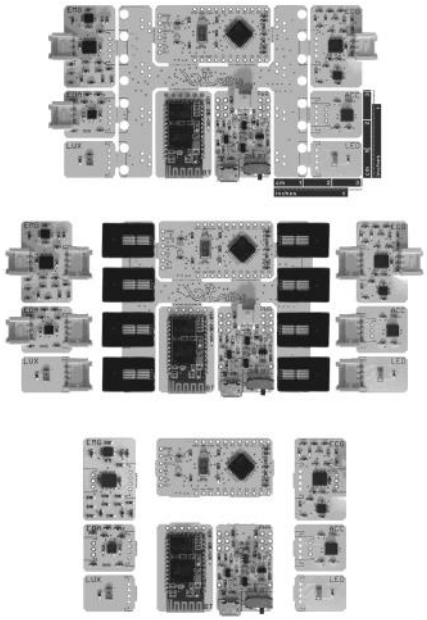

Figure 3.7: Bitalino©'s hardware modalities: standard credit-sized board on top, plugged version in the middle and freestyle kit in the bottom [60].

Regardless of the chosen modality, the device includes the following features:

- **Control Block** based on the ATmega328P microcontroller, with a sampling rate that is configurable to 1, 10, 100 or 1000 Hz;
- **6 Analog Ports** from which 4 are 10-bit inputs and 2 are 6-bit inputs;
- **8 Digital Ports**, 4 inputs and 4 outputs, all 1-bit;
- **5 Sensors** that include 3 electrophysyiological (ECG, EMG and EDA) and 2 environmental ones (ACC and LUX);
- **1 Actuator**, an LED;
- **Wireless Communication** with a class II Bluetooth v2.0 module (approximate range of 10 m);
- **Power Block** associated with a 3.7 V LiPo battery.

3.4 Hand Tracking Devices

Being able to interface with visual display systems in real-time and at a distance using nothing but one's hand motion and gestures offers many advantages over traditional interaction schemes, particularly in scenarios where either immersion or sterilization are at stake. Consequently, *Hand Tracking Devices* that can do this in a seamless and touch-free manner are becoming increasingly popular, not only in the VR/AR industry but also in fields that value contamination avoidance (*e.g.* medicine) [57, 71].

3.4.1 Leap Motion©

The *Leap Motion*© controller is essentially a markerless optical tracking device, that uses range imaging (discussed in section 2.6.5) to track hand motion, as well as that of tools.

From a hardware perspective, the device's core can be summed up as two monochromatic IR cameras and three IR LEDs. The latter emit pattern-less flashes of light intermittently while the former generate over 300 Frames Per Second (FPS) of reflected imagery data referring to an interaction volume of roughly 250 cm^3 (shown in figure 3.8). The boundaries of its stereoscopic FOV are ultimately limited by IR light propagation, which in turn is intertwined with the current driving the LEDs and thus constrained by the maximum current that be drawn over the USB 2.0 connection [56].

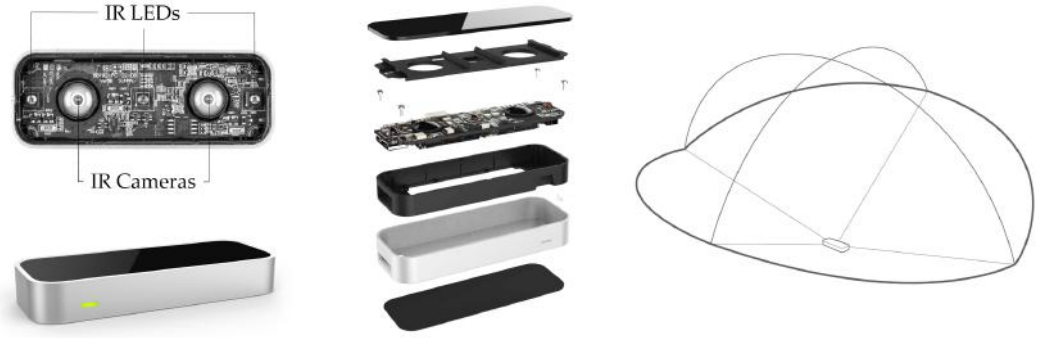

Figure 3.8: Exploded representation of a Leap Motion© controller and its interaction area (results from the intersection of the binocular cameras' FOVs). Adapted from [56]

After being streamed to Leap Motion©'s proprietary tracking software, the 2D sensor data from each camera takes the form of a low resolution grayscale image of the near-IR light spectrum. Ideally, the only visible objects in these images would be those being directly illuminated by the controller's LEDs but other IR sources (*e.g.* sunlight and incandescent bulbs) can light up the scene and thereby compromise tracking fidelity. To compensate for this, the software filters out background objects such as heads and highly reflective surfaces and uses the remaining raw data to identify and extract features of the hands, fingers and tools. 3D representations of these can then be synthesized, even when occluded, in which case position is inferred from temporal and physical coherence [56].

3.4.2 Nimble Sense©

Similarly to Leap Motion©, Nimble VR© has built a compact depth sensing camera (portrayed in figure 3.9) that can be used as a natural input controller in HCI applications and easily mounted onto an HMD. Unlike the Leap, *Nimble Sense*© utilizes only one IR camera associated with an IR laser and employs the TOF method (report to equation 2.3) to capture dense 3D point clouds every 20 ms. Computer-vision algorithms can subsequently process these in order to not only accurately bring the user's hands into VR/AR without any markers, gloves or other external parts, but also build 3D models for pretty much any physical object that the device can "see" [88].

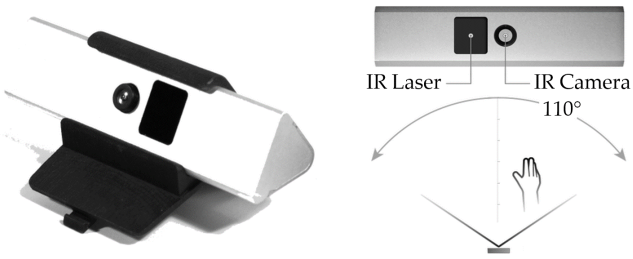

Figure 3.9: Pictorial representation of the Nimble Sense© in its VR mount (on the left) and a schematic of its FOV (on the right). Adaptation form [88]

The fact that Nimble VR© was procured by Oculus before its Kickstarter© campaign was through certainly attests to the technology's appraisal, and might hint towards a future where headsets with integrated skeletal hand tracking are a reality. Be that as it may, ever since the two companies merged, not much was disclosed about the current status of the project.

3.4.3 Myo©

Thalmic Lab™'s *Myo*© armband (see figure 3.10) is a very unique hand tracking device, in the sense that unlike the previously debated technologies, it does not use optics to capture motion but rather deduces it from IMU (9-axis) readings and EMG tracings. These can be used to accurately detect translations and rotations of the hand and forearm, as well as up to 5 gestures. Moreover, it can produce both visual and haptic cues to create affordances for its user, further adding to its potential in motor rehabilitation applications [83].

Figure 3.10: Myo© expandable armband [83].

3.5 Game Engines

As we have contemplated in section 2.7, *Game Engines* are packed with native graphics representation and physics simulation capabilities that make them powerful development platforms. For this reason, they are becoming progressively more popular within the scientific community, a trend that is further catalyzed by the ease-of- both -access and -use that often characterize them.

3.5.1 Unity3D©

Conceivably the most popular of its kind, *Unity3D*© is a flexible and robust development tool that provides out-of-the-box functionality and allows for straightforward integration with external media (using the package system). Despite obviously leaning towards game design, its simulation and visualization capabilities for creating high-end crossplatform interactive content have justified its use in countless other industries, such as architecture, medicine and the military.

Unity Technologies© offers individuals and companies a Personal Edition with no fees, provided that their gross annual revenue stays below 100 000 US $. Alternatively, Unity Pro and all the premium features it includes can be acquired in either a 75 US $ monthly subscription format or in a permanent one-time purchase one, costing 1 500 US $ [81]. Both these editions are shipped with a customized version of MonoDevelop ©, an open-source IDE that supports JavaScript, C# and Boo (Python-inspired language).

In terms of actual application development, Unity3D© projects deploy event-driven scripted programming and structure their assets in accordance with the game object hierarchy and the component model (schematized in figure 3.11). This setup allows for a high-level creation of programs featuring encapsulation, inheritance, polymorphism, modularization and other aspects that define object-oriented programming [93].

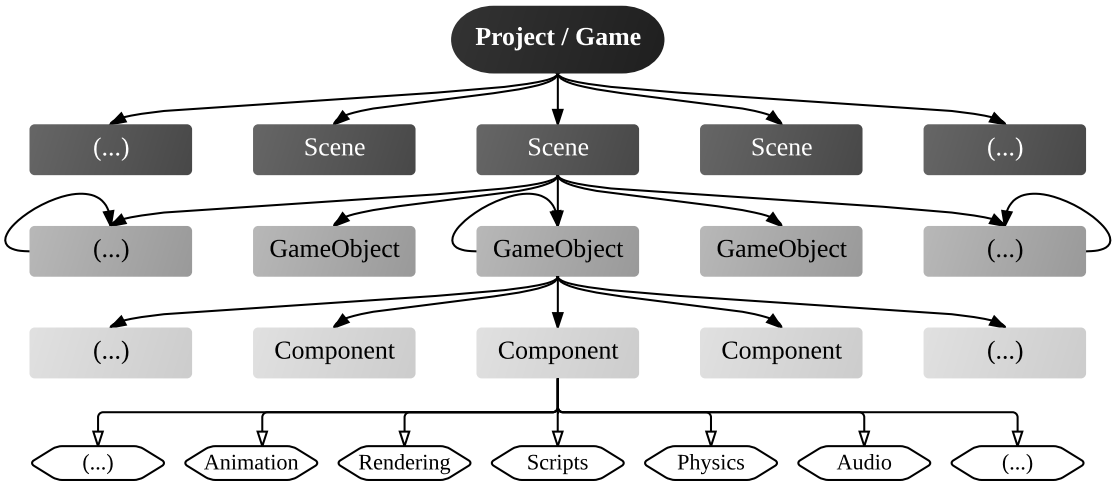

Figure 3.11: Structure of a typical Unity3D© project. As per indicated by self-feeding arrows, the game object hierarchy system allows for object parenting. Inspired by [93].

3.5.2 Unreal Engine©

Made by game developers and for game developers, Epic Games©'s *Unreal Engine*© is a multiplatform development suite that some argue outshines Unity3D© when it comes to end results. Nevertheless, general opinion claims that it is not as friendly in terms of available documentation and learning curves.

A paramount distinction from other game engines lies in it being completely open-source. The fact that any developer who adopts the system immediately has access to its complete C++ source code greatly increases the power of customization, optimization and debugging, specially for experienced programmers.

On the other hand, this coupled with an equally distinctive nomenclature and overall workflow might be intimidating for novice users and therefore make getting started or transitioning from other game development platforms slightly more perilous than one would expect. Unreal's blueprint-based visual scripting mechanic (represented in figure 3.12) somewhat atones for this by hastening prototyping and general testing.

Where pricing and distribution are concerned, no fees are enforced until a revenue of atleast 3 000 US $ per quarter is achieved. From that point on, a royalty of 5 % is due (not applicable to film, contracting and consulting projects).

Not unlike Unity, Unreal has built-in VR/AR support that is compatible with the flagship HMDs in the industry, meaning that adapting an existing project to virtual reality takes only a "couple of clicks" and requires no coding additions or alterations [28].

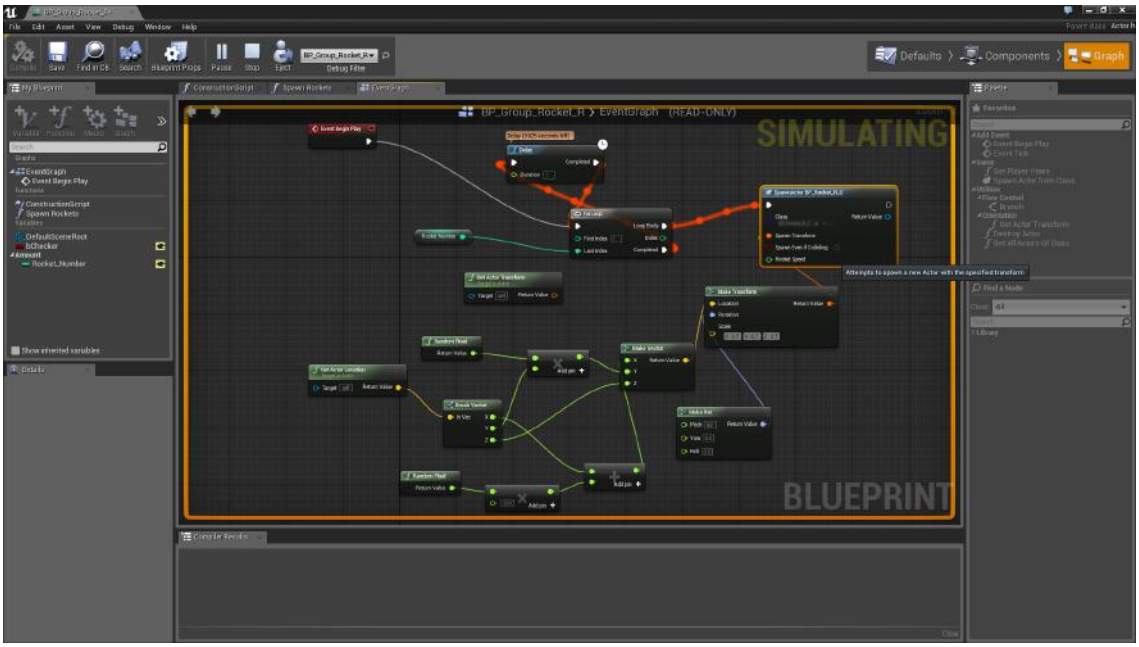

Figure 3.12: Diagram illustrating Unreal Engine©'s editor as well as its visual scripting functionality (blueprint mechanic).

3.6 Connectome Visualization Tools

In section 2.9 we introduced the topic of brain connectomics and recognized how its emergence could not be dissociated from technological advances in non-invasive neuroimaging modalities like fMRI and DTI.

Traditionally, connectivity data is represented mathematically in its 2D matrix form. Depending on whether matrices are binary or weighted, they describe how each region of the brain, *i.e.* node, relates to the remainder by attributing each row-column intersection a "1", a "0" or an arbitrarily defined connection strength. The common practice in most of the contemporary research in the field is to extract either global or regional statistical parameters from these matrices and use them when surmising conclusions [20]. Here we will present a collection of recent efforts that aim towards making 3D visualization of these highly sophisticated structural and functional maps as rewarding as possible.

3.6.1 BRAINtrinsic

BRAINtrinsic is a VR compatible web-based 3D analysis tool that approaches connectome data in a visual and interactive manner. Furthermore, it introduces the concept of Intrinsic Geometry, defined by G. Conte *et al.* as being "the topological space as informed by brain connectivity, via dimensionality reduction." In other words, each node's position relative to its cohorts is dictated not by its anatomical location but rather by its role and influence in the overall connectivity network. In the authors' scope, visualizing and analyzing such relations in this intrinsic dimension could prove vital when screening longitudinal changes in individual brains and administrating precision medicine.

Broadly speaking, the more complex and dense a given network is, the more its visualization is susceptible to visual clutter. However, the heterogeneity in the distribution of its interconnections means that different points of view will reveal regions with varying levels of occlusion and cluttering. With this mindset, it follows as natural that molding a static visualization tool into an interactive and immersive one would aid the user in discerning what is being displayed (a frame of this can be seen in figure 3.13) [20].

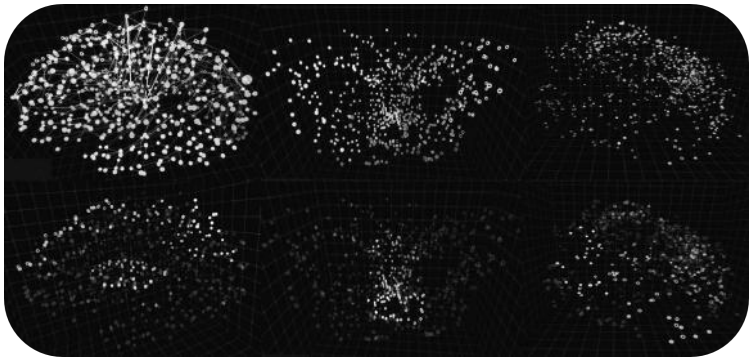

Figure 3.13: BRAINtrinsic's UI showcasing the intrinsic geometries of DTI-derived structural and the resting-state fMRI connectomes (middle and right column, respectively) as well as their reference in neuroanatomical space (left column). Adapted from [20].

3.6.2 BRAINX^3

Meant as a large-scale VR simulation environment for contemplating brain activity and analyzing complex dynamic networks with real-time interaction, *BRAINX*^{3} (phonetically intended as "brain cubed") denotes a remarkable symbiosis of computational power and human intuition (an illustration of the simulation chamber is shown in figure 3.14).

By disturbing the human connectome with localized and transient stimuli, the user can (among other things) [4]:

- Observe their reverberations across the brain's network;
- Simulate lesion dynamics and scrutinize their repercussions;
- Implement network analysis functions from a library of graph theory metrics;

This novel and immersive approach can thus be used for exploring the dynamics of activity patterns in connectivity networks, both for resting- and task-related state datasets, for unveiling the signaling pathways that characterize brain function and dysfunction and for surgical planning [4].

Figure 3.14: Depiction of the BRAINX^3 visualizer. The 3D connectome and its overlaying simulations are projected onto the central screen. The one the the right displays regional information referring to the selected areas while the left screen shows 2D axial slices of the brain and highlights regions of activity. Adapted from [4].

In addition, seeing as the brain and body are not only intricately coupled but also mutually constrictive, BRAINX^3's researchers are planning on embodying robots with their synthesized virtual brains to quote, "better understand the physical foundations of consciousness" [87].

Chapter 4

Methods & Materials

4.1 Development Environment

In order to assemble a framework that would accommodate the creation of applications featuring aspects of VR/AR, motion tracking, haptic feedback and electrophysiology, several choices had to be made. The most pressing of which had to do with electing an appropriate development platform that was amenable to be integrated with the listed media. For this and the reasons presented in the preceding chapters, game engines stood as the logical and most viable candidates for the role.

Following a brief evaluation of the available systems within the category and pondering both the resources and the expertise of the team members at *Instituto de Biofísica e Engenharia Biomédica* (IBEB) in the equation, Unity3D© and by extension MonoDevelop©, were selected.

Throughout the course of this thesis and ensuing from the uncannily organic growth of the gaming industry, the software's version was upgraded manifold (each time requiring minor adjustments), as per reported by table 4.1.

Version	Date
5.0.1	1 April, 2015
5.0.2	13 May, 2015
5.0.3	9 June, 2015
5.1.0	9 June, 2015
5.1.1	18 June, 2015
5.0.4	6 July, 2015
5.1.2	16 July, 2015
5.1.3	24 August, 2015
5.2.0	8 September, 2015

Table 4.1: Utilized versions of Unity3D© in chronological order.

So as to better understand some of the terms and references we will be making from this point onward, a brief discussion regarding the layout of Unity3D©'s editor and some of the terminology that accompanies it is due. This issue is thoroughly dealt with below.

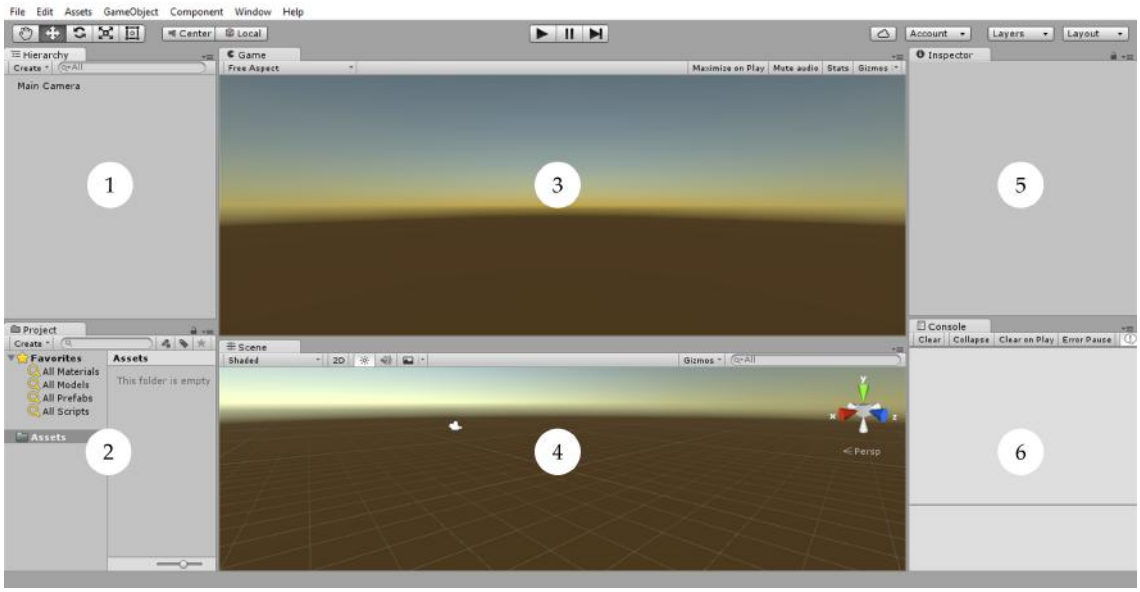

Figure 4.1: Capture of a customized layout of Unity's editor. The position of each of its constituents is highly configurable. Alternatively, one of multiple presets can be selected.

1 → the Hierarchy contains every game object in the current scene. Selecting and dragging game objects onto and out of each other is how one handles parenting;
2 → Project Browser where the assets (scripts, materials, plugins, *etc.*) that are included in the current project can be accessed and managed. It is through this tab that one can go about importing and exporting either standard or customized packages[1];
3 → the Game View is a rendered perspective of the main camera[2]'s FOV;
4 → the Scene view is an interactive "sandbox" in which the user can select and position the environments, cameras, models and all other game objects in the current hierarchy;
5 → as section 3.5.1 showed us, a typical Unity scene is made up of multiple game objects, which in turn contain components such as meshes, scripts, sounds and/or other graphical elements like lights. By displaying detailed information about the currently selected game object, all its components and their corresponding properties, the Inspector allows for a high-level comprehension and modification of their functionality;
6 → Console Window where Unity-generated messages such as errors and warnings are displayed. In addition, custom messages can be printed for debugging and/or other purposes if scripted to do so;

[1] Packages are essentially collections of assets (scripts, materials, plugins, *etc.*) that can be imported into and exported out of a Unity project at any given time.

[2] Even though having more than one camera is customary in most games, for the purpose of this thesis we shall restrain ourselves to one, the main camera.

4.2 Head Mounted Display

Given its pioneer stature in the VR/AR scenario, Oculus Rift©'s HMDs and their corresponding SDKs stand as the most well documented and therefore agreeable with integration into development suites such as Unity3D©.

As a result of availability, the DK1 headset was used in this dissertation up until the collaboration with the Luso-Illyrian Institute for Human Development (iLIDH) regarding the Museum of Universal Values (MUV) project commenced in mid April, 2015. From that point on the DK2, a 350.00 $ piece of hardware, was gratuitously and generously lent to our cause. Thereafter, it was used in any and all subsequent VR/AR-related work.

Regarding software overhauls, the VR/AR scene is on par with the gaming one. Facetiously speaking, it is often said that one cannot sleep if he/she hopes to keep up with them. In the meantime since this project started, Oculus has released numerous versions of its SDK, runtime and Unity integration package. Nevertheless, the release of Unity 5.1.0 with its integrated VR support has deemed the discontinuance of the latter.

In light of this, the process of creating Unity projects that are compatible with the DK2 has been immensely simplified and can now be achieved with a few elementary steps (illustrated in figure 4.2):

(i) Downloading and installing Unity3D©'s latest version;

(ii) Downloading and installing the latest runtime from Oculus Rift©;

(iii) Starting a new Unity project;

(iv) Ticking "Virtual Reality Supported" under Edit, Project Settings, Player.

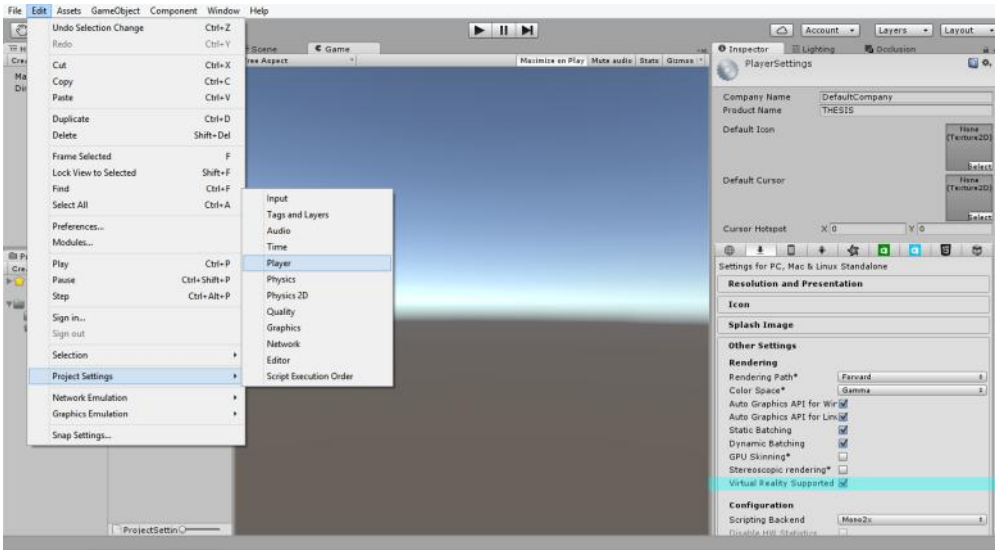

Figure 4.2: Screenshot of the UI of Unity3D©'s editor showcasing just how straightforward the process of creating and adapting content for virtual reality display has become. The checkbox highlighted in cyan in the inspector is the one that controls VR support.

4.3 Interaction Controller

One of the aboriginal realizations that dawn on first-time users of VR interfaces (AR's nature makes it less susceptible to this) has to do with the loss of spatial awareness regarding the means of input with which they are accustomed - keyboard and mouse.

To circumvent this issue, our initial approach was to use a console controller (*e.g.* the PlayStation 4 controller) to interact with the program. Although it performed far better than the alternative, which at that point consisted in frantically trying to find the mouse and/or a reference key, we felt it detracted from the sense of immersion we were aiming for. Besides, barring resorting to one-handed controllers, conflicts with the envisioned wearable device were bound to arise once we reached that stage in development.

Hand tracking devices on the other hand, posed no such problems, and added a layer of motion capture to the system that could prove invaluable in rehabilitation applications. Postliminary to mulling over criteria analogous to that that led to the choice of Unity3D© as our development environment and Oculus Rift©'s DK2 as our HMD, the Leap Motion© controller, a 89.99 € device, was chosen as our primary source of input.

Short of installing its runtime[3] and importing the Leap Motion© core assets package onto a Unity project, no further steps are needed to start developing. One needs only drag the "HandController" prefab[4] onto the scene's main camera, offset and scale it to where the user's hands would be and hit play. To actually use the tracking data as a source of input instead of just visualizing it though, requires a deeper understanding of this and some of the additional C# classes that are defined in the package's scripts:

- **HandController** serves as the anchor point for the drawing of hands in the current scene and its properties define where and how these are drawn (*e.g.*, "Is Head Mounted" is a boolean property that informs the program of the controller's placement and orientation in the physical world);
- **HandModel** is the base class that interfaces between the "HandController" game object and the concrete objects containing both the graphics and physics of a hand[5]. It implements most of the public methods that allow the program to retrieve the tracking data for the hand in question;
- **FingerModel** is similar to the previously listed class, but instead refers to a finger along with its respective game object and tracking information;
- **ToolModel** is a simpler variation of the classes itemized above, as having no internal articulations means only its global position and orientation need tracking.

[3] Leap Motion©'s software runs as a service, or daemon, on the host computer, which analyses images produced by the hardware and sends tracking information to applications.

[4] A prefab is an asset type within Unity that allows the storage of a game object alongside their components and properties. It acts as a template from which new instances can be created.

[5] Graphics hands are rigged meshes that cover the physics hands, which consist of compound colliders.

4.4 VR/AR Mount

Having established the primary development coalition that would allow us to start creating VR/AR content featuring hand/tool motion tracking, all that was needed to start experimenting was a physical mount that would hold the Leap Motion© controller in place at the front of the VR headset (see figure 4.3).

Figure 4.3: Ideal configuration for mounting the Leap Motion onto a HMD [57].

For this very purpose, Leap Motion© has an official VR Developer Mount that is compatible with Oculus's HMDs and can either be bought[6] or printed, since its .STL files have been made available for free[7]. Unaware of this and apprehensive about shipping times, we had to resort to a custom-made unofficial surrogate. At least that is how it started, seeing as even after the DK2 had been procured, we refrained from purchasing the official alternative. The realization of how simple, affordable and quite frankly rewarding it was to tailor our own personalized model and then see it come to fruition, drove us into sticking with and improving upon our designs. Ensuring that their cavities and flaps pondered the dimensions of both the Leap Motion controller and the Oculus's headsets meant that 3D representations of the devices had to be created beforehand.

To meet all our modeling needs, we resorted to Autodesk©'s Maya, a tool that offers a comprehensive creative feature set for 3D computer animation, modeling, simulation, rendering and compositing on a highly extensible production platform. Despite being distributed as a pay-to-use software with 200 € monthly subscriptions or 1 600 € yearly ones, three-year-long free of charge licenses are available for educators and students.

When it came to printing the models, we used an Ultimaker© Original printer with polylactic acid for feedstock material. In spite of having registered the actual settings (*e.g.* temperature, density, layer thickness, and speed) for each printing session, these were regrettably lost prior to the writing of this thesis.

Purely for the sake of aesthetics, each printout was painted using black acrylic paint.

[6] Retails for 14.99 € (plus shipping costs).
[7] 3D printing is not without its associated costs.

4.5 Glove Design

Once the concerns addressed in the previous sections had been dealt with to a satisfactory degree, the time had come to move onto designing and manufacturing the actual wearable device apace with its underlying haptics and electrophysiology components.

4.5.1 Textiles

Originally, we had envisioned an e-textile design (shown in figure 4.4) that would use conductive thread for wiring and have its remaining electronics encapsulated in the glove's fabric. To do so, we started by consulting with the designers Inês Braga[8], João Melo Costa and Rachel Freire[9], from whom we received encouraging replies. However, the overall confection process soon proved incompatible with both the time-frame and budget of this dissertation.

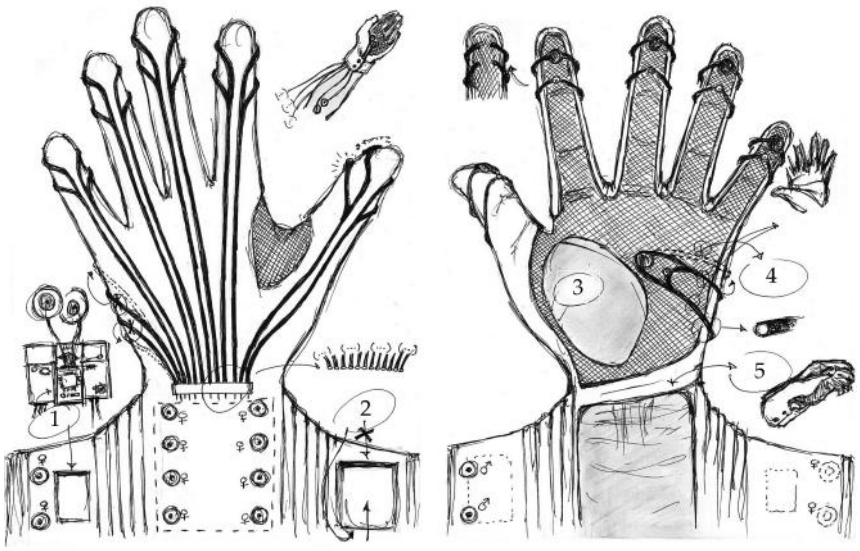

(a) Dorsal view. (b) Palmar view.

Figure 4.4: Early sketches showcasing the design intended for the wearable device. The thick black lines indicate where the wires would pass whereas the flat open surface on the base of the wrist's topside (on the left) pinpoints the placement site for the haptic module. Male (♂) and Female (♀) symbols illustrate where their corresponding snap connectors would be sewn. Tactors and their signaling LEDs were respectively drawn as big and smaller circles at the fingertips and palm of the hand (visible on the palmar view).

1 → pouch that would hold the glove's electrophysiology module;
2 → pouch that would hold the glove's battery;
3 → orifice that would allow for a direct measurement of EDA using skin electrodes;
4 → flexible fabric covering the palmar portion of the glove;
5 → rigid fabric that would support the glove's electronics and cables;

[8] Founder of the Kitess© brand.
[9] Textile pattern cutter for the Mi.Mu© glove project.

Seeing as time was of the essence, we postponed our initial plans and started working on a simpler design that used thermal tennis gloves[10] (depicted in figure 4.5) as its basis. To facilitate the acquisition of EDA signals with standard skin electrodes, a hemmed hole was cut in the palm of the left glove, which would ultimately become our final prototype. As for its right counterpart, it was kept in its original condition and used as an intermediary prototype with which most of the preliminary tests were conducted.

Figure 4.5: Different perspectives of the thermal gloves from Artengo©'s tennis collection.

Lastly, to compensate for the encountered setbacks and mitigate their repercussions in terms of amount of electronics left in sight, a pattern (visible in figure 4.6) was cut out of lycra to serve the dual purpose of holding the device's main circuit modules and covering each tactor unit[11] that was to be placed at the fingertips and palm of the glove.

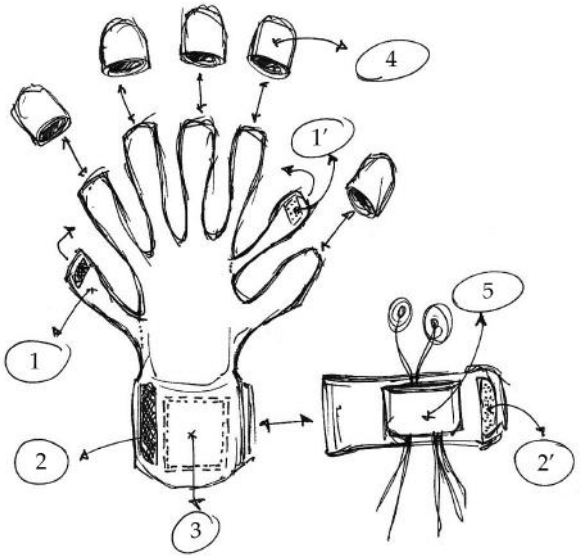

Figure 4.6: Sketch portraying the pattern design for the glove's cover.

1 – 1′ → straps that once connected (through velcro bands) conceal the palm's tactor unit;
2 – 2′ → velcro terminals that once tightened ensure that the cover stays in place;
3 → flat surface where the device's haptic module is to be attached;
4 → finger caps that hide the fingertips' tactor units (5 in total);
5 → pouch that will hold the glove's electrophysiology module;

[10] Purchased for 9.95 €.
[11] Comprised of an ERM vibration motor and its respective signaling LED.

4.5.2 Haptic Feedback Module

The core functionality of the developed glove is its ability to convey tactile feedback to its wearer while he/she is immersed in a VR/AR experience. Accomplishing this encompassed tackling many an issue, not the least of which was selecting the appropriate components for the job.

4.5.2.1 Control Unit

First and foremost, we had to define how to dynamically control the haptic module, *i.e.*, how and when to trigger tactile feedback on the appropriate tactor unit. As section 3.3.1 showed us, the microcontroller-based prototyping boards from the Arduino© platform are ideal for this sort of applications.

Had we gone through with the initial e-textile design and the LilyPad would likely have been the board to use. Barring that possibility, there was no reason not to go with the cheaper, easier to deploy and more familiar UNO Rev3 alternative. Using its Pulse Width Modulation (PWM) pins[12] as outputs enabled us to fabricate different vibration intensities simply by varying the duty cycle of the generated signal.

Most of the hardware verification tests as well as some elementary attempts at making PHL applications were directed with resort to simple sketches[13] made with Arduino©'s official IDE. The following listing is an example of one such a sketch, that once uploaded to a board, sets pin 3 as an output and subsequently activates it intermittently with a frequency of 0.5 Hz (even though pin 3 is a PWM one, it is not being used in that capacity).

```
1  void setup() {                    // pin configuration code, runs once
2      pinMode(3, OUTPUT);
3  }
4  void loop() {                     // main program, runs repeatedly
5      digitalWrite(3, HIGH);
6      delay(2000/2);
7      digitalWrite(3, LOW);
8      delay(2000/2);
9  }
```

To actually enable the constructed haptic module to be responsive to the wearer's actions inside a VR/AR application, the two parties (*i.e.* glove and user) have to be exchanging information constantly. The link between them is indirectly entrenched in Unity3D©. The user informs Unity of his/her movements through the Leap Motion© controller and the DK2 HMD. This data is processed internally and then streamed to the UNO Rev3 board (programmed with the "Standard Firmata" sketch), using a communication protocol that is established by the Uniduino©[14] plugin.

[12] The fact that the UNO Rev3 board only has 6 PWM I/O pins was one of the reasons that led us to settle for 6 tactor units.

[13] A sketch is the unit of code that is uploaded to and ran on an Arduino© board.

[14] Published by Edwon©, available at Unity's asset store for 32.96 €.

4.5.2.2 Tactor Units

As we have examined in section 2.3.2, tactile feedback can be produced with a variety of different vibration actuators. Despite having initially leaned towards LRAs for their superior haptic response, the fact that they are also less affordable and demand more complex driving circuitry eventually led to the choice of Precision Microdrives™'s 310-118 ERM model (look to appendix C for its datasheet) as our primary source of actuation (report to table 4.2 for further details).

To assemble that which would become our version of a tactor unit, a 3 mm blue signaling LED was soldered in conjunction with an ERM motor onto a custom-cut prototyping stripboard, measuring roughly 2 x 1 cm (an example is displayed in figure 4.7). This configuration greatly simplified the process of placing each of these units in its rightful place, as having a planar surface meant there was a larger area of contact between the unit, the glove's fabric and the intermediary ethyl cyanoacrylate adhesive[15].

Category	Characteristics	ID	Quantity	Unitary Price
Vibration Motor	ERM	310-118	6	5.83 €
LED	100 mcd	PTR002901	6	0.20 €
		TOTAL	12	36.18 €

Table 4.2: Specifications of the components used to make the final tactor units.

Taking into account that the ERMs from Precision Microdrives™ were by far the most expensive components of the entire glove, these were spared from experimental tests and early prototyping endeavors. In their stead, ERM vibration motors that had been scavenged from malfunctioning or damaged mobile phones were used.

Figure 4.7: Devised tactor entity. The final prototype (beta) holds 6 of these units (placed at the tips of the thumb, fingers and palm), while the early one (alpha) has but 5.

For this and any preceding or succeeding soldering necessities, we used standard lead-free solder and one of Parkside©'s iron sets.

[15] More broadly known as "super glue".

4.5.2.3 Driving Circuit

When it comes to the circuitry that is required to drive vibration motors such as those that compose the formerly described tactor units, there are several integrated circuits[16] that can perform the task. Nonetheless, if the application design already features a power supply with an appropriate voltage as well as high impedance signal sources (*e.g.* the output pins of a microcontroller) it is often cheaper to resort to discrete components.

With this in mind, the directives for driving vibration motors provided in Precision Microdrives™'s bulletin were used as guidelines when dimensioning the circuit [50]. The components used in the process are listed in the table below.

Category	Characteristics	ID	Quantity	Unitary Price
Transistor	BJT-NPN	P2N2222A	6	0.20 €
Resistor	75 kΩ	PTR003699	6	0.16 €
Capacitor	100 nF	PTR000513	6	0.18 €
Diode	Schottky	NRVB120ESF	6	0.12 €
		TOTAL	24	3.96 €

Table 4.3: Specifications of the parts that where used in the making of the driving circuit.

These were then used to implement 6 instances of the circuit schematized in figure 4.8 (one for each tactor unit). For the pilot prototype (alpha), this was done in a standard breadboard, whereas for the final one (beta), the parts were soldered onto a custom-made shield[17] for the UNO Rev3 board (thoroughly examined in the upcoming chapter) in order to minimize the total volume occupied by the haptic module.

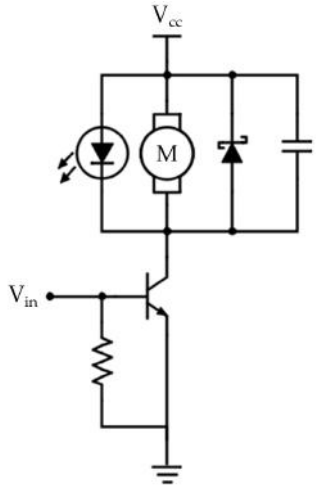

Figure 4.8: Schematic showing the circuit configuration used to drive each of the tactor units (which are also visible). Based on the diagrams suggested in [50].

[16] Texas Instruments™'s DRV2605 chip was initially considered, but eventually discarded as it was only shipped in packages compliant with Printed Circuit Board (PCB) mounting.

[17] Modular circuit boards that "piggyback" atop an Arduino board to instill it with extra functionality.

4.5.3 Electrophysiology Module

Though not quite as crucial to the glove's operation as its haptic cohort, this physical computing module added a lot of flexibility to the potential HCI interfaces that could be developed with the final framework.

Incipient conundrums relating to which biosignals to focus on, how to acquire and afterwards transmit them to Unity, culminated in us opting for Bitalino© as our electrophysiology toolkit. Namely its freestyle kit, that we molded and soldered into a compact module featuring the parts presently tabled, all of which generously lent by Plux©.

Category	Characteristics	ID	Quantity	Unitary Price
Sensor	ECG	SENSECG1	1	27.50 €
Sensor	EMG	SENSEMG1	1	27.50 €
Sensor	EDA	SENSEDA1	1	22.50 €
Component	PWR	COMPPOW1	1	12.50 €
Component	MCU	COMPMCU1	1	15.00 €
Component	Bluetooth 2.0	COMPBLU1	1	20.00 €
Battery	LiPo 3.7 V, 500 mA h	BAT500M1	1	7.50 €
Electrode	Pre-gelled, self-adhesive	ELECTR001	8	12.50 €
Cable	Lead accessory	ELCTRDCAB	8	10.00 €
		TOTAL	23	310.50 €

Table 4.4: Specifications of the parts that where used in the assembly of the glove's electrophysiology module. It is important to note that the prices listed are unitary and that the actual freestyle kit (which includes some additional parts) is quoted at 159 €.

Readings from the OpenSignals software served as ground truth for comparison with those collected in Unity via the BITalino-Unity3D API[18]. Not only does this open-source package deal with the communication between the module's Bluetooth block and Unity but it also takes each sensor's transfer function (appendix C) into account, thus converting the dimensionless sampled values into physically meaningful and properly scaled ones.

Conducive to a dynamic extraction of events and other relevant features (*e.g.* heart beats, muscle contractions and SCRs) from each channel, its respective buffered data is treated in real-time using a C# signal processing library that we developed for the effect. This Unity toolkit is mostly composed by generic albeit adjustable time-domain filters:

- **Bandpass** filters with signal-specific lowpass- and highpass-cutoff frequencies;
- **Rectification** filters that can either be set to half- or full-length;
- **Smoothing** filters with malleable window-sizes that can be moving average- or root mean square-based.

[18] Developed by Adrien Verhulst and Paulin Doux from the University of Angers and Tokyo University of Science, respectively.

In the interim of implementing and perfecting the preceding filters, we generated artificial EDA, ECG, and EMG signals (figure 4.9). This allowed us to both discriminate which of the available filters to apply to each of the examined biosignals and to later experiment and calibrate these in order to facilitate event detection and feature assessment.

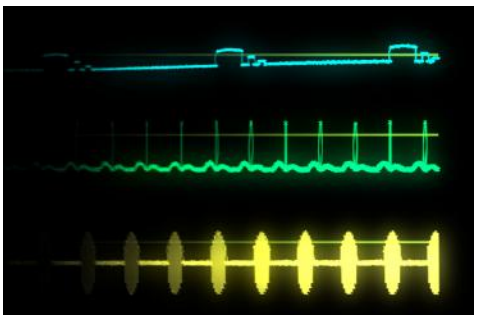

Figure 4.9: Stand-in signals that were fabricated to aid in the calibration of the implemented filters. From top to bottom: EDA (cyan), ECG (green) and EMG (yellow). For each of these, an event-related threshold that is calculated dynamically can be seen (olive).

The results of this channel-specific fine-tuning and its confluence with our literature revision are summarized in table 4.5 and better appreciated by analyzing figure 4.10.

	EDA	**ECG**	**EMG**
High-pass Cutoff Frequency	0 Hz	0.5 Hz	20 Hz
Low-pass Cutoff Frequency	3 Hz	25 Hz	300 Hz
Rectification Type	None	Half-Length	Full-Length
Moving Average Window Size	10	10	50
Mean Square Root Window Size	10	10	50

Table 4.5: Channel-specific filter configuration that was used in any and all interfaces that featured our electrophysiology module. *N.B.*, these are mere recommendations reflecting what resulted best for our applications and as such, ought to be adjusted if required.

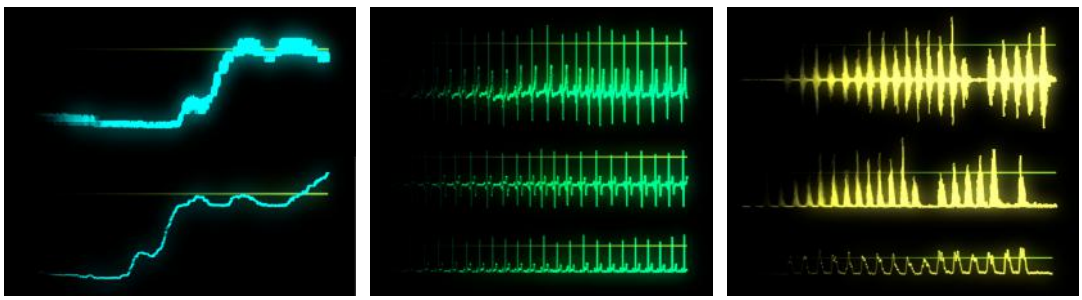

(a) EDA. (b) ECG. (c) EMG.

Figure 4.10: Plots showcasing the outcome of applying the implemented filters as per specified in table 4.5. In each channel's tracings, the raw data (at the top) and the end result (at the bottom) are displayed. Additionally, intermediary stages of filtering illustrating the effects of a bandpass filter and a full-length rectification can be seen for the ECG and the EMG signals, respectively. All captures pertain to buffers with 20 000 points.

4.6 Connectomics Data

Here, we will expose the processes of genesis, pre- and post-processing of the data that was used in the making of Brain Connectivity Leap (BCL) (thoroughly presented in the chapters ahead), prior to its visualization in this 3D interactive environment.

4.6.1 MRI Reconstructions

The first step towards doing so was reconstructing T1-weighted MR images [19] into accurately segmented meshes, one for each of the implemented parcellation atlases (report to table 2.1). Said volumes were converted from Digital Imaging and COmmunication in Medicine (.DICOM) to the Neuroimaging Informatics Technology Initiative (.NIFTI) format and then imported onto FreeSurfer©. This open-source processing suite is where the actual brain meshes were first generated, split into independent parcels and therein outputted as .OBJ files, in a process that took approximately 12 hours per atlas [67].

Considering that the resulting 3D brain models had exceedingly high poly-counts (nearing on 2 M), Autodesk©'s Maya was used as a mediator optimization tool (look to figure 4.11 for an example). After filtering out lamina faces[20], matching polygons and other inefficient geometries, the compressed models were exported as Filmbox (.FBX) files. Given that it preserves hierarchy and is amenable to being animated, this is usually the preferred format for Unity3D© imports.

Once in Unity, these models work as regular assets and as such, can be used to populate the scene. Concerning segment labeling, it was done at run time by interpreting a Text (.txt) file containing the correct atlas's labels.

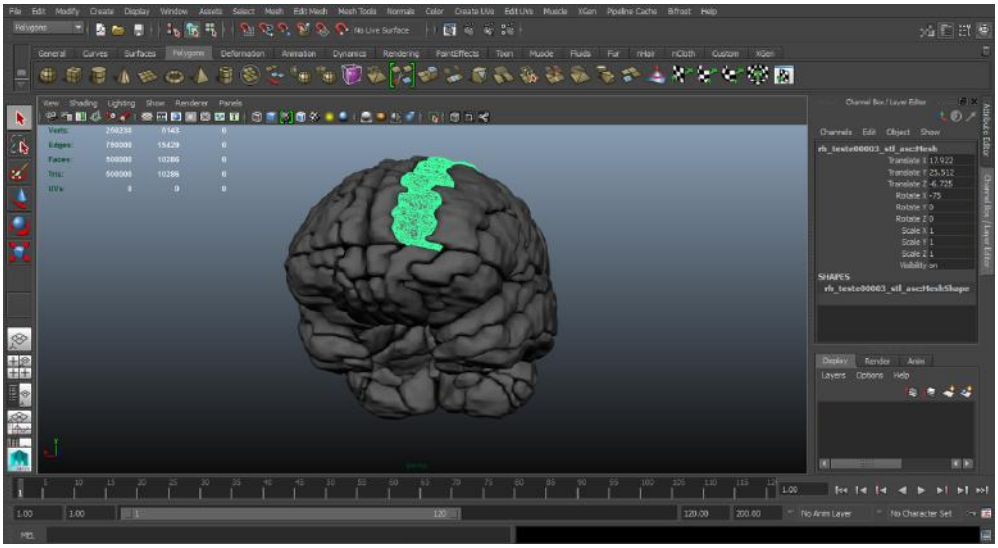

Figure 4.11: Screenshot of Maya's UI after optimizing an AAL brain model. The process lowered the mesh's poly-count from 1.8 M to 0.5 M (72.2 % reduction).

[19] These MRI datasets were provided by IBEB, where they had been used in previously conducted studies.
[20] Redundant polygons sharing all edges.

4.6.2 Connectivity Matrices

Now that the basis for the connectome had been dealt with, we had but to draw a web of connectivity graphs onto it. To contrive the 2D matrices that would be translated into said 3D network, we used the Multimodal Imaging Brain Connectivity Analysis (MIBCA) toolbox [66]. This open-source application pipelines well-known neuroimaging software[21] in a straightforward manner that allows for the pre-processing of MRI (functional and anatomical), PET and DTI data and its subsequent use in computing connectivity matrices[22] as well as related graph theory metrics [65].

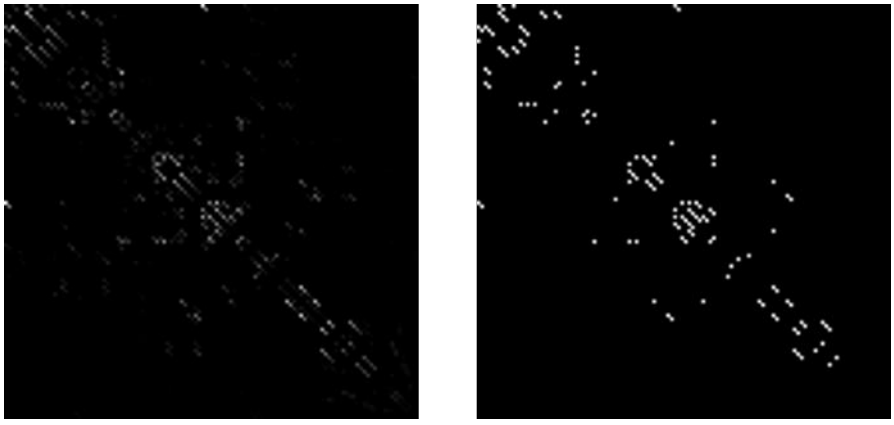

Figure 4.12: 2D representations of an AAL connectivity matrix in its weighted (on the left) and binary (on the right) forms. On the former, each pixel's gray level encodes the connection strength[23]between the ROIs associated with its respective row and column. On the latter however, each non-black pixel represents a connection that is "stronger" than the arbitrated binarization threshold, but reveals nothing about its intensity.

The matrices used in this dissertation where derived from DTI datasets, whence 20 referred to healthy subjects and 2 epilepsy patients. Much like the aforementioned 3D brain models, their use in Unity is dependent on an association with the appropriate label-containing file.

For performance reasons, the matrix that ends up being interpreted and visualized as a 3D network is often a hybrid between its weighted and binary forms (both shown in figure 4.12), meaning that even though it is thresholded it still retains information about the weights of each connection. Not only does drastically reducing the number of graphs in the scene improve overall performance and increase the average FPS count, but it also diminishes the visual clutter caused by lesser connections.

Lastly and befitting their use in a comparative, qualitative and visual analysis feature, atlas-specific reference matrices were calculated using a simple Matlab© script that averages the 20 healthy matrices into a single one.

[21] Such as FreeSurfer©, SPM©, FSL© and TrackVis©'s Diffusion Toolkit.
[22] MIBCA includes routines for constructing structural, functional and effective connectivity matrices.
[23] Arbitrated as the number of axonal fibers connecting two parcels/ROIs.

4.6.3 Tractography

In the hopes of representing the morphology of the intricate neural networks that emerge from the connections among different cortical and subcortical ROIs, these had to be somehow cataloged in tractography files that Unity could decipher.

To create them, we started by feeding DTI volumes to TrackVis©'s Diffusion Toolkit, a set of command-line tools that performs data reconstruction as well as fiber tracking on diffusion MR images. Essentially, it takes in raw .DICOM or .NIFTI data and outputs a Track (.trk) file that is ready to be analyzed and visualized once inside TrackVis©'s graphic UI (displayed in figure 4.13).

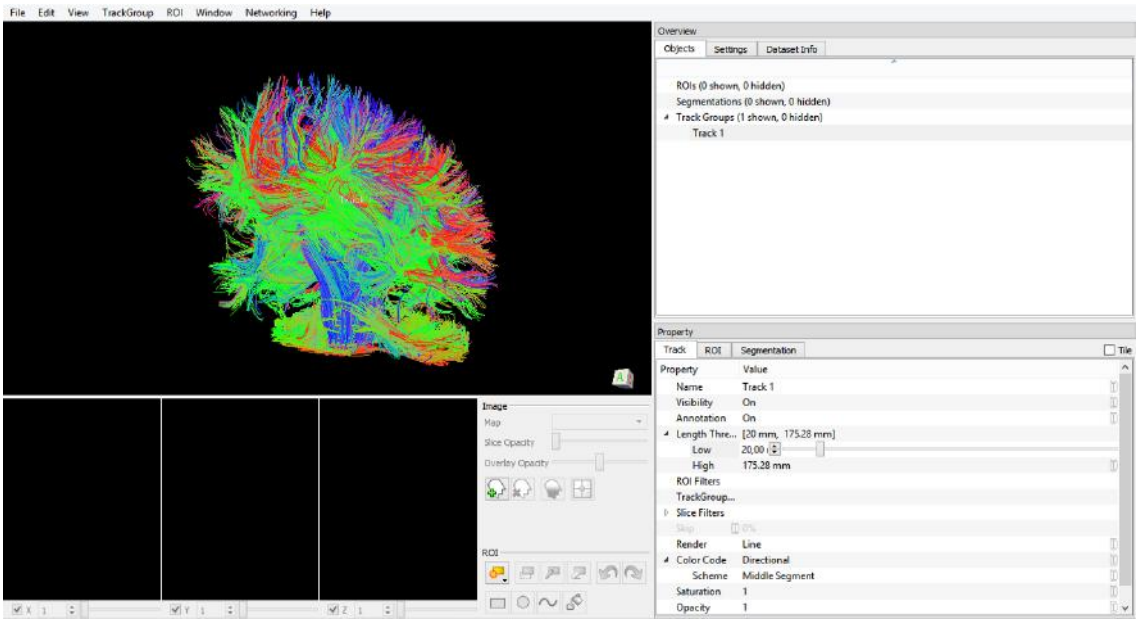

Figure 4.13: Sreenshot of TrackVis©'s graphic UI. This particular capture is showing every tract whose length measures more than 20.00 mm and less than 175.28 mm. *N.B.*, each tract's voxel is color coded according to how its absolute orientation in a 3D-coordinate system translates into RGB "space" (where right-left corresponds to Red, anterior-posterior to Green and superior-inferior to Blue) - Anisotropic color code.

The conversion from a .trk to a Unity-readable tractography file, was only possible thanks to Luis Lacerda, a colleague at IBEB that has been actively involved in the development and improvement of the MIBCA toolbox. He is responsible for a Matlab© routine that interprets a .trk file and outputs a 2D array containing the metadata of all tracts in one column and their corresponding Cartesian positions (x, y, z coordinates) in the other. The latter can then be saved and exported as a .txt file, which like we have formerly seen, Unity can "understand".

Chapter 5

Results & Discussion

5.1 Framework

All the research, efforts and methodologies described thus far, eventually culminated in the creation of what in our scope, is a high-level development framework, acquiescent to being deployed in the conception of clinically or academically relevant VR/AR content[1].

Its cursory demeanor notwithstanding, we feel that figure 5.1 paints a more accurate picture when summarizing said framework's intricate nature and Unity's pervasive role in it than words ever could.

Figure 5.1: Illustration of our final development framework that emphasizes Unity's ubiquity in the integration of all its software elements. The logo on the far right is a mock-up for our wearable device whereas the leftmost one represents our VR mount.

[1] The assembled framework is by no means restricted to these fields.

5.1.1 Leap Rift Mount

Creating a physical model that would hold the Leap Motion© controller in front of the DK1 and DK2 HMDs from Oculus was a challenge in and off itself. In total, three prototypes were printed and countless more were designed in Autodesk©'s Maya.

5.1.1.1 DK1 Mount v1

Being that it was the result of our first contact with not only Maya but also 3D printing, this was by far the most time-consuming model to build. After 27 nerve-wrecking hours, the .STL files pertaining to the two parts that make up the mount (shown in figure 5.2) were finally printed and hence ready to be painted and glued together (see figure 5.3).

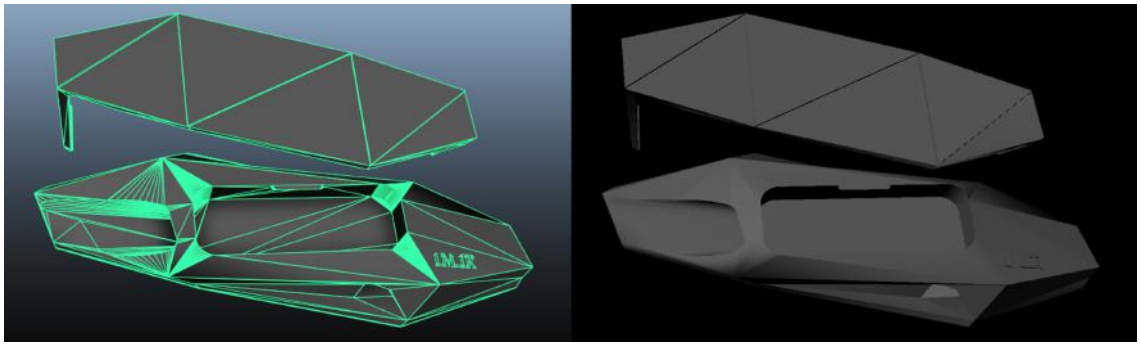

Figure 5.2: Maya visualizations of the DK1 mount, both in shaded wireframe mode (on the left) and post-rendering (on the right). Though it it is meant to be used as a single unit, the model was designed as a two-part piece to facilitate the printing process.

Much to our surprise, our first attempt at reproducing the mount was a success, in the sense that it fit almost perfectly on the DK1 HMD. Its most noticeable flaw was that its side flaps, the pieces that assured it stayed tightly attached to the headset, were somewhat loose. A result of the excessive tolerance margin that they had been given in the designing phase. To overcome it, strips of rubber were taped to their inner sides, thus increasing the grip of the mount as a whole.

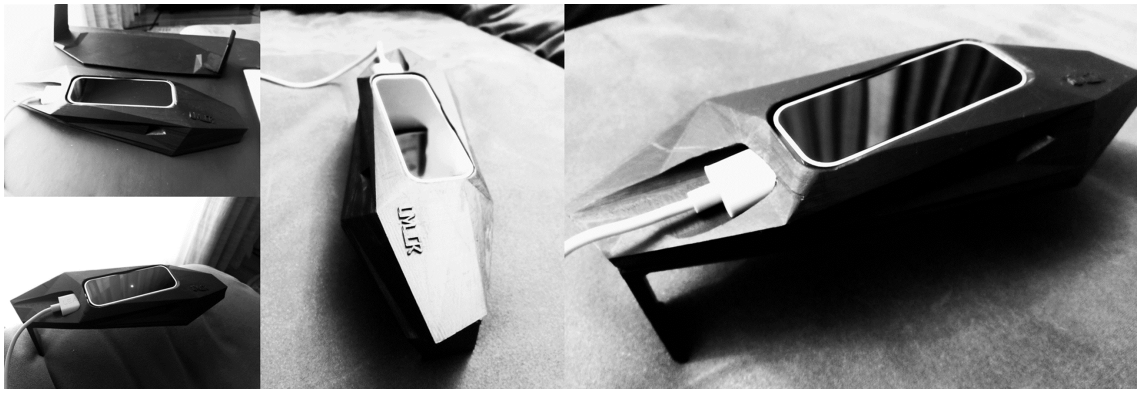

Figure 5.3: Photographic composition of the DK1 mount, once printed, assembled (the picture on the top left corner features the mount's two constituent pieces) and painted.

5.1.1.2 DK2 Mount v1

If there is one thing to apprehend from section 3.1.1 it is that the HMDs from Oculus Rift© are strikingly different from one another. This meant that when we found ourselves in the possession of a DK2 headset, we could not simply use the mount we had devised for its predecessor. Conversely a new mount had to be modeled, one that not only pondered the appreciably curvier edges of the DK2's design but also contemplated the positions of the IR LEDs that it uses to track position. The results are visible in the figures below.

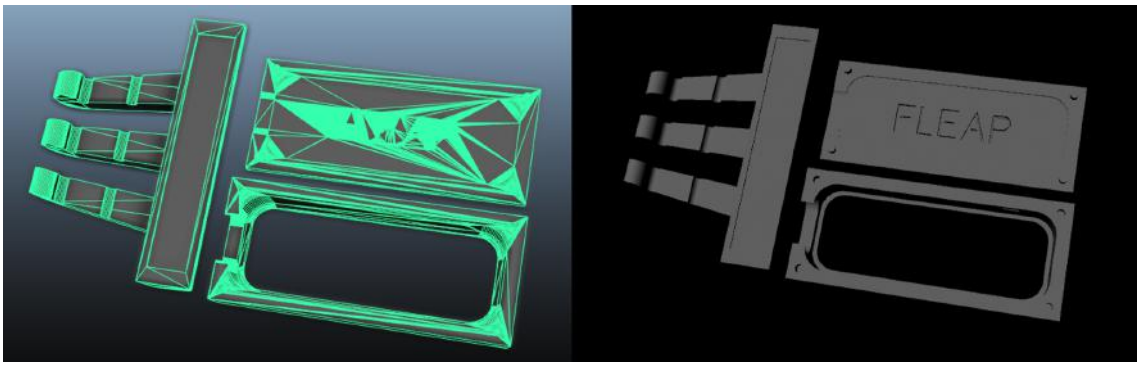

Figure 5.4: Maya visualizations of the DK2's first mount. The fork-like component is meant to be glued to the one with the Leap-shaped hole, whereas the remaining flat one is a cover that snaps onto the rest and secures the controller.

Contrasting with what had happened with our previous attempt, this one did not pan out as anticipated. Besides having some major design flaws that prevented the pieces from properly fitting together and could only be fixed with a hot blade, a mishap with the painting process almost rendered it useless. As one would and should expect, leaving a piece of thermoplastic material to dry out in the sun may cause some adverse effects. Nevertheless, using a standard hair dryer, we managed to mold it back into something resembling its original design and therefore salvage its functionality. All things considered, we could not help but be pleased with the outcome, a deformed albeit serviceable mount.

Figure 5.5: Photographic composition of the first version of the DK2 mount portraying the various stages it underwent prior to being ready.

5.1.1.3 DK2 Mount v2

Yet unsatisfied with the mount in hand, we set out to redesign it from scratch and enforce that which we had learned from its precursors. The result was the lighter, smaller and more befitting model that we present here (illustrated in figure 5.7).

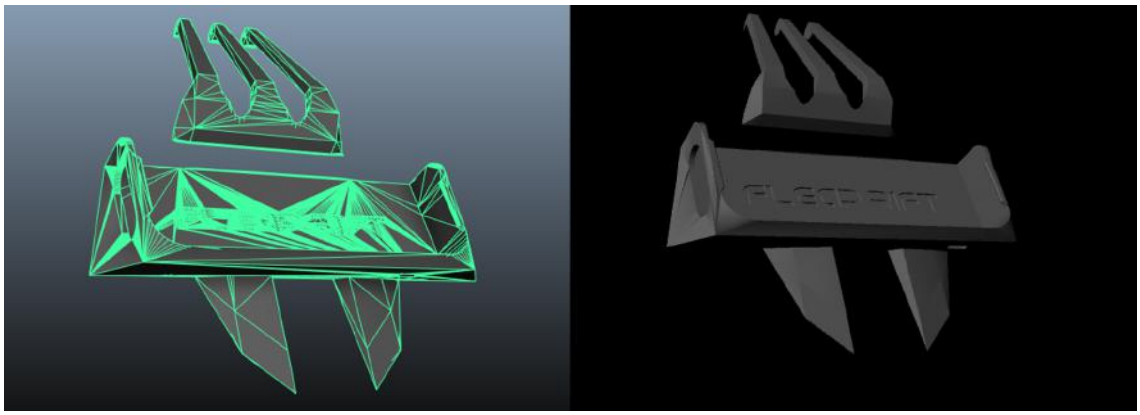

Figure 5.6: Maya visualizations of the DK2's second and final mount, showing its polygonal mesh (on the left) and the result of rendering said mesh (on the right). The trident-shaped sub-piece is to be glued to its Leap-holding counterpart. The latter features two laminae that further add to the overall stability of the model, once it is mounted.

Appeased with the Leap Rift mount we now had at our disposal and reassured by the comfort of having Unity do all the heavy-lifting for us in terms of SDK integration, we deemed the matter of interfacing the DK2 HMD with the Leap Motion© controller as sealed, with respect to both hardware and software. The time had then come to move onto the development of the wearable device.

Figure 5.7: Photographic composition of the final version of the DK2 mount illustrating the various production stages that led to its final outlook.

5.1.2 Haptic Mitt Bit

As we have previously ascertained, one of cornerstones of this dissertation was the development of a wearable device that could invoke tactile sensations on its user all the while measuring some of his/her biosignals - the Haptic Mitt Bit (HMB)[2]. In doing so, not only have we endowed our framework with a layer of physical computing, but also with the ability to stimulate the human haptic sense, a paucity in current VR/AR systems.

Leading up to our final design, many prototypes were assembled. Even though this happened continuously throughout our campaign, some breakthroughs did occur, particularly in terms of hardware. In our view, the most notorious of these milestones justified a discrete categorization of the development process, that we now move to present.

5.1.2.1 Pre-alpha Prototypes

Pre-alpha prototypes is what we are calling those hastily mustered circuits that were used in parallel with the Arduino© UNO Rev3 board in the earliest of development stages, during which our strategy was still being tweaked. A testament to this is the fact that integrating an electrophysiology module had not yet been considered at this point. These forebears of the haptic module abstracted from a physical glove entirely and did not feature tactile actuators *per se*, but rather emulated them with standard LEDs. Figure 5.8 illustrates some of the tests that were conducted with a setup that used these prototypes in conjunction with the Leap Motion© controller.

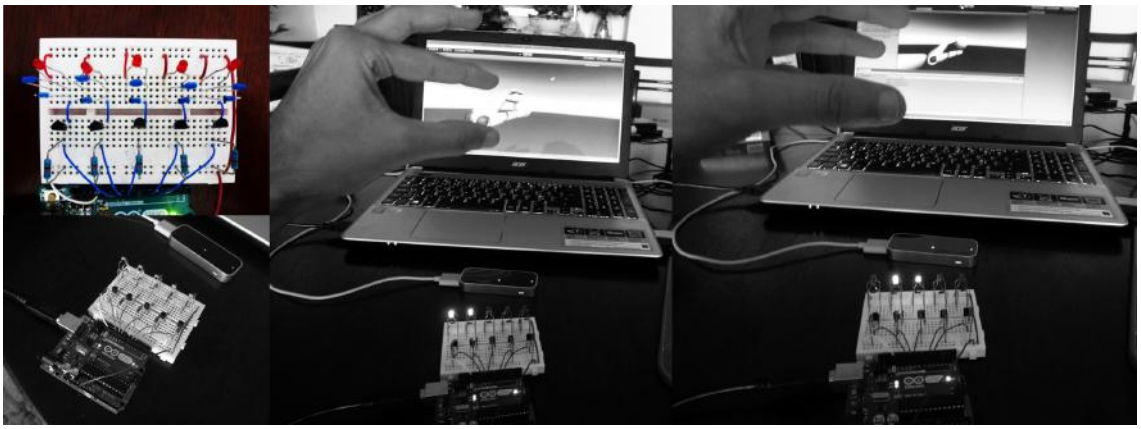

Figure 5.8: Assortment of photographs that depict some of the tests that were performed with the early versions of the glove's haptic module. Using Unity's physics engine, we were able to detect collisions between the user's hand and a haptically responsive object (the sphere that is barely visible in the laptop's screen) with finger specificity.

Simple as they were, these modules quenched our doubts about the communication between the various constituents of our architecture, by showing imperceptible response times and delays between onscreen collisions and LED actuation.

[2]Play on words with the terms "Haptic", "Mitt" (as in glove) and "Bit" (allusion to Bitalino©).

5.1.2.2 Alpha Prototype

Despite yet lacking integrated modules in its design, this system was the first to successfully incorporate electrophysiology in its plans. Granted, it did so with a less than suitable standard Bitalino© board but that was not a pressing concern at the time. As such, this did not keep it from serving its intended purpose, which was allowing us to familiarize ourselves with the BITalino-Unity API.

Furthermore, this setup is where the vast majority of the tests that concerned the haptic feedback module took place. Featuring 5 ERM vibration motors (depicted in figure 5.9) that had been ransomed from inoperative or defective cellphones, this early haptic wearable stood as the perfect guinea pig for extremist experiments. These would have otherwise been unthinkable as we could not afford to perform them with the ERMs that we had purchased from Precision Microdrives™.

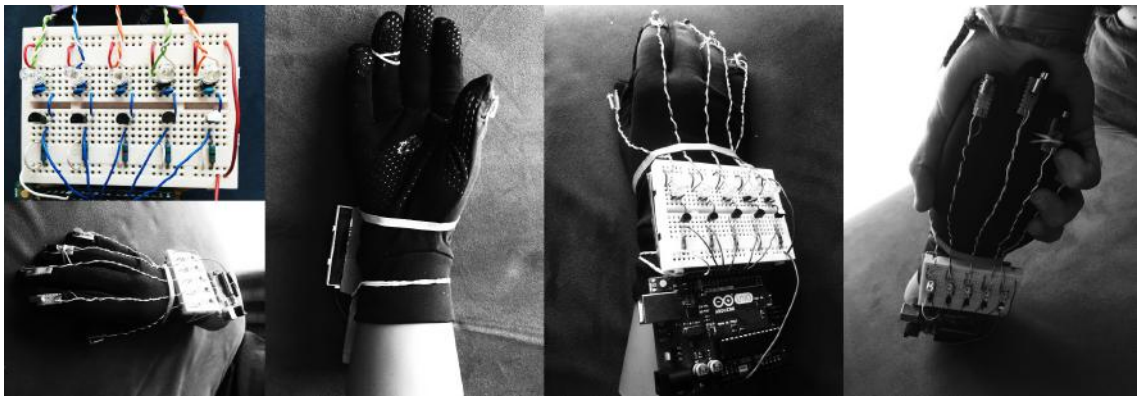

Figure 5.9: Collection of photographs that show the alpha prototype of our haptic device. These images display our right thermal glove (reffered in section 4.5.1) worn by a mannequin's hand, a prop that aided us immensely when defining the layout for our electronics. Pictures of the Bitalino hardware that was used at the time were unfortunately lost before the writing of this thesis.

Convenience dictated that we would place this version's rudimentary tactor units on top of each fingernail, which is an innately less sensible area when compared to the bottom side of the fingertip. This and other issues (*e.g.* inserting an additional tactor unit at the palm of the glove and moving the LEDs onto said units) were addressed in the ensuing and incidentally, final prototype.

5.1.2.3 Beta Prototype

"Beta" is how we officially labeled our most polished wearable device, whereas officiously, it was the first to be baptized as the Haptic Mitt Bit. Using what we had learned from its earlier cohorts, we came up with a more deliberate and unobtrusive design that not only did a better job at concealing its electronics, but also enabled the integration of its two core modules (hardware-wise). Preceding said assimilation though, both of these had to be scaled-down as much as it were possible without hindering their functionality.

With regards to the glove's electrophysiological element, this preparation process consisted in a thoughtful arrangement and subsequent soldering of the parts that make up our customized Bitalino© freestyle kit (discussed at greater depths in section 4.5.3). The outcome was the compact module that figure 5.10 epitomizes.

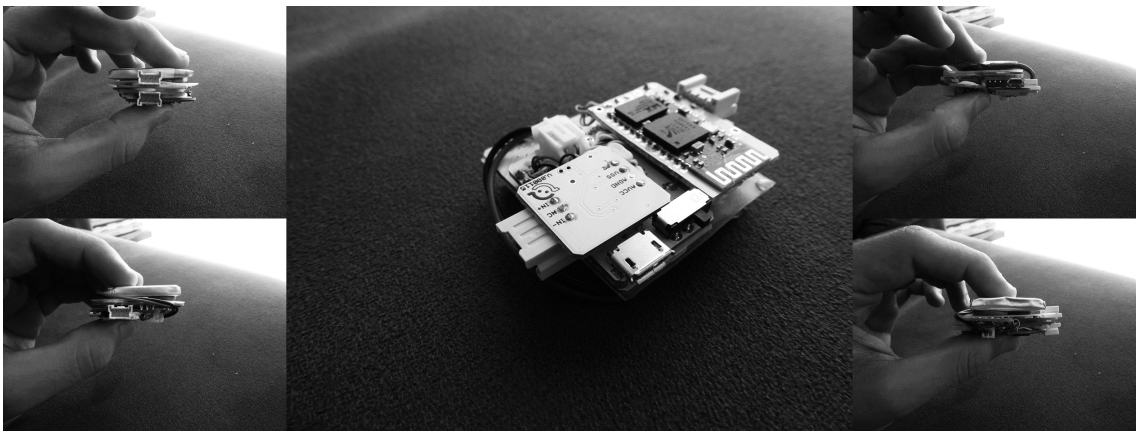

Figure 5.10: Brief portfolio of photographs that showcase the final electrophysiology module. The two smaller images on the left focus the plug-in entry points for the ECG, EMG (both on the top left corner) and EDA (bottom left) sensor-blocks while the pair on the right, emphasizes the micro USB port on the power block (top right corner) and the battery's hookup site (bottom right corner).

Barring the reallocation of the LEDs to the tactor units (shown in section 4.5.2.2), the addition of one such a unit to the palm of the glove and the replacement of the temporary ERM motors with those that came from Precision Microdrives™, the haptic module's operation did not change much when compared to its alpha predecessor. In terms of solidity and wearability on the other hand, we believe the beta version to surpass the preceding prototypes immeasurably. A claim that figure 5.11 vouches for.

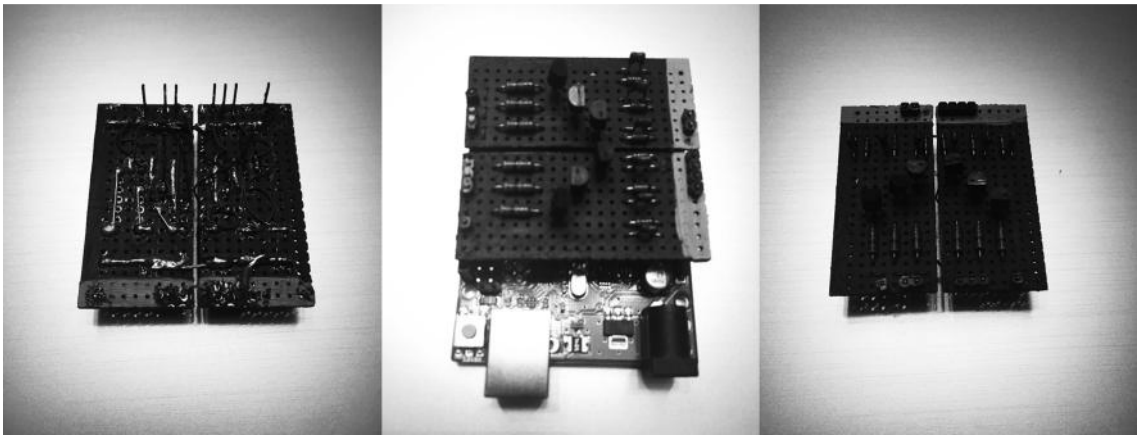

Figure 5.11: Photographic composition that exhibits our final haptic module (minus the tactor units). The two images on the extremities display the custom-made shield with the driving circuitry soldered onto it, whereas the one on the middle portrays it plugged into the Arduino© UNO Rev3 board.

All that remained was then to combine the aforementioned modules with the device's tactor and textile components (reported in section 4.5). The resulting prototype made use of our custom-tailored cover in confluence with the left pair of the thermal gloves, which it used as its foundation. The hemmed opening that had been cut into the latter's palmar region accommodated the acquisition of the wearer's EDA by providing a direct access point to the skin portion where the pre-gelled electrodes were to be attached. This and other aspects of the integration process are encapsulated in figures 5.12 and 5.13.

Figure 5.12: Series of photographs that summarize the device's integration process. The larger picture on the right portrays its final product, whilst those on the left display the tactor-concealing cover (two at the top) as well as the thermal glove by itself, with the EDA hole cut into it and the tactor units already in place (two at the bottom).

As it is often the case with vibration, the hardware produces audible noise than can detract from a complete sense of immersion and borderline on the irritating, thus rendering the whole experience as ostensible. To circumvent the issue, the use of headphones or alternative sound systems that can muffle the motors' buzzing is highly recommended.

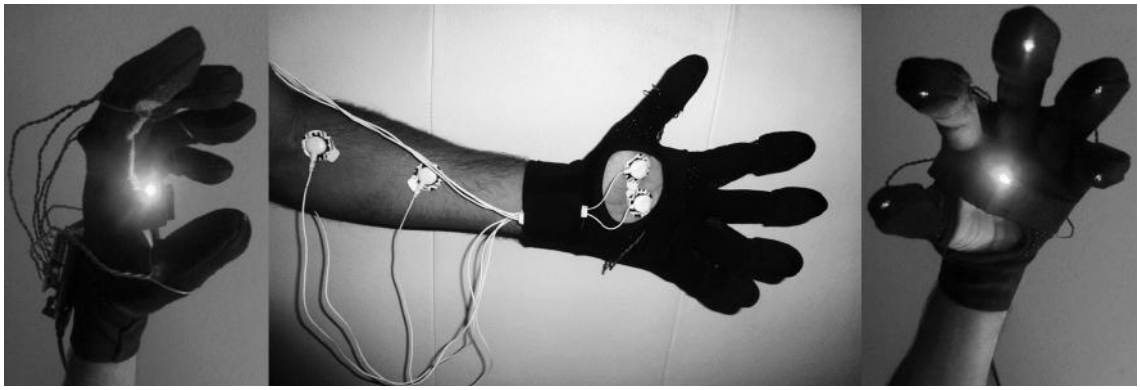

Figure 5.13: Assemblage of photographs that illustrate the constructed wearable device in use. The two images on the far ends captured the glove while all its tactor units were simultaneously active, whereas the one in the middle shows the proper configuration of the device's EMG and EDA electrodes.

Software-wise, the all but organic nature of the development process prevents us from classifying discrete landmarks that could be affiliated with the prototypes listed above. Conversely, we will simply present some of the core aspects of the final Unity package that complements our device (*e.g.* prefabs and classes), so that we might shed some light on how it is to be applied.

- **HMBArduino** is an adaptation of Uniduino©'s "Uniduino" prefab. Essentially, it is a game object that has the "Arduino" script attached to it, *i.e.*, it is an instance of the "Arduino" class. As such, it deals with the communication between Unity3D © and the Arduino© board by providing standard configurable settings (*e.g.* serial port name and baud-rate);

- **HapticsManager** is a class that in addition to defining which finger is related to each pin on the actual Arduino© board, also contains the public methods that manage their activity. It can the thought of as the closest thing in Unity to a sketch in Arduino©'s IDE (report to section 4.5.2.1);

- **HMBBitalino** is a variation of the "Bitalino" prefab that comes with the BITalino-Unity API. Analogously to what happens with its Arduino© cohort, it is used to configure the communication between Unity and the Bitalino© hardware. Moreover, it also deals with common acquisition parameters, such as sampling rate, buffer size and register options (which channels to record and whether or not to record them);

- **ElectrophysiologyManager** is a class that stores the features and events that can be extracted from the acquired signals (*e.g.* heart rate, muscular contractions and SCRs). Furthermore, it also contains the definition for the abstract "Biosignal" class, which specifies how each of the implemented filters (addressed in section 4.5.3) is applied to any signal that inherits from it;

- **ECG, EMG & EDA** classes inherit most of their functionality from the "Biosignal" class and differ from it mainly in the plotting capabilities and feature-specific methods they implement, *i.e.*, peak detection, contraction detection and SCR/SCL assessment, respectively;

- **HMBHandController** is a tweaked version of the "HandController" prefab that is included in Leap Motion©'s core assets Unity package. The most notorious distinction between the two being that the HMB one uses our "HapticPhysXHand" as its physics model. This compound collider is layered in a way that allows for the detection of finger- and palm-specific collisions, which can then be translated into localized tactile feedback;

The Haptic Mitt Bit was complete at last, and therefore ready to be deployed in the development of multimodal VR/AR applications, alongside the remaining constituents of the described framework.

5.2 Applications

When all is said and done, a tool is only as good as its applicability. Determined to prove the worth of ours, we set out to employ it in the conception of a number of cohesive experiences, that would advocate its potential in educational and medical exploits.

5.2.1 Brain Connectivity Leap

Network studies of the human brain are dominantly motivated by the idea that brain function is not solely attributable to individual regions and connections, but rather emerges from the topology of the network as a whole, the connectome of the brain.

The visualization of such an intricate system in a comprehensive albeit intuitive manner remains as challenging a feat as it ever were. This has never held more true than it does so today, in the age of big data, wherein brain-related information is constantly being provided and by multiple sources, ranging anywhere from genetics and neuropsychology to electrophysiology and neuroimaging.

Standing as the apex of what was created with the framework we assembled, Brain Connectivity Leap (BCL) is a VR/AR interface that hopes to address this issue by providing an immersive, interactive and novel means of navigating the human connectome. Some of the key traits it features towards accomplishing its goal are presently listed:

- Multiple Parcellation Atlases;
- T1-weighted MRI Reconstructions of the Brain;
- DTI-estimated Connectivity Matrices;
- Graph Color Coding;
- Tractography
- Head Tracking & Display;
- Hand Tracking & Interaction;
- Gesture Recognition;
- Haptic Feedback;
- Electrophysiological Computing;
- Signal Processing;

Although most of these elements have been contiguously addressed throughout this dissertation, there are some that merit additional clarification. So as to better understand their role and implementation in BCL's overall structure, we shall briefly go through the process that one would have to undergo in order to make proper use of it.

5.2.1.1 Setup

Once Unity is launched and either of the BCL scenes is opened (desktop or VR), the user is faced with a layout that by design, presents him/her with a narrow set of configurable properties. Although some of these should be reserved for developers that are familiar with Unity's syntax and mechanics, those that relate to the "Connectome" game object (highlighted in figure 5.14) are meant to be accessible to even the most novice of users:

- **Parcellation Atlas** is the most important of said options, as not only does it define which brain mesh will be loaded onto the scene when the application is executed but it also conditions the majority of the remaining choices. Using the dropdown menu of the "Segmentation" component, the user can select one among the implemented segmentation atlases (report to table 2.1);
- **Connectivity File** refers to the 2D matrix that will be translated into a 3D network of connectivity graphs once the program is ran. As expected, the matrix's labeling has to coincide with the parcellation atlas that was selected (otherwise, an exception will be thrown). Atlas-specific matrices can be found in the the project folder (Assets, Resources, Connectivity Data);
- **Reference Connectivity File** is the connectivity matrix against which the previously discussed one will be compared. By default, the current atlas's health reference (discussed in section 4.6.2) is used;
- **Connection Threshold** defines the minimum connection strength a graph has to have in order to be drawn. By disregarding lesser connections, we are able to boost performance and minimize visual clutter.

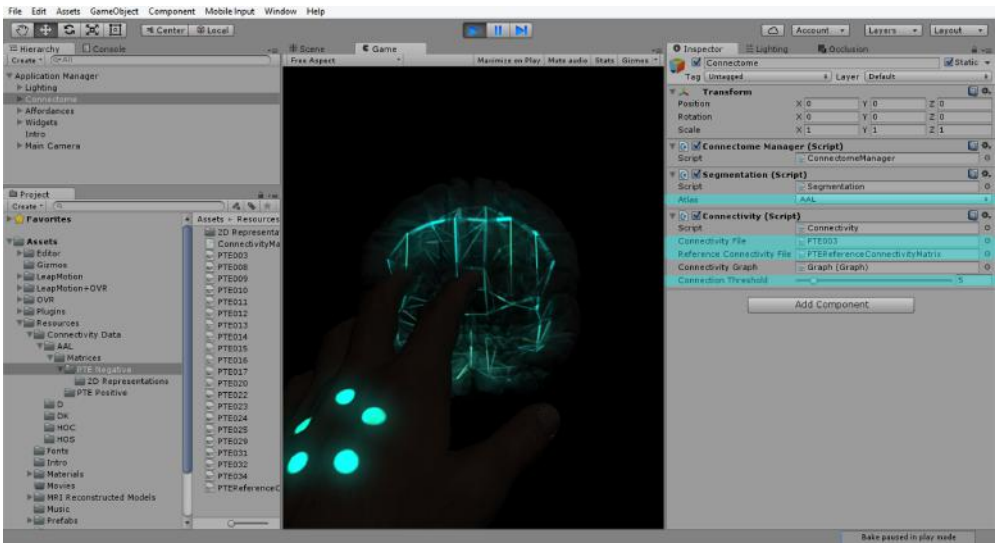

Figure 5.14: Screenshot of Unity's editor while running BCL. The variables highlighted in cyan inside the "Connectome" inspector are the ones we presented in this section.

5.2.1.2 Connectome Visualization

Above all else, BCL is a visualization tool. In order to grasp how it interprets .txt connectivity files and subsequently translates them into networks of weighted and cataloged connections, we should first examine how it is structured, *i.e.*, how it organizes the classes[3] that relate to the rendering of the actual connectome.

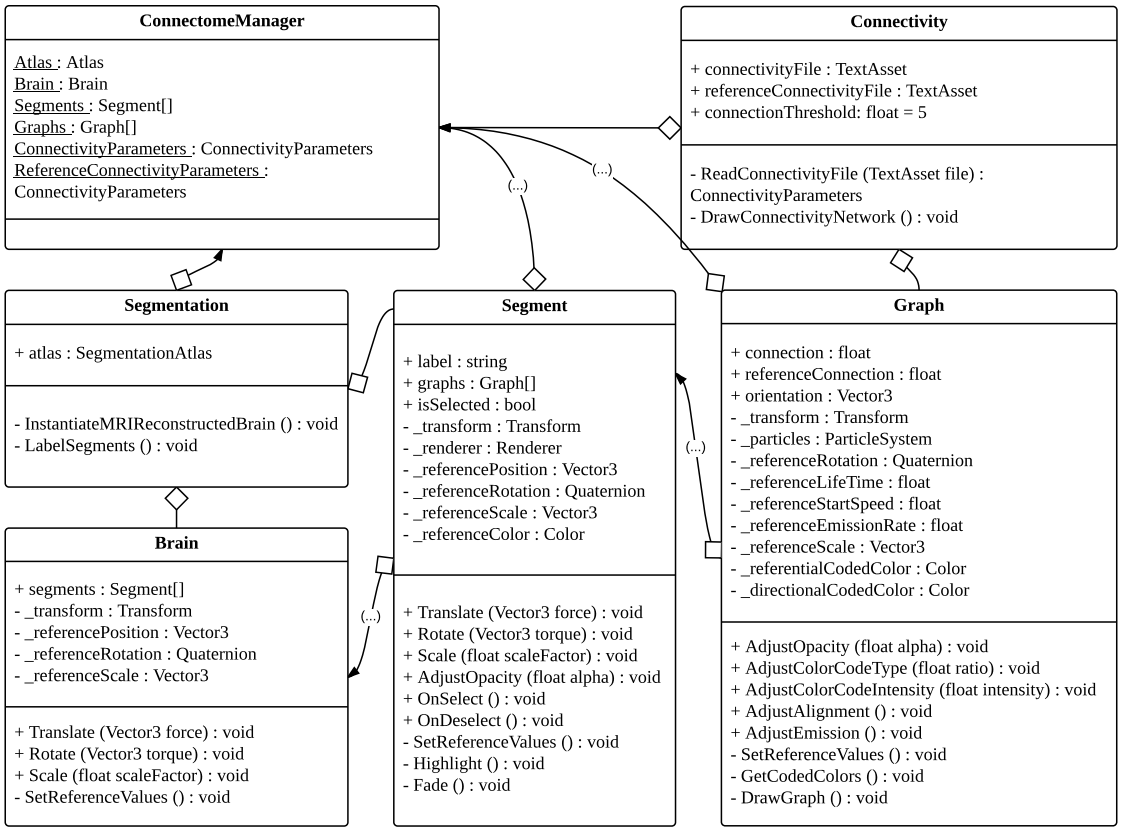

Figure 5.15: Class diagram that schematizes the connectomic portion of BCL's structure. Plus (+) and minus (-) signs refer to public and private members, respectively. Links with solid arrowheads represent the storage of instances of the originating class in the receiver's, while plain ones denote instantiations (*e.g.* "Graph" instances are created in the "Connectivity" script, and assigned to member variables in the two "Segment" instances they connect as well as in the "ConnectomeManager").

As figure 5.15 shows us, the portion of the program that deals with instantiating an accurately parcellated brain, its labeled ROIs and their respective weighted interconnections, is highly modularized yet still centralized. What we mean by this, is that by storing all the relevant constituents of the connectome under the "ConnectomeManager" singleton[4], we facilitate their retrieval and affectation in other limbs of the application, namely those that deal with interaction.

[3] *N.B.* in Unity, a class is instantiated by attaching the script that defines it onto a game object.
[4] The singleton pattern is a design pattern that restricts the instantiation of a class to a single object.

As informative as it is, diagram 5.15 provides no insights about the chronological sequence in which the various constituents of the connectome are drawn. For this reason, we will now enumerate the primary events that lead to the visualization of said structure:

(i) Instantiation of a properly parcellated brain mesh. Each of the implemented atlases has a mesh associated with it (all shown in figure 5.16). In order to reproduce meaningful networks of connectivity, all ROIs, or segments, have to be labeled in accordance with the atlas that defines them;

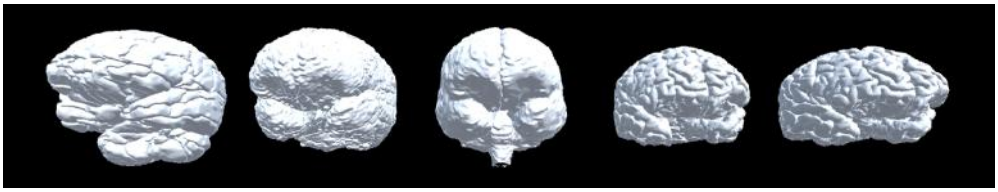

Figure 5.16: Instances of the MRI reconstructed brain meshes in Unity. From left to right: AAL, HOA (cortical), HOA (subcortical), DKCA and DCA parcellated models.

(ii) Interpretation of the atlas-concordant connectivity files. Prior to storing the 2D labeled connectivity matrices in the appropriate member variables of the "ConnectomeManager" singleton, standard statistics (*e.g.* count, minimum, maximum and average) are extracted from them and fed back to the user through Unity's UI;

(iii) Actual drawing of the graphs, which consist of particle systems that ponder both the strength of the connection they represent and the distance between the two segments they connect. In other words, each graph emits particles with a speed, direction, life time, rate and diameter that encode the connection it embodies;

(iv) Coloring of the graphs according to one of two codes (visible in figure 5.17). In the Referential code, each graph is colored in a manner that illustrates how its underlying connection strength fairs against its counterpart in the reference matrix. Red represents connection deficits, cyan denotes similarity and yellow indicates excesses. The resulting tone reflects the degree of deviation by interpolating the three colors. Alternatively, the user can choose to apply the Anisotropic color code, which is the one used in standard tractography (covered in section 4.6.3);

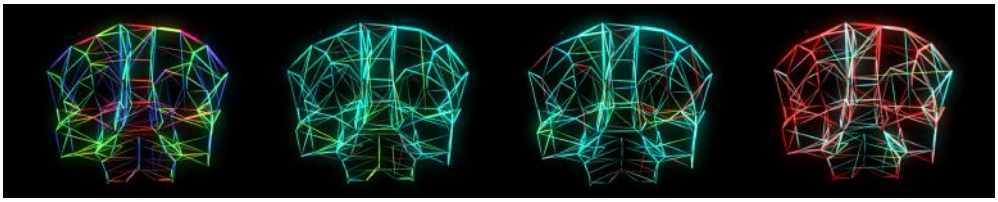

Figure 5.17: Screen captures of AAL connectivity networks with different color codes applied onto them. The leftmost one is colored according to the Anisotropic code whereas the one adjacent to it showcases a healthy matrix encoded with Referential colors. As do the two images on the right, though these stemmed from two distinct epileptic matrices.

The resulting connectome cannot be truly appreciated in static imagery, but is nonetheless portrayed in the composition below.

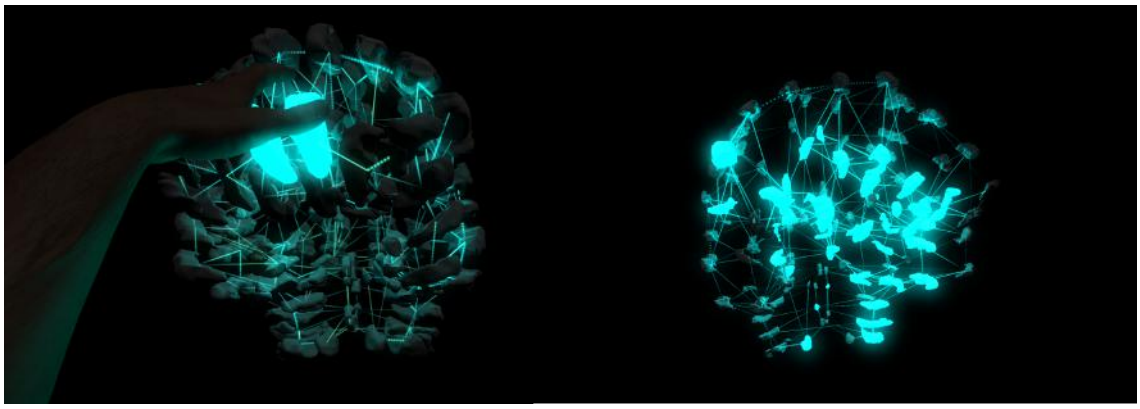

Figure 5.18: Screenshots of an AAL connectome, after is has been expanded/exploded.

Despite not being depicted in the class diagram we presented above (figure 5.15), BCL also features a "Tractography" script, that takes Unity-readable .txt files (generated as described in section 4.6.3) as input and converts them into a collection of static particle systems, one per tract. Even though we were very pleased with the results in terms of accuracy, visibility and aesthetics (shown in figure 5.19), we were less than so regarding the performance impact that having such an excessively high particle-count posed to our system. This vexing limitation deemed it incompatible with the levels of interaction and fluidity[5] we were aiming for and as a result, the inclusion of tractography in BCL was temporarily postponed.

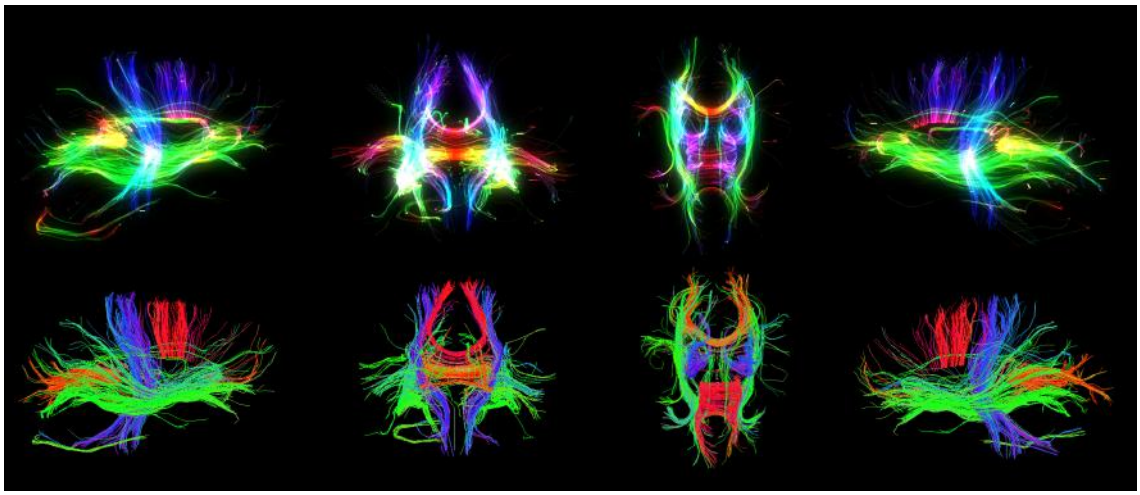

Figure 5.19: Comparison between the tractography visualization tool we created in Unity (top row) and TrackVis©'s one (bottom row). Both tractographies were set to only display tracts that were longer than 90.00 mm and shorter than 200.00 mm. From left to right, the captures refer to the right lateral, coronal, top and left lateral views, respectively.

[5]Tractography caused drops from 50-60 FPS to 10-20 FPS.

5.2.1.3 Interaction Scheme

Having established how BCL generates and displays its connectomic components, it is time to move on to how to interact with them. The designed scheme includes:

- **One Handed Interaction** that provides the user with different tools depending on how many fingers he/she has extended (see figure 5.20). When only one finger is stretched, the segments at which said finger is pointing at become selected. Extending two fingers enables the translation of the currently selected segments by an amount that is proportional to the hand's velocity. Analogously, holding up three fingers and moving the hand in question causes the current selections to rotate. Fully opening a hand (5 fingers stretched) enables selection and deselection by hovering, *i.e.*, by increasing or decresing the distance (past an arbitrated threshold) between the hand and a segment, it either becomes or ceases to be selected, respectively. Lastly, a closed fist deselects all active selections;

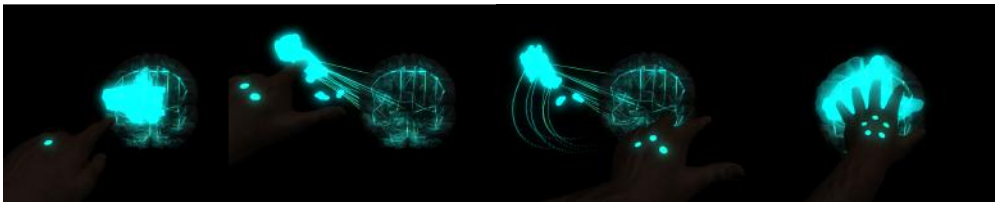

Figure 5.20: Portrayals of each of the One Handed Interaction tools. From left to right: Point & Select, Translate, Rotate and Hover & Select/Deselect. Notice how the pattern on the back of the hand changes to indicate how many extended fingers the Leap is seeing.

- **Two Handed Interactions** are a lot less complex than the ones we have just examined. When 2 hands are on the screen, the whole connectome rotates in order to always be facing the center of mass of the hands. By "paddling" with both hands, said connectome is translated in the direction in which the hand motion is occurring. It bears reminding that One and Two handed interactions are not mutually exclusive, meaning that they can happen simultaneously;

- **Haptic Feedback** is enabled provided that the user is wearing the HMB. If so, whenever he/she virtually touches a connectivity graph, the glove produces a vibration that is proportional to the connection strength of said graph. Additionally, when Hover mode is active, all tactor units are triggered with a low duty cycle input signal. This is perceived by the user as a tingling sensation;

- **Physiological Computing** is also present if a Bitalino© device (not necessarily the one from the HMB) is connected to the system. By contracting his/her forearm (or whichever muscle the EMG electrodes are monitoring), the user hides/shows the plots for his/her biosignals. We are aware that this is not the most impressive of HCI features but it bears reminding that it was devised as a proof of concept, and that it could easily be adapted to any other discrete functionality;

- **VR Widgets**, a set of tools that Leap Motion© provides in its core assets package. With it, typical UI elements like dials, sliders, buttons and scrollers can be brought into the VR scene, thus opening new yet familiar channels of interaction between the user and the application. Presently, BCL utilizes 4 sliders to manage rendering adjustments of the connectome and 2 scrollers that list the current hand-specific selections (all of which are visible in figure 5.21). These are contained in an invisible cube that surrounds the user's avatar and can rotate into and out of the FOV. Additionally, one scroller is used at the beginning of each execution to display BCL's credits, motivations and instructions;

Figure 5.21: Representation of BCL's use of the VR Widgets. From left to right: Introduction scroller, Adjustment sliders and Selections scrollers. Also from left to right, each slider's function is to: adjust the brain's opacity, adjust the network's luminosity, control the type of color code being applied (Referential or Anisotropic) and lastly, its amount.

- **Library of Recognizable Gestures** that hopes to fill the void left by the absence of a mouse and keyboard. Although Leap Motion©'s Unity package does offer a collection of pre-defined gestures (*e.g.* swipe, circle and tap), these felt neither intuitive nor adequate for the tools we had in mind. Consequently, we decided to implement our own set of recognizable hand poses (demonstrated in figure 5.22), in which both the Trigger[6] and Pinch[7] gestures are defined. The former controls the rotation of the widgets cubic container, which happens in a clockwise fashion when the left hand Triggers and in an anti-clockwise one when a right Trigger is detected. Pinching does nothing when performed by a single hand but could easily be set to purpose. When a double Pinch is detected however, the user enters scaling mode, in which the whole connectome can be exploded or imploded;

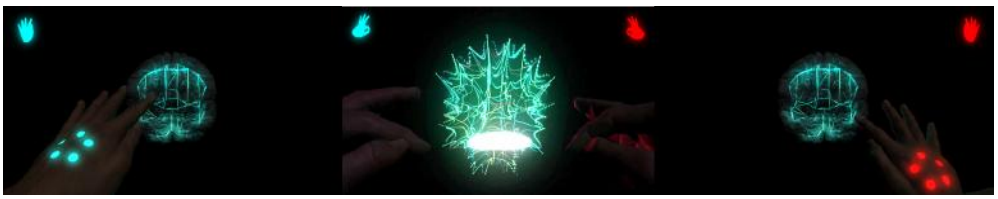

Figure 5.22: Depiction of our recognizable gestures. The images on the extremities illustrate the left and right Trigger gestures, while the one in the center shows a double Pinch. Notice that visual cues specific to each gesture and hand appear on the respective corner of the screen when a gesture is properly performed.

[6]Tip of the thumb touching the index knuckle while the remaining fingers are extended.
[7]Tip of the index touching the tip of the thumb while the remaining fingers are extended.

- **Keyboard Commands**, though vestigial, do exist. To dismiss the initial introductory scroller, one needs but to press the "ENTER" key. Thenceforth, the left and right cursor movement keys (← and →) allow the user to swap between male (♂) and female (♀) hand models (shown in the figure below). Pressing the "B" key toggles the bloom effect[8] on/off and finally, the escape key ("ESC") exits the application.

Figure 5.23: Gender-specific hand models included in BCL. The male ones can be seen on the images to the left while their female cohorts are displayed on the right. Notice how each hand has its own signature color and how it is the negative of its counterpart's.

5.2.2 Ode to PHL

Contrasting with the previously discussed BCL, Ode to PHL is a more rudimentary application that makes only partial use of our framework [9] towards the passive learning of simple one-handed piano sequences. It was inspired by previous research in the field and as such should not be construed as original work [40, 48]. Nevertheless, our fascination with the PHL effect, its potential in rehabilitation and the all but logical marriage of such an application with HMB moved us to develop Ode to PHL.

Even though the original plan was to include a considerable collection of melodies from which one could be selected at will, time constraints dictated that only one could be properly implemented - excerpted from the final movement of Beethoven's 9th simphony, Ode To Joy (its musical sheet is shown in figure 5.24). Not surprisingly, this is where the application got its name.

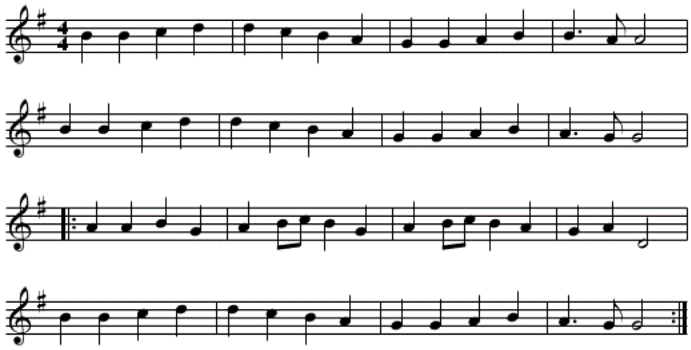

Figure 5.24: Ode to Joy's musical sheet. Arrangement by Lester Bailey.

[8] Blooming is the optical effect whereby light from a bright source appears to leak into surrounding objects. Though it adds to the realism and aesthetics of the experience, it takes its toll on performace.

[9] Its development encompassed only Unity and the tactile feedback module of the HMB.

In order for it to work, musical sheets such as the one shown above had to be translated into Unity-readable files (see table 5.1) that contained information about the sequence of notes and their relative duration (relative to the tempo[10] of the piece).

Note	Si	Si	Do	Re	Re	Do	Si	La	Sol	Sol	La	Si	Si	La	La
Duration	1	1	1	1	1	1	1	1	1	1	1	1	1.5	0.5	2
Finger	M	M	I	T	T	I	M	R	P	P	R	M	M	R	R

Table 5.1: Portion of the .txt file that translates the first line of Ode to Joy's musical sheet into something Unity can decipher and subsequently transmit to the haptic module of the HMB. For a left handed configuration: "P" stands for pinky, "R" for ring, "M" for middle, "I" for index and "T" for thumb.

Once these associations are taken care of and the application is executed, the user will feel a sequence of buzzes in his/her fingers that mirrors the sequence of key strokes he/she would have to perform in order to play the corresponding melody on a keyboard. The idea here is that by repeatedly using the glove for extended periods of time[11], one could learn and retain simple passages through sheer muscle memory.

Furthermore, Ode to PHL reinforces haptic stimuli with both auditory and visual cues. These are produced in Unity, which in addition to interpreting the aforementioned musical sheet and overseeing the activity of the HMB's haptic module, also reproduces the appropriate audio clip for each note and represents it graphically (as shown 5.25) in a synchronous manner.

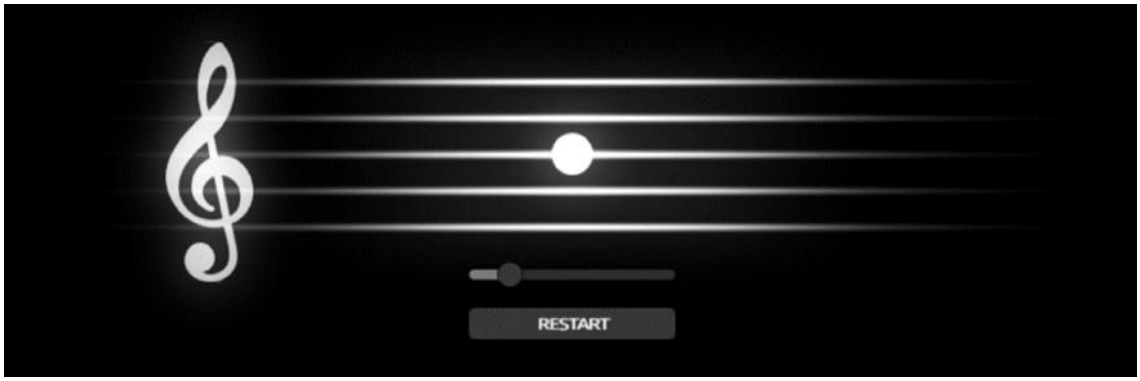

Figure 5.25: Graphical UI of Ode to PHL. The white circle in the middle of the screen moves according to the note that is being played. The standard slider adjusts the tempo and the "Restart" button resets the sequence (which is continuously looping otherwise).

Unfortunately, the time-frame of this thesis prevented us from conducting any actual studies that could corroborate and advocate the deployment of Ode to PHL in motor rehabilitation therapy. Withal, after revising the existing literature on the matter we are both confident and expectant with the prospect.

[10] In musical terminology, tempo is the speed or pace of a given piece or subsection thereof.
[11] Literature reports high success for able-bodied subjects with biweekly sessions of 30 minutes each [40].

5.2.3 Surgery Simulator

Yet another elementary application whose underlying principle is far from it, this VR surgical simulator seemed like a mandatory usage of the framework we assembled. Even though the tool tracking capabilities of the Leap Motion© and any concurrent optical devices cannot deliver the reliability and robustness that an actual telesurgery application would require, they are sufficient for the development of a preliminary training environment. Bestowing said interface with haptic feedback and an electrophysiology component that could access the hypothetical surgeon's stress level and constrict his/her movements accordingly, would further add to its cause in educational endeavors.

With these premises in mind, we set out to create one such a platform. The first order of business was to model a standard surgical tool, such as the scalpel. Using Maya, we came up with the design that figure 5.26 showcases.

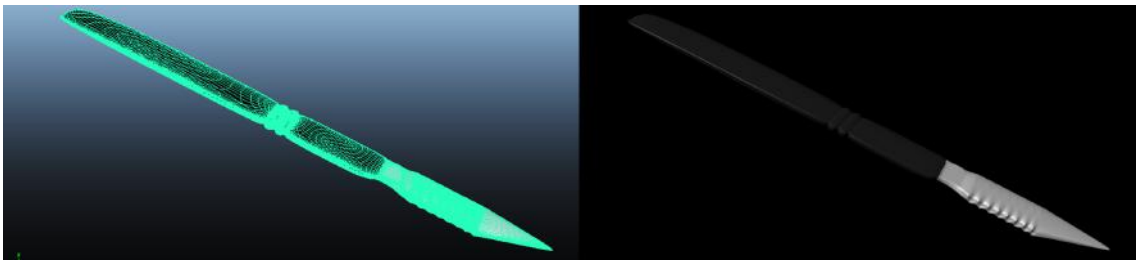

Figure 5.26: Maya visualizations of the scalpel model that was created for the Surgery Simulator, both in shaded wireframe mode and rendered mode.

Thereupon, we were left with the task of conceiving a deformable object that would serve as a proxy for the actual body of the patient. In order to enable the conveyance of tactile feedback, this surrogate had to have a physical component to it, *i.e.*, a collision detection mechanic. For this, we used Unity's particle system and created a grid that emulates a planar membranous structure, resembling human skin (visible in figure 5.27).

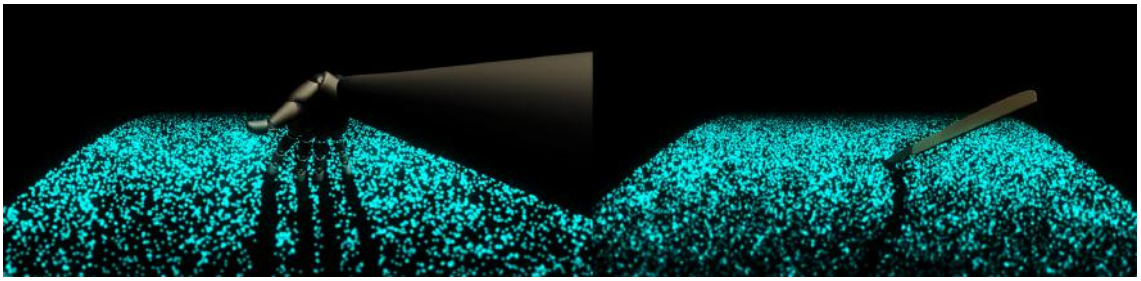

Figure 5.27: Screenshots of an execution of our Surgery Simulator application. The picture on the left shows the user interacting with the deformable membrane with his hand whereas the one on the right depicts an interaction with our custom-made scalpel.

Having laid out the foundations for the construction of our simulator, all that remained was to implement the actual haptic and electrophysiological aspects that would complement it.

Haptics-wise, the devised approach resembles the ones we have examined thus far. When the user's reconstructed hands collide with a haptically responsive object, such as our particle grid, a tactile sensation is produced by the HMB in the appropriate tactor units. However, seeing as this is the first application to feature tool tracking, we had to formulate a vibration pattern that would mimic that which is felt when we touch an object indirectly, through a tool. To do this, we arbitrated that whenever a collision between the tip of the tool and an haptic game object was detected, the HMB would produce a vibration in the index, middle and thumb tactor units that was proportional in intensity to the velocity of the tool's end-effector.

As far as electrophysiology is concerned, we focused mainly on the acquisition and processing of the user's ECG and EDA signals. Using the heart rate and SCRs we were able to extract from these tracings, we defined a rudimentary stress metric. After an initial calibration in which the user's basal pulse and SCL are asserted, we start delimiting the range of his/her motions in accordance to the level of stress that is being recorded. In other words, the sensitivity of the Leap Motion© controller to the movements of hands and/or tools is defined by the user's state of stress. Besides eradicating spurious and heedless actions on the trainee's end, this approach provides educators and overseers with valuable information that could prove useful when it came to the evaluation of the student in question.

As was the case with Ode to PHL, the scope of this dissertation prevented us from directing any actual user trials. Even so, we were satisfied with the exploratory results, limited as their were.

Chapter 6

Conclusions

6.1 Final Thoughts

The present dissertation revolved around the gathering of state the art VR/AR media and their subsequent integration with a wearable device of our own design - a glove that is capable of conveying tactile feedback to its wearer while simultaneously acquiring and processing his/her ECG, EMG and EDA tracings, the Haptic Mitt Bit.

The ensuing conclave of software and hardware is a versatile framework that enables the development of cohesive interfaces, featuring aspects of virtual reality, motion capture, multisensory stimulation and electrophysiological computing. Provided one has access to each and every constituent of said framework, *i.e.* a DK1/DK2 from Oculus Rift©, a Leap Motion© controller with the appropriate VR/AR mount (official or otherwise), an Arduino© prototyping board and a Bitalino© device, he/she needs but to follow simple directives in order to start designing multimodal experiences in Unity3D©.

Though not at all restricted to them, clinical and educational themes were what prompted the assemblage of the proposed framework. As such, when the time to deploy it was due, we restricted ourselves to the conception of interfaces that could be set to purpose in the aforesaid fields. Cursory as they yet are, the developed applications have nonetheless scratched the surface of what we hold as possible to achieve with our system.

Among these, Brain Connectivity Leap stands as the magnum opus of what was produced. A visualization tool that by exploiting all the aforementioned capabilities of our development suite and complementing them with external programs (*e.g.* Matlab©, Maya©, Freesurfer©, TrackVis© and MIBCA) allows for a qualitative analysis of brain connectivity data in a visceral albeit simplified way. To the best of our knowledge, this constitutes a novel approach in dealing with connectome-related data that therefore deems BCL as potentially appealing to researchers, educators and clinicians alike.

Furthermore, our repertoire also includes the less polished Ode to PHL and Surgery Simulator applications. The former uses the haptic module of HMB to steadily stimulate the user's muscle memory in the hopes that by doing so, he/she will unwittingly retain the sequence in which said stimuli were applied, effectively enabling the learning of simple piano passages. If properly ameliorated and validated by preliminary group studies, this could prove an invaluable tool in rehabilitation for patients with motor impairments. The latter on the other hand, was our first attempt at designing a haptically responsive simulator environment for medical training. By measuring, processing and then merging the trainee's ECG and EDA signals into an embryonic stress metric, this application is able to restrict the movement of his/her hands as well as that of the tool he/she wields. In addition to preventing unwanted drifts that would otherwise issue catastrophic results in a real surgical scenario, the fact that the mentioned biosignals are registered and ergo susceptible to *a posteriori* analysis on the educator's end could translate into more quantitative, accurate and insightful evaluations.

6.2 Limitations

As it is often the case in thesis such as this one, there was no shortage of setbacks and obstacles during its campaign, of which time constraints were by far the most hindering. By no means are we oblivious to the fact that deadlines affect all uniformly and are often used as alibis for less than desirable results. Nevertheless, we could not go without mentioning its weight in some of our decisions. Namely the choice of ERM motors as HMB's tactile actuators, which reflected not only budgetary limitations but also temporal ones, seeing as alternatives such as LRAs would have required specialized driving integrated circuits that in turn would demand that our driving circuitry be adapted to PCB. It is only admissible to assume that this would have been both a time-consuming and expensive endeavor, hence one that we could not afford to pursue. Additionally, it cannot be left tacit that we would have preferred to have used our own integral design for the glove's textile components, but once again, schedule limitations along with third-party dependencies instigated us to seek safer courses of action. Lastly, as we have briefly voiced in the previous chapter, both Ode to PHL and Surgery Simulator would have benefited deeply if a little extra time had been put towards their improvement and validation.

On a different note, the adaptable and extensible manner in which BCL was developed all but begged for extra datasets with which to test its performance. Its scarcity notwithstanding, let it be stated that we could not be more grateful for the data that was made available to us, and to all who collaborated in its acquisition and preparation.

As far as distribution is concerned, we are aware that that of our framework's software could be made more amenable to dissemination. As is it is now, the sole impediment to creating a single Unity3D© package that could easily and gratuitously be redistributed among the research community is the fact that the communication between the Arduino© UNO Rev3 and Unity is regulated by Uniduino©, which is itself a paid package.

6.3 Future Work

If anything, the limitations that we have just gone through and all the discussions that stemmed from them strengthened our resolve and filled us with plans for the future. Amid these, the following warrant particular consideration:

- **Exploration of alternative tactors for HMB**: As we have have addressed in section 2.3.2, there are several other vibration actuators besides the ERM motors. Some of which have notoriously better haptic responses and would thus be more suitable for the role of HMB's tactor units;
- **Circumvention of HMB's dependency on Uniduino©**: By establishing our own communication protocol between Unity3D© and Arduino©'s prototyping boards we would greatly add to our framework's appeal among developers and students who otherwise might be reluctant to utilizing it;
- **Condensation of HMB's electronics into a single wireless module**: This would be the next logical step, as it would enable us to build a more compact, portable and lightweight version of HMB. Presumably, this could be the turning point at which we would forego both the Arduino© and the Bitalino© prototyping platforms;
- **Substitution of HMB's wiring with embedded conductive thread** Yet another step towards wearability and perchance even a consumer product. At this stage it would be almost mandatory to design a glove from the ground up, which would also sate our longing for doing so;
- **Pilot studies for concept validation**: This would be an irrevocable task if the applications we developed are ever to be adopted in any and all sorts of both academic pursuits and clinical practices;
- **Testing BCL in the 280° cave at the Imperial College of London**: Postliminary to our oral presentation of BCL in this year's Brain Informatics & Health (BIH) conference (examined at greater depth in appendix A), an invitation for the adaptation of BCL to the 280° immersion room at the university was extended. If all goes as planned, we shall proceed with said undertaking come the end of October;
- **Complementing Surgical Simulator with a robotic arm**: Associating the motion of a tool with a robot's end-effector has been an enduring ambition of ours ever since we first saw Leap Motion©'s tool tracking potential;
- **Introducing EEG to HMB's electrophysiolgy component**: The irony of building a connectome visualization tool that is able to ponder ECG, EMG and EDA readings into its operation but does not do so for Electroencephalography (EEG) acquisitions is not lost with us. In fact, as we "speak" there is another master's thesis that is addressing this very issue.

6.4 Contributions

Throughout this project's journey, there have been many collaborations of as much a scientific nature as a colloquial one. Befitting its conclusion, some of the most prominent of these are summarized below in a chronological fashion:

- **Museum of Universal Values (MUV)**: Ever since this year's 27th of April, IBEB and iLIDH have been actively collaborating towards the creation of a live sciences museum in Mafra that will feature VR in most of its exhibits. As a result, I was granted access to a DK2 HMD as well as a standard bachelor's scholarship (cc 6248-1A PT) in reciprocity for the development of two carefully scripted applications;
- **BITalino-Unity integration tutorial**: In an unspoken contract type of dealing, it was agreed upon that in exchange for the loan of both a standard board and a freestyle kit from Bitalino©, I was to produce a video tutorial in which I would explain how to integrate Unity3D© with the BITalino-Unity API. A compromise I gladly accepted. The resulting video is now featured at Bitalino©'s official webstite;
- **Participation in *Noites de Ciência, Noites de Luz***: In celebration of the international year of light, the Faculty of Sciences of the University of Lisbon has organized a series of monthly lectures and demonstrations directed at the general public. On the 26th of June, we showcased an early version of BCL in one such a session;
- **Participation in Lisbon Machine Learning School (LxMLS) 2015**: The LxMLS Demo Day is an informal gathering that brings together a number of highly technical companies and research facilities alongside their savvy students, with the goal of solving current machine learning problems. I was fortunate enough to participate with BCL in this year's edition, which was hosted at *Instituto Superior Técnico*;
- **Participation in the Brain Informatics & Health (BIH) 2015 conference** The BCL-related abstract that was submitted, accepted and orally presented as a type-II paper at this year's BIH conference (held in London) can be found apace with its corresponding poster in appendix A;
- **Participation in *II Congresso Internacional da Saúde Gaia-Porto* (IICISGP)**: An abstract regarding BCL's most up to date version was submitted and accepted for an oral/poster presentation at the international congress of health that is to take place in Gaia-Porto between the 19th and the 21st of November, 2015 (see appendix B);
- **Online Presence & Visibility**: On a more relaxed yet still relevant closing statement, it is worth noting that BCL is currently featured in a multitude of VR galleries and stores. Among the ones hosted by Leap Motion©, Oculus Rift©, Unimersiv© and WEARVR©, it has amassed close to 1 000 downloads and 7 000 visualizations. Granting that it is directed at a much smaller niche, our Leap Rift mount is not straggling far behind with its total of 250 views and 40 downloads at Thingiverse®.

Bibliography

[1] M. F. Alhamid, M. Eid, and A. El Saddik. "A multi-modal intelligent system for biofeedback interactions". In: *MeMeA 2012 - 2012 IEEE Symposium on Medical Measurements and Applications, Proceedings* (2012), pp. 1–5.

[2] Arduino. *LilyPad*. 2015. URL: https://www.arduino.cc/en/Main/ArduinoBoard/LilyPad (visited on 09/12/2015).

[3] Arduino. *UNO Rev3*. 2015. URL: https://store.arduino.cc/product/A000066 (visited on 09/12/2015).

[4] X. D. Arsiwalla, R. Zucca, A. Betella, E. Martinez, D. Dalmazzo, P. Omedas, G. Deco, and P. F. M. J. Verschure. "Network dynamics with BrainX3: a large-scale simulation of the human brain network with real-time interaction". In: *Frontiers in Neuroinformatics* 9.February (2015), pp. 1–14.

[5] M. Azadi and L. A. Jones. "Vibrotactile actuators: Effect of load and body site on performance". In: *IEEE Haptics Symposium, HAPTICS* (2014), pp. 351–356.

[6] M. Barandas. "Range of Motion Measurements Based on Depth Camera for Clinical Rehabilitation". MSc thesis. Faculdade de Ciências e Tecnologia - Universidade NOVA de Lisboa, 2013.

[7] E. Barnes. *Radiology, News, Education, Service*. 2012. URL: http://www.auntminnie-europe.com/index.aspx?sec=ser\&sub=def\&pag=dis\&ItemID=606734 (visited on 09/07/2015).

[8] P. W. Battaglia, J. B. Hamrick, and J. B. Tenenbaum. "Simulation as an engine of physical scene understanding." In: *Proceedings of the National Academy of Sciences of the United States of America* 110.45 (2013), pp. 18327–32.

[9] T. E. J. Behrens and O. Sporns. "Human connectomics". In: *Current Opinion in Neurobiology* 22.1 (2012), pp. 144–153.

[10] M. Benali-khoudja, M. Hafez, and J.-m. Alexandre. "Tactile interfaces : a state-of-the-art survey". In: *35th Interational Symposium on Robotics* 23-26 March (2004).

[11] W. M. Bergmann Tiest, N. D. Kosters, A. M. L. Kappers, and H. A. M. Daanen. "Haptic perception of wetness". In: *Acta Psychologica* 141 (2012), pp. 159–163.

[12] G Bianchi, B Knoerlein, G Szekely, and M Harders. "High Precision Augmented Reality Haptics". In: *Simulation* 6 (2006), pp. 169–178.

[13] A. Binstock. *Powering the Rift*. 2015. URL: https://www.oculus.com/en-us/blog/powering-the-rift/ (visited on 09/09/2015).

[14] J. W. Bohland, H. Bokil, C. B. Allen, and P. P. Mitra. "The brain atlas concordance problem: Quantitative comparison of anatomical parcellations". In:*PLoS ONE* 4.9 (2009).

[15] C. P. Botha, B. Preim, and A. Kaufman. "From individual to population: Challenges in Medical Visualization". In: *arXiv preprint* (2012), pp. 1–19. arXiv: 1206.1148.

[16] L. Bouarfa, P. Bembnowicz, B. Crewther, D. Jarchi, and G. Z. Yang. "Profiling visual and verbal stress responses using electrodermal heart rate and hormonal measures". In: *2013 IEEE International Conference on Body Sensor Networks, BSN 2013* (2013).

[17] J. Braithwaite, D. Watson, J. Robert, and R. Mickey. "A Guide for Analysing Electrodermal Activity (EDA) & Skin Conductance Responses (SCRs) for Psychological Experiments". In: (2013), pp. 1–42.

[18] Y. O. Carrim. *SA Medical - General Medicine questions: The Cardiovascular system, Heart Muscle, The Heart as a pump*. 2010. URL: http://samedical.blogspot.pt/2010/08/heart-muscle-heart-as-pump.html (visited on 10/04/2015).

[19] R. H. Chowdhury, M. B. I. Reaz, M. A. B. M. Ali, A. A. A. Bakar, K. Chellappan, and T. G. Chang. "Surface electromyography signal processing and classification techniques." In: *Sensors (Basel, Switzerland)* 13.9 (2013), pp. 12431–12466.

[20] G. Conte, A. Q. Ye, A. G. Forbes, O. Ajilore, and A. Leow. "BRAINtrinsic : A Virtual Reality-Compatible Tool for Exploring Intrinsic Topologies of the Human Brain Connectome". In: *Interational Conference on Brain Informatics and Health* August-September (2015), pp. 1–10.

[21] C. J. De Luca, A. Adam, R. Wotiz, L. D. Gilmore, and S. H. Nawab. "Decomposition of surface EMG signals". In: *J Neurophysiol* 96.3 (2006), pp. 1646–1657.

[22] R. S. Desikan, F. Ségonne, B. Fischl, B. T. Quinn, B. C. Dickerson, D. Blacker, R. L. Buckner, A. M. Dale, R. P. Maguire, B. T. Hyman, M. S. Albert, and R. J. Killiany. "An automated labeling system for subdividing the human cerebral cortex on MRI scans into gyral based regions of interest". In: *NeuroImage* 31.3 (2006), pp. 968–980.

[23] C. Destrieux. "Automatic parcellation of human cortical gyri and sulci using standard anatomical nomenclature". In: *NeuroImage* 34.1 (2010), pp. 1–15.

[24] L. Dos, S. Machado, M. Cristina, and F. D. E. Oliveira. "Realidade Virtual: Definições, Dispositivos e Aplicações". In: *Revista Eletrônica de Iniciação Científica da SBC* (2002), pp. 1–33.

[25] DutchOps. *Gyroscopes Theory - DutchOps.com powered*. 2009. URL: http://www.dutchops.com/Portfolio_Marcel/Articles/Instruments/Gyroscopic_Instruments/Theory_Gyroscopes.htm (visited on 10/07/2015).

[26] EMBS. *Biomedical Signal Processing - Engineering in Medicine and Biology Society*. 2014. URL: http://www.embs.org/about-biomedical-engineering/our-areas-of-research/biomedical-signal-processing/ (visited on 08/19/2015).

[27] K. Friston. "Functional and effective connectivity: a review." In: 1.1 (2011).

[28] E. Games. *Unreal Engine*. 2015. URL: https://www.unrealengine.com/what-is-unreal-engine-4 (visited on 09/14/2015).

[29] V. Geroimenko. "Augmented reality technology and art: The analysis and visualization of evolving conceptual models". In: *Proceedings of the International Conference on Information Visualisation* (2012), pp. 445–453.

[30] Gloveone. *Gloveone: Feel Virtual Reality by NeuroDigital Technologies*. 2015. URL: https://www.kickstarter.com/projects/gloveone/gloveone-feel-virtual-reality/description (visited on 09/10/2015).

[31] B. E. Griffith. "Electrophysiology". In: (2013).

[32] J. Hartshorne. *The Video Game Engine in Your Head*. 2014. URL: http://www.scientificamerican.com/article/the-video-game-engine-in-your-head/?print=true (visited on 09/06/2015).

[33] M. P. van den Heuvel and O. Sporns. "Rich-Club Organization of the Human Connectome". In: *Journal of Neuroscience* 31.44 (2011), pp. 15775–15786.

[34] C.-p. Hsiao, R. Li, X. Yan, and E. Y.-l. Do. "Tactile Teacher : Sensing Finger Tapping in Piano Playing". In: *Proceedings of the 9th International Conference on Tangible, Embedded, and Embodied Interaction - TEI '15* (2015), pp. 257–260.

[35] HTC. *HTC Vive*. 2015. URL: http://www.csmonitor.com/Technology/2015/0304/HTC-Vive-review-roundup-Virtual-reality-gets-real (visited on 09/10/2015).

[36] Intel. *Open Source Game Development | Intel® Developer Zone*. 2012. URL: https://software.intel.com/en-us/articles/open-source-game-development (visited on 09/06/2015).

[37] H. Kalagher and S. S. Jones. "Young children's haptic exploratory procedures". In: *Journal of Experimental Child Psychology* 110 (2011), pp. 592–602.

[38] M. G. Kevin Koch, Thor Walker, Yi Ji, Kevin Gravesmill, Julia Kwok. *HandsOmni*. 2015. URL: http://news.rice.edu/2015/04/22/gamers-feel-the-glove-from-rice-engineers/ (visited on 09/10/2015).

[39] J. Kim and H. Jun. "Implementation of image processing and augmented reality programs for smart mobile device". In: *Proceedings of the 6th International Forum on Strategic Technology, IFOST 2011* 2 (2011), pp. 1070–1073.

[40] D. Kohlsdorf and T. Starner. "Mobile music touch: The effect of primary tasks on passively learning piano sequences". In: *Proceedings - International Symposium on Wearable Computers, ISWC*. 2010.

[41] H. E. Krugman and E. L. Hartley. "Passive Learning from Television". In: *Public Opinion Quarterly* 34.2 (1970), pp. 184–190.

[42] D. Levac, S. Glegg, and P. Miller. "Supporting therapists to integrate virtual reality systems within clinical practice : A knowledge translation study". In: (2013), pp. 204–205.

[43] J. Lobo and P. Trindade. "Interactive demonstration of InerTouchHand - iTH: A glove device with distributed inertial sensors and vibro-tactile feedback". In: *Proceedings - 2013 2nd Experiment@ International Conference, exp.at 2013* (2013), pp. 178–179.

[44] Z. Lv, A. Tek, F. Da Silva, C. Empereur-mot, M. Chavent, and M. Baaden. "Game On, Science - How Video Game Technology May Help Biologists Tackle Visualization Challenges". In: *PLoS ONE* 8.3 (2013).

[45] Z. Ma, S. Member, P. Ben-tzvi, and S. Member. "RML Glove — An Exoskeleton Glove Mechanism With Haptics Feedback". In: 20.2 (2015), pp. 641–652.

[46] E. Macdonald, R. Salas, D. Espalin, M. Perez, E. Aguilera, D. Muse, and R. B. Wicker. "3D Printing for the Rapid Prototyping of Structural Electronics". In: *IEEE Access* 2 (2014), pp. 234–242.

[47] K. E. MacLean. "Putting haptics into the ambience". In: *IEEE Transactions on Haptics* 2.3 (2009), pp. 123–135.

[48] T. Markow, N. Ramakrishnan, K. Huang, T. Starner, M. Eicholtz, S. Garrett, H. Profita, a. Scarlata, C. Schooler, A. Tarun, and D. Backus. "Mobile Music Touch: Vibration stimulus in hand rehabilitation". In: *Pervasive Computing Technologies for Healthcare (PervasiveHealth), 2010 4th International Conference on Assistive Technologies* (2010).

[49] D. Marr. "Vision - A Computational Investigation into the Human Representation and Processing of Visual Information". In: 1982, p. 3.

[50] P. Microdrives. *Discrete Driver Circuits for Vibration Motors Guide*. URL: http://www.precisionmicrodrives.com/application-notes-technical-guides/application-bulletins/ab-001-discrete-driver-circuits-for-vibration-motors (visited on 09/16/2015).

[51] P. Microdrives. *How To Drive A Linear Resonance Vibration Actuator*. 2015. URL: http://www.precisionmicrodrives.com/application-notes-technical-guides/application-bulletins/ab-003-how-to-drive-linear-resonance-actuators-lra-vibrating-motors (visited on 08/22/2015).

[52] P. Microdrives. *Linear Resonant Actuator Characteristics - Precision Microdrives*. 2015. URL: http://www.precisionmicrodrives.com/application-notes-technical-guides/application-bulletins/ab-020-understanding-linear-resonant-actuator-characteristics (visited on 08/21/2015).

[53] P. Microdrives. *Linear Resonant Actuator Vibrator Motors Guide | for Haptic Feedback*. 2015. URL: http://www.precisionmicrodrives.com/vibrating-vibrator-vibration-motors/linear-resonant-actuator-lra-haptic-vibration-motors (visited on 08/21/2015).

[54] P. Microdrives. *Understanding Eccentric Rotating Mass (ERM) Vibration Motor*. 2015. URL: http://www.precisionmicrodrives.com/application-notes-technical-guides/application-bulletins/ab-004-understanding-erm-characteristics-for-vibration-applications (visited on 08/20/2015).

[55] MIT. *The Future of Medical Visualisation | MIT Technology Review*. 2012. URL: http://www.technologyreview.com/view/428134/the-future-of-medical-visualisation/ (visited on 09/07/2015).

[56] L. Motion. *How Does the Leap Motion Controller Work?* 2014. URL: http://blog.leapmotion.com/hardware-to-software-how-does-the-leap-motion-controller-work/ (visited on 09/05/2015).

[57] L. Motion. *VR Best Practices Guidelines*. Tech. rep. 2015.

[58] P. Nogueira. *Motion Capture Fundamentals*. Tech. rep. 2011.

[59] J Perry, C. S. Easterday, and D. J. Antonelli. "Surface versus intramuscular electrodes for electromyography of superficial and deep muscles." In: *Physical therapy* 61.1 (1981), pp. 7–15.

[60] H. Plácido and A. Fred. "Biosignals for Everyone". In: (2014), pp. 64–71.

[61] Plux. *Electrocardiography (ECG) Sensor Data Sheet*. Tech. rep. 2015.

[62] Plux. *Electrodermal Activity (EDA) Sensor Data Sheet*. Tech. rep. 2015.

[63] Plux. *Electromyography (EMG) Sensor Data Sheet*. Tech. rep. 2015.

[64] Q. L. Qiao. "Electrophysiology course with quantitative method". In: *ITME2009 - Proceedings 2009 IEEE International Symposium on IT in Medicine and Education* (2009), pp. 706–710.

[65] A. S. Ribeiro, L. M. Lacerda, and H. A. Ferreira. *MIBCA*. 2015. URL: http://www.mibca.com/ (visited on 09/18/2015).

[66] A. S. Ribeiro, L. M. Lacerda, and H. A. Ferreira. "Multimodal Imaging Brain Connectivity Analysis (MIBCA) toolbox". In: *PeerJ* 3 (2015), e1078.

[67] R. Ribeiro, F. Henriques, and H. A. Ferreira. "Desenvolvimento de uma interface de visualização de conectividade cerebral usando realidade virtual e controlo por gestos". PhD thesis. Faculdade de Ciências e Tecnologia - Universidade NOVA de Lisboa, 2014.

[68] O. Rift. *Oculus Best Practices*. Tech. rep. 2015.

[69] D. Robotics. *Dexmo f2*. 2014. URL: http://www.dextarobotics.com/ (visited on 10/07/2015).

[70] D. A. Rodriguez-Silva, F. Gil-Castineira, F. J. Gonzalez-Castano, R. J. Duro, F. Lopez-Pena, and J. Vales-Alonso. "Human Motion Tracking and Gait Analysis: a Brief Review of Current Sensing systems and Integration with Intelligent Environments". In: *2008 International Conference on Virtual Environments, Human-Computer Interfaces, and Measurement Systems* July (2008), pp. 14–16.

[71] N. Rossol, I. Cheng, R. Shen, and A. Basu. "Touchfree Medical Interfaces". In: (2014), pp. 6597–6600.

[72] Samsung. *Gear VR Innovator Edition for GS6 and GS6 edge*. 2015. URL: http://www.samsung.com/us/mobile/wearable-tech/SM-R321NZWAXAR (visited on 09/10/2015).

[73] Samsung. *Samsung Gear VR*. 2015. URL: http://www.samsung.com/global/microsite/gearvr/gearvr_specs.html (visited on 09/10/2015).

[74] C. Seim, J. Chandler, K. Desportes, S. Dhingra, M. Park, and T. Starner. "Passive Haptic Learning of Braille Typing". In: (2014).

[75] C. Seim, T. Estes, and T. Starner. "Towards Passive Haptic Learning of Piano Songs". In: (2015), pp. 445–450.

[76] C. Setz, B. Arnrich, J. Schumm, R. L. Marca, G. Tr, and U. Ehlert. "Using a Wearable EDA Device". In: 14.2 (2010), pp. 410–417.

[77] SHIVR. *SHIVR piezoelectric haptic actuators | Pack & Tactor*. 2015. URL: http://www.mide.com/products/shivr-haptics/SHIVR-piezoelectric-haptic-actuators.php (visited on 08/21/2015).

[78] E. Siegel. *Haptics technology: picking up good vibrations*. 2011. URL: http://www.eetimes.com/document.asp?doc_id=1278948 (visited on 10/04/2015).

[79] Sony. *Project Morpheus*. 2015. URL: https://www.playstation.com/pt-pt/explore/ps4/features/project-morpheus/ (visited on 09/09/2015).

[80] O. Sporns. "Structure and function of complex Brain Networks". In: (2013), pp. 247–262.

[81] U. Technologies. *Unity3D*. URL: http://unity3d.com/ (visited on 09/14/2015).

[82] Texas Instruments. "Haptics Solutions for ERM and LRA". In: (2013).

[83] Thalmic Labs. *Myo Gesture Control Armband*. 2015. URL: https://www.myo.com/techspecs (visited on 09/13/2015).

[84] S. P. Tomlinson, N. J. Davis, H. M. Morgan, and R. M. Bracewell. "Hemispheric specialisation in haptic processing". In: *Neuropsychologia* 49.9 (2011), pp. 2703–2710.

[85] N Tzourio-Mazoyer, B Landeau, D Papathanassiou, F Crivello, O Etard, N Delcroix, B Mazoyer, and M Joliot. "Automated anatomical labeling of activations in SPM using a macroscopic anatomical parcellation of the MNI MRI single-subject brain." In: *NeuroImage* 15.1 (2002), pp. 273–289.

[86] B. Y. University. *TekBots - Accelerometer MMA*. URL: http://eecs.oregonstate.edu/education/hardware/accelerometer/ (visited on 10/07/2015).

[87] P. F. M. J. Verschure. *BrainX3*. 2015. URL: http://www.brainx3.com (visited on 09/15/2015).

[88] N. VR. *Nimble Sense: Bring Your Hands into Virtual Reality & Beyond by Nimble VR*. 2014. URL: https://www.kickstarter.com/projects/nimblevr/nimble-sense-bring-your-hands-into-virtual-reality (visited on 09/13/2015).

[89] H. Wang, D. Kaleas, R. Ruuspakka, and R. Tartz. "Haptics using a smart material for eyes free interaction in mobile devices". In: *Haptics Symposium 2012, HAPTICS 2012 - Proceedings* 1714 (2012), pp. 523–526.

[90] S. Wei and Z. Wen-qi. "Virtual Reality Technology in Modern Medicine". In: (2010), pp. 557–561.

[91] P Wellman, W Peine, G Favalora, and R Howe. "Mechanical Design and Control of a High-Bandwidth Shape Memory Alloy Tactile Display". In: *In International Symposium on Experimental Robotics* June (1997), pp. 56–66.

[92] A. Wright. "The touchy subject of haptics". In: *Communications of the ACM* 54 (2011), p. 20.

[93] J. Xie. "Research on key technologies base Unity3D game engine". In: *ICCSE 2012 - Proceedings of 2012 7th International Conference on Computer Science and Education* Iccse (2012), pp. 695–699.

[94] K. Yang. "Research and application of new inserted shape memory alloy actuators". In: *IEEE Transactions on Industrial Electronics* 57.8 (2010), pp. 2845–2850.

[95] C. Youngblut, R. E. Johnston, S. H. Nash, R. A. Wienclaw, and C. A. Will. In: July (1996), pp. 117–123.

[96] H. Zhou and H. Hu. "Human motion tracking for rehabilitation-A survey". In: *Biomedical Signal Processing and Control* 3.1 (2008), pp. 1–18.

Appendix

International Conference on Brain Informatics & Health 2015

The present appendix contains both the abstract and the accompanying poster that were presented in this year's edition of BIH, which was held at the Royal Geographical Society[1] in London between the 31st of August and September 2nd. These documents were subsequently featured in the locally published BIH 2015 type-II proceedings.

[1] Adjacent to the Imperial College of London.

Brain Connectivity Leap: Interacting with the Brain Connectome

Filipe Sobreira Rodrigues[1,2], Ricardo Ribeiro[1], Hugo Alexandre Ferreira[1]
(1) Universidade de Lisboa, Faculdade de Ciências, Instituto de Biofísica e Engenharia Biomédica, Campo Grande, 1749-016 Lisboa, Portugal
(2) Universidade Nova de Lisboa, Faculdade de Ciências e Tecnologia, Departamento de Física, Quinta da Torre, 2829-516, Caparica, Portugal

Abstract: Visualizing the brain in a comprehensive and intuitive manner is a challenging feat. This is particularly true in the age of big data, where brain data is being provided from multiple sources ranging from genetics and neuropsychological testing to electrophysiology and neuroimaging.

Here, we present Brain Connectivity Leap (BCL), an application for seamless visualization and interaction with the brain and brain connectivity data, based on featuring aspects of Virtual Reality, Gesture Recognition and Haptic Feedback. This application is developed in a Unity3D environment into which a model reconstruction of a subject's brain is imported alongside with his/her demographic (e.g. age, gender), neuropsychological (e.g. mini-mental state examination scores), imaging (e.g. cortical thickness and fractional anisotropy) and connectivity data (e.g. graph theory metrics such as node degree and global efficiency). In particular, the brain graph visualization itself is made possible through processing of imported connectivity matrices. Subject-specific brain image models and connectivity matrices can be prepared resorting to different software tools such as Freesurfer and Diffusion Toolkit for example. Alternatively, the Multimodal Imaging Brain Connectivity Analysis toolbox (http://www.mibca.com) can be used. MIBCA consists of an application that pre-processes and analyses both MRI and PET data and computes connectivity matrices and related graph theory metrics in a straightforward manner. BCL makes use of the Leap Motion controller, a hand tracking device that enables the user to navigate and interact with the virtual brain and connectome using a library of gestures and mechanics developed for the effect. The interaction includes: moving (translation/rotation) and expanding the brain model and its connectivity network; toggling on/off the visualization, and adjusting the color palette/transparency/rendering of these elements; toggling on/of the visualization of demographic, neuropsychological, imaging and graph data; selection of specific regions-of-interest and displaying their correspondent regional connections and existing complementary data. The BCL experience can be enhanced through usage of a specially developed haptic glove that makes use of the Arduino platform interfaced with Unity3D and vibration motors placed at the fingertips and palm of the hand. This glove provides a haptic feedback that is proportional to the strength of a connection when the user virtually "touches" the brain graph. Here, hand and finger positions in the virtual environment are also provided by the Leap Motion interface. Finally, BCL also interfaces with the virtual reality goggles Oculus Rift, enabling a complete immersion of the user in the virtual scenario. This allows the user to "navigate" inside the brain connectome.

We believe that Brain Connectivity Leap is an application that provides a novel and intuitive means of visualizing brain connectivity data, which could appeal to researchers, clinicians, educators, students and enthusiasts.

Keywords: Connectome, Brain Connectivity, Visualization, Virtual Reality, Gesture recognition, Haptic Feedback.

BIH 2015

2015 International Conference on Brain Informatics & Health

30 August – 2 September 2015, London, UK

*contact: hhferreira@fc.ul.pt

BRAIN CONNECTIVITY LEAP. MULTIMODAL INTERACTION WITH THE HUMAN CONNECTOME

B307. F. S. RODRIGUES | R. RIBEIRO | H. A. FERREIRA

KEY FEATURES:

PARCELLATION ATLASES:
- HARVARD-OXFORD CORTICAL & SUBCORTICAL
- AUTOMATED ANATOMICAL LABELING
- DESIKAN-KILLIANY CORTICAL
- DESTRIEUX

MAGNETIC RESONANCE IMAGING DATA:
- T1-WEIGTHED 3D RECONSTRUCTIONS
- DTI ESTIMATED TRACTS

CONNECTIVITY DATA:
- PATIENT DATA
- HEALTHY SUBJECTS REFERENCE

GRAPH COLOR CODING:
- REFERENTIAL
- DIRECTIONAL

VIRTUAL REALITY:
- HEAD TRACKING & DISPLAY
- HAND TRACKING & INTERACTION
- GESTURE RECOGNITION

HAPTIC FEEDBACK
- 6 VIBRATION ACTUATORS

ELECTROPHYSIOLOGICAL FEEDBACK:
- ELECTROCARDIOGRAM
- ELECTRODERMAL ACTIVITY
- ELECTROMYOGRAM

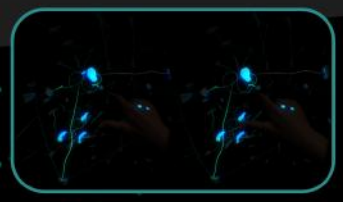
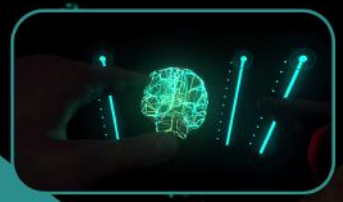


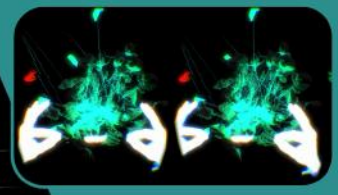


bitalino

unity

oculus

LEAP MOTION

ARDUINO

U LISBOA | UNIVERSIDADE DE LISBOA

IBEB Instituto de Biofísica e Engenharia Biomédica

FCT FACULDADE DE CIÊNCIAS E TECNOLOGIA UNIVERSIDADE NOVA DE LISBOA

FCT Fundação para a Ciência e a Tecnologia

plux

Ciências ULisboa

Research supported by Fundação para a Ciência e Tecnologia (FCT) and Ministério da Ciência e Educação (MCE) Portugal (PIDDAC) under grants UID/BIO/00645/2013 and PTDC/SAU-ENB/120718/2010

Appendix B

II Congresso Internacional da Saúde Gaia-Porto

This appendix includes the abstract that was recently submitted and accepted to the second edition of the International Congress of Health of 2015, that will unfold between the 19th and the 21st of November with the *Auditório Magno* of *Instituto Superior de Engenharia do Porto* as its venue.

Brain Connectivity Leap: Multimodal Interaction with the Human Connectome

Filipe Sobreira Rodrigues[1,2], Ricardo Ribeiro[1], Hugo Alexandre Ferreira[1]
(1) Universidade de Lisboa, Faculdade de Ciências, Instituto de Biofísica e Engenharia Biomédica, Campo Grande, 1749-016 Lisboa, Portugal
(2) Universidade Nova de Lisboa, Faculdade de Ciências e Tecnologia, Departamento de Física, Quinta da Torre, 2829-516, Caparica, Portugal

Abstract: Visualizing the Brain in a comprehensive albeit intuitive manner remains a challenging feat. This holds particularly true in the age of big data, wherein brain-related information is provided by sources ranging from genetics and neuropsychology to electrophysiology and neuroimaging.

Here, we present Brain Connectivity Leap (BCL), a Virtual Reality (VR) interface that features multisensory integration, motion capture and electrophysiology in hopes of providing an innovative, immersive and interactive means of exploring the human Connectome.

BCL is being developed in a Unity3D© environment, into which a 3D mesh of a parcellated brain is imported alongside its demographic, imaging and connectivity data. Subject-specific and atlas-concordant brain models, together with their associated connectivity matrices were prepared with a consortium of software tools, such as Freesurfer©, Maya© and the Multimodal Imaging Brain Connectivity Analysis (MIBCA) toolbox. Navigation-wise, BCL makes use of an Oculus Rift© headset, onto which a Leap Motion© controller is mounted. The designed interaction scheme includes:

- Library of Recognizable Gestures;
- Whole Brain Translation, Rotation, Explosion & Implosion;
- Hand-specific ROI Selection, Translation & Rotation;

The experience can be enhanced through usage of a custom-made wearable haptic device, developed using the Arduino© prototyping platform. Its tactile feedback relies on six vibration actuators, placed at the fingertips and palm of the hand. Additionally, the glove incorporates a customized Bitalino© on its wrist, thus enabling a non-intrusive acquisition of ECG, EDA and EMG tracings.

The integration of the aforementioned tools and methodologies allowed for a qualitative analysis of Brain Connectivity data in a visceral yet simplified way.
We believe this deems BCL as potentially appellative to researchers, clinicians, educators and enthusiasts alike.

Research supported by Fundação para a Ciência e Tecnologia and Ministério da Ciência e Educação Portugal under grants UID/BIO/00645/2013 and PTDC/SAU-ENB/120718/2010.

Keywords: Connectome, Brain Connectivity, Neuroimaging, Electrophysiology, Biofeedback, Haptics, Motion Capture, Virtual Reality, Haptic Feedback.

Appendix C

Relevant Datasheets

Here, we shall present the datasheets of the most vital components that were used in the construction and confection of the beta prototype of the HMB. Namely, those referring to the ERM vibration motors that constitute the tactor units of its haptic feedback module and those pertaining to the sensors comprised in its electrophysiological module.

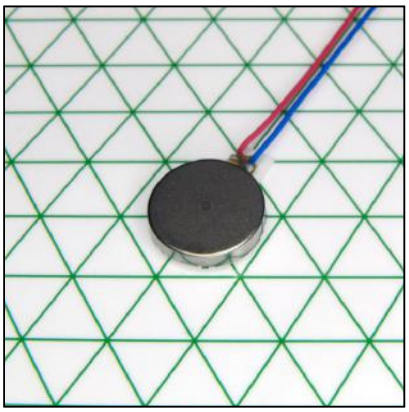

10mm Vibration Motor - 2mm Type
Shown on 6mm Isometric Grid

PRECISION MICRODRIVES™

Product Data Sheet
Pico Vibe™
10mm Vibration Motor - 2mm Type

Model: 310-118

Ordering Information

The model number 310-118 fully defines the model, variant and additional features of the product. Please quote this number when ordering.
For stocked types, testing and evaluation samples can be ordered directly through our online store.

Datasheet Versions

It is our intention to provide our customers with the best information available to ensure the successful integration between our products and your application. Therefore, our publications will be updated and enhanced as improvements to the data and product updates are introduced.
To obtain the most up-to-date version of this datasheet, please visit our website at:
www.precisionmicrodrives.com
The version number of this datasheet can be found on the bottom left hand corner of any page of the datasheet and is referenced with an ascending R-number (e.g. R002 is newer than R001). Please contact us if you require a copy of the engineering change notice between revisions.

If you have any questions, suggestions or comments regarding this publication or need technical assistance, please contact us via email at:
enquiries@precisionmicrodrives.com or call us on +44 (0) 1932 252 482

Key Features

Body Diameter:	10 mm [+/- 0.1]
Body Length:	2.05 mm [+/- 0.1]
Rated Operating Voltage:	3 V
Rated Vibration Speed:	14,000 rpm [+/- 3,500]
Typical Rated Operating Current:	60 mA
Typical Normalised Amplitude:	1.1 G

Typical Vibration Motor Performance Characteristics

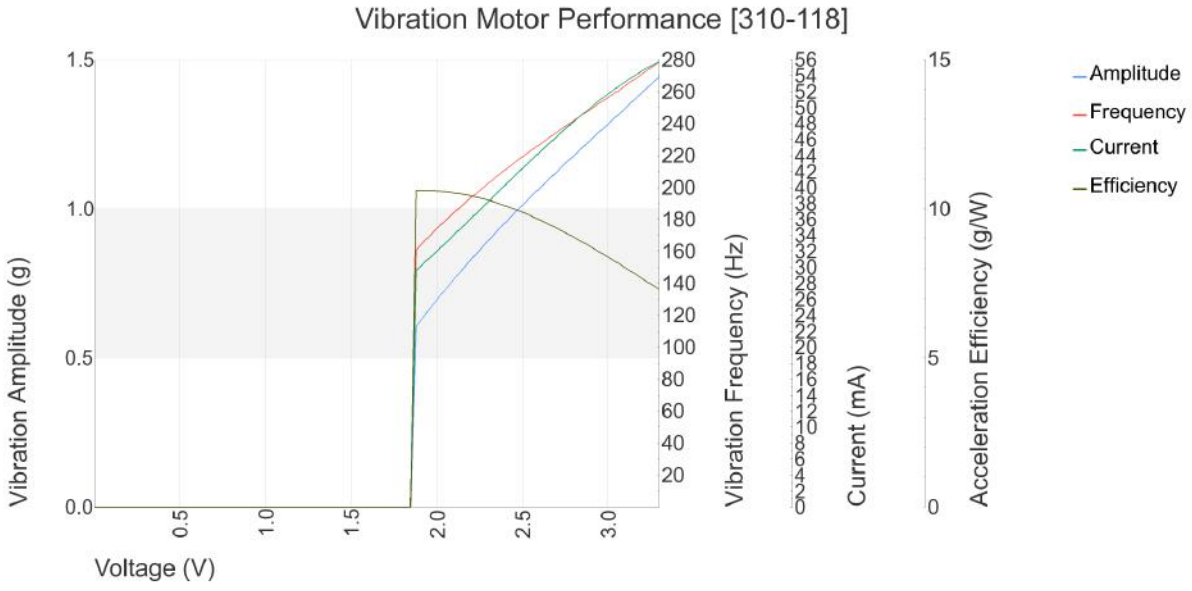

Understanding Precision Microdrives Specification and Production Stages

Precision Microdrives Specification Stages

Precision Microdrives is run on processes and we guide all customers through sets of predefined specification stages as they move from prototype to production. These are designed to allow the flexibility to iterate designs with the eventual certainty required for production parts.

Base	Sampling	Pre-Production	Production	EOL
Used for factory downselection Typically 0 units	Used for validating prototypes Typically ~ 10 units	Used for validating initial production Typically ~ 1k units	Used for validating mass production Typically >5k+ units	Used as basis for product replacement 'Base' spec Typically 0 units

Precision Microdrives Capabilities and Competences

Precision Motor Testing and Motor Testing Services

When we started PMD there were no commercial testing machines available, so we built our own. Ever since we've continued to develop new motor testing machines & procedures each year. Fast forward to today and we now have the most extensive testing facilities in the world for sub 40mm diameter motors, gear motors and vibration motors. These are used to validate motors through specification stages and during manufacturing. We also test motors as a service, provide easy to read reports and assist customers with their interpretation.

Motor Customisation, Design, and Manufacturing

To be useful motors need to be integrated with other parts, such as housings or couplings . We routinely develop and produce complete assemblies, from motors with customised leads or connectors to complete electromechanical mechanisms and integrated control electronics. We will support and guide you through the specification stages from prototype to signing-off for mass production.

Competent and Dependable Supply Chains for Production

Most of the worlds miniature motors are made in Asia, and you need engineers on the factory floor who can maintain the Western values of "doing things right" whilst supporting the Asian values of "getting things done". As a customer you are supported by expert eyes, right at the heart of the manufacturing process where it is needed: On the ground in the UK, Hong Kong, and China.

Quality Engineers on the Ground and Local Engineering Teams

The nature of our business is to confidently produce and supply motors 'On time & To spec'. Our customers benefit from our certified ISO 9001 quality systems, reliable motor production infrastructure, and experience. We have a core competence in helping customers design out over-specified and expensive European drives, with more cost-effective, adequately specified, and verified Asian alternatives.

Physical Specification

PARAMETER	CONDITIONS	SPECIFICATION
Body Diameter	Max body diameter or max face dimension where non-circular	10 mm [+/- 0.1]
Body Length	Excl. shafts, leads and terminals	2.05 mm [+/- 0.1]
Unit Weight		0.8 g

Construction Specification

PARAMETER	CONDITIONS	SPECIFICATION
Motor Construction		Flat Coreless
Commutation		Precious Metal Brush
No. of Poles		6
Bearing Type		Sintered Bronze

Leads & Connectors Specification

PARAMETER	CONDITIONS	SPECIFICATION
Lead Length	Lead lengths defined as total length or between motor and connector	100 mm [+/- 2]
Lead Strip Length		1.5 mm [+/- 0.5]
Lead Wire Gauge		32 AWG
Lead Configuration		Straight

Operational Specification

PARAMETER	CONDITIONS	SPECIFICATION
Rated Operating Voltage		3 V
Rated Vibration Speed	At rated voltage using the inertial test load	14,000 rpm [+/- 3,500]
Max. Rated Operating Current	At rated voltage using the inertial test load	90 mA
Rated Inertial Test Load	Mass of standard test sled	100 g
Max. Start Voltage	With the inertial test load	2.3 V
Min. Vibration Amplitude	Peak-to-peak value at rated voltage using the inertial test load	0.8 G
Max. Operating Voltage		3.3 V
Max. Start Current	At rated voltage	130 mA
Min. Insulation Resistance	At 50V DC between motor terminal and case	10 MOhm

Important: The characteristics of the motor is the typical operating parameters of the product. The data herein offers design guidance information only and supplied batches are validated for conformity against the specifications on the previous page.

Typical Performance Characteristics

PARAMETER	CONDITIONS	SPECIFICATION
Typical Rated Load Power Consumption	At rated voltage and load	180 mW
Typical Rated Operating Current	At rated voltage using the inertial test load	60 mA
Typical Vibration Amplitude	Peak-to-peak value at rated voltage using the inertial test load	1.1 G
Typical Start Current	At rated voltage	100 mA
Typical Vibration Efficiency	At rated voltage using the inertial test load	6.1 G/W
Typical Normalised Amplitude	Peak-to-peak vibration amplitude normalised by the inertial test load at rated voltage	1.1 G
Typical Start Voltage	With the inertial test load	1.8 V
Typical Terminal Resistance		63 Ohm
Typical Terminal Inductance		330 uH

Typical Haptic Characteristics

PARAMETER	CONDITIONS	SPECIFICATION
Typical Lag Time	At rated voltage using the inertial test load	41 ms
Typical Rise Time	At rated voltage using the inertial test load	96 ms
Typical Stop Time	At rated voltage using the inertial test load	128 ms
Typical Active Brake Time	Time taken from steady-state to 0.04 G under inverse polarity at max. voltage	50 ms

Environmental Characteristics

PARAMETER	CONDITIONS	SPECIFICATION
Max. Operating Temp.		60 Deg.C
Min. Operating Temp.		-20 Deg.C
Max. Storage Temp.		70 Deg.C
Min. Storage Temp.		-30 Deg.C

Typical Packing Conditions

PARAMETER	CONDITIONS	SPECIFICATION
Carton Type		Boxed Trays

Product Dimensional Specification

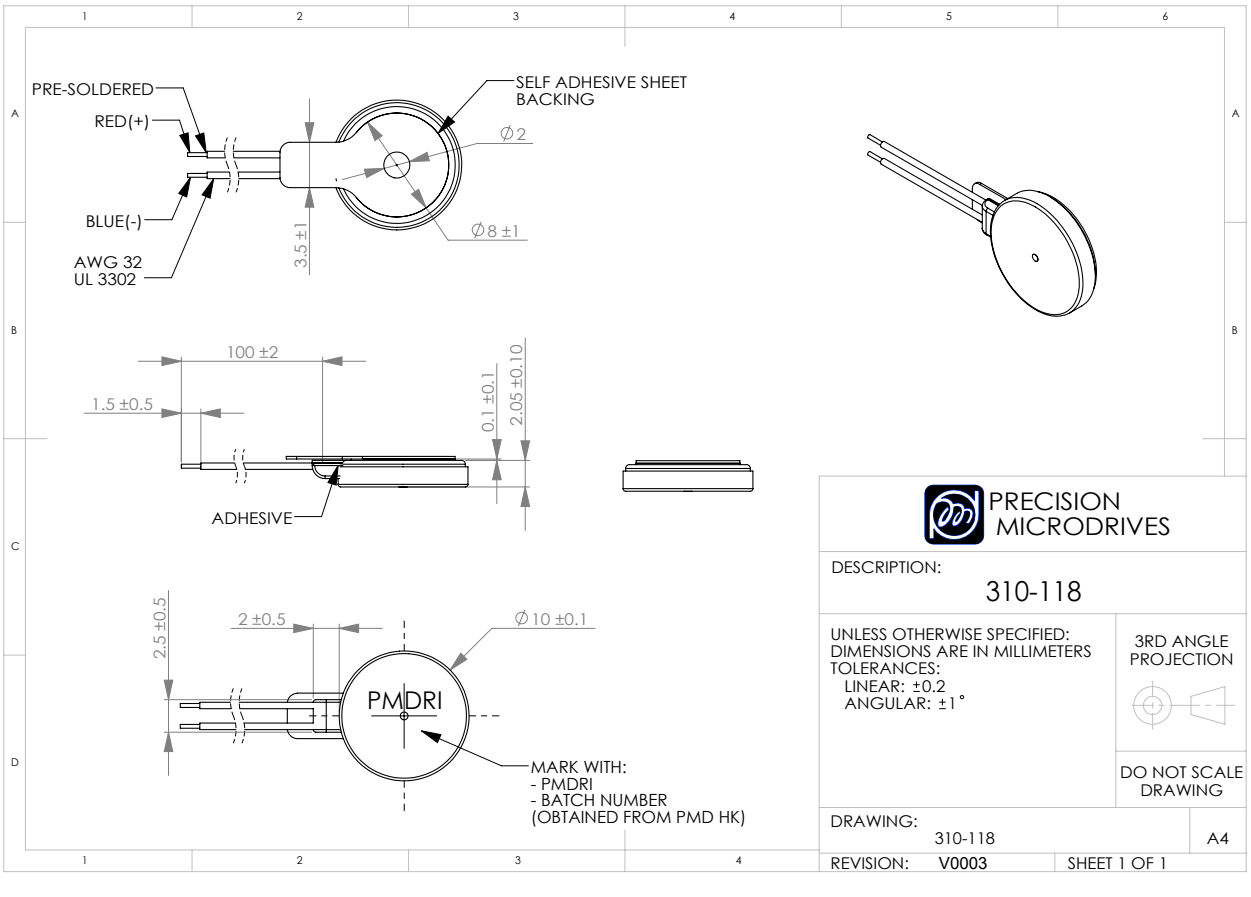

Life Support Policy

PRECISION MICRODRIVES PRODUCTS ARE NOT AUTHORISED FOR USE AS CRITICAL COMPONENTS IN LIFE SUPPORT DEVICES OR SYSTEMS WITHOUT THE EXPRESS WRITTEN APPROVAL OF PRECISION MICRODRIVES LIMITED.
As used herein:

1. Life support devices or systems are devices or systems which, (a) are intended for surgical implant into the body, or (b) support or sustain life, and whose failure to perform when properly used in accordance with instructions for use provided in the labeling, can be reasonably expected to result in a significant injury to the user.

2. A critical component is any component of a life support device or system whose failure to perform can be reasonably expected to cause the failure of the life support device or system, or to affect its safety or effectiveness.

Precision Microdrives Limited

Canterbury Court, 1-3 Brixton Road
London
SW9 6DE
United Kingdom

Tel: +44 (0) 1932 252482
Fax: +44 (0) 1932 325353
Email: enquiries@precisionmicrodrives.com
Web: www.precisionmicrodrives.com

Registered in England and Wales No. 5114621
VAT registration. GB 900 1238 84

Electrocardiography (ECG) Sensor Data Sheet

ECG 080115

SPECIFICATIONS

> **Gain:** 1100
> **Range:** ±1.5mV (with VCC = 3.3V)
> **Bandwidth:** 0.5-40Hz
> **Consumption:** ~4mA
> **Input Impedance:** 100GOhm
> **CMRR:** 110dB
> **Electrodes:** 3 or 2 (virtual REF)

FEATURES

> Bipolar differential measurement
> Pre-conditioned analog output
> High signal-to-noise ratio
> Small form factor
> Raw data output
> Easy-to-use
> "On-the-person" and "off-the-person" use

APPLICATIONS

> Heart rate & heart rate variability
> Human-Computer Interaction
> Biometrics
> Affective computing
> Physiology studies
> Psychophysiology
> Biofeedback
> Biomedical devices prototyping

GENERAL DESCRIPTION

Heartbeats are triggered by bioelectrical signals of very low amplitude generated by a special set of cells in the heart (the SA node). Electrocardiography (ECG) enables the translation of these electrical signals into numerical values, enabling them to be used in a wide array of applications. Our sensor allow data acquisition not only at the chest ("on-the-person"), but also at the hand palms ("off-the-person"), and works both with pre-gelled and most types of dry electrodes. The bipolar configuration is ideal for low noise. Here are a few examples:

http://vimeo.com/98075534h
https://www.youtube.com/watch?v=hQ3BUBV-BBMh
https://www.youtube.com/watch?v=lKWM2TL1toM

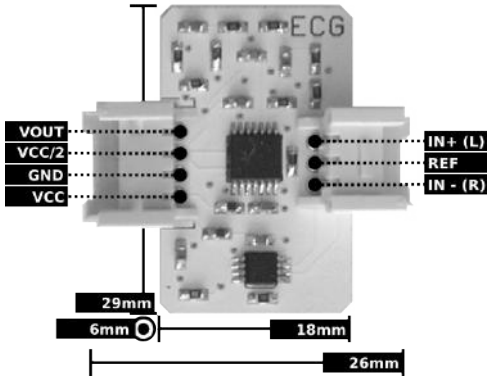

Fig. 1. Pin-out and physical dimensions.

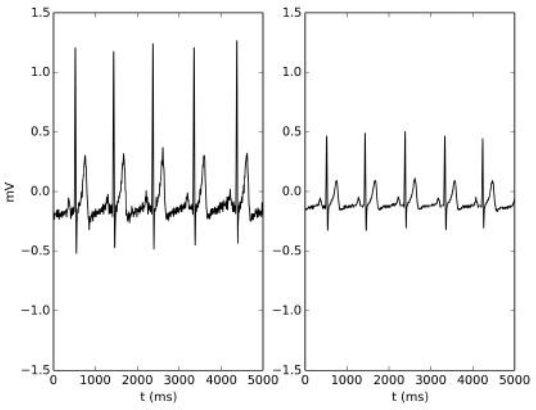

Fig. 2. Typical raw ECG data (acquired with BITalino) using 2 electrodes at the hands (left) and 3 electrodes at the chest (right).

Fig. 3. Example of a 2 electrodes placement at the hands (left) and a 3 electrodes placement at the chest (right).

PLUX – Wireless Biosignals, S.A.
Av. 5 de Outubro, n. 70 – 8.
1050-059 Lisbon, Portugal
bitalino@plux.info
http://bitalino.com/

REV A

BEWARE: DIRECT OR INDIRECT COUPLING TO THE MAINS MAY RESULT IN SHOCKING HAZARD

Electrocardiography (ECG)
Sensor Data Sheet

TRANSFER FUNCTION

[-1.5mV, 1.5mV]

$$ECG(V) = \frac{\left(\frac{ADC}{2^n - 1} - \frac{1}{2}\right).VCC}{G_{ECG}}$$

$$ECG(mV) = ECG(V) * 1000$$

$VCC = 3.3V$ (operating voltage)
$G_{ECG} = 1100$ (sensor gain)

$ECG(V)$ – ECG value in Volt (V)
$ECG(mV)$ – ECG value in millivolt (mV)
ADC – Value sampled from the channel
n – Number of bits of the channel[1]

[1] The number of bits for each channel depends on the resolution of the Analog-to-Digital Converter (ADC); in BITalino the first four channels are sampled using 10-bit resolution ($n = 10$), while the last two are sampled using 6-bit ($n = 6$).

Electromyography (EMG) Sensor Data Sheet

EMG 080115

SPECIFICATIONS

> **Gain:** 1000
> **Range:** ±1.65mV (with VCC = 3.3V)
> **Bandwidth:** 10-400Hz
> **Consumption:** ~4mA
> **Input Impedance:** 100GOhm
> **CMRR:** 110dB

FEATURES

> Bipolar differential measurement
> Pre-conditioned analog output
> High signal-to-noise ratio
> Small form factor
> Raw data output
> Easy-to-use

APPLICATIONS

> Human-Computer Interaction
> Robotics & Cybernetics
> Physiology studies
> Psychophysiology
> Biomechanics
> Biofeedback
> Muscle reflex studies
> Nerve conduction measurement
> Biomedical devices prototyping

GENERAL DESCRIPTION

Muscle activation is triggered by bioelectrical signals of very low amplitude sent from motor control neurons on our brain to the muscle fibers. Electromyography (EMG) enables the translation of these electrical signals into numerical values, enabling them to be used in a wide array of applications. Our sensor is especially designed for surface EMG, and works both with pre-gelled and most types of dry electrodes. The bipolar configuration is ideal for low-noise data acquisition, and the raw data output enables it to be used for human-computer interaction and biomedical projects alike. Here are a few examples:

https://www.youtube.com/watch?v=pVAaFeym8TQ
https://www.youtube.com/watch?v=7Q4HC0vxFsc
http://www.physioplux.com/

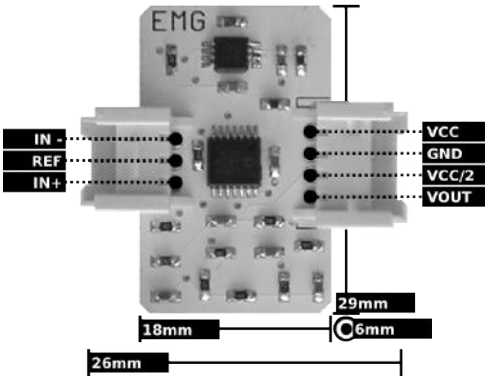

Fig. 1. Pin-out and physical dimensions.

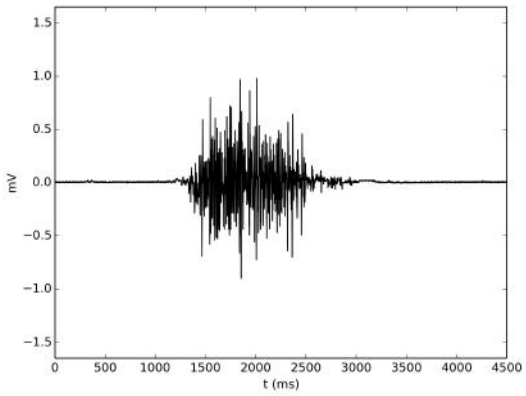

Fig. 2. Typical raw EMG data (acquired with BITalino).

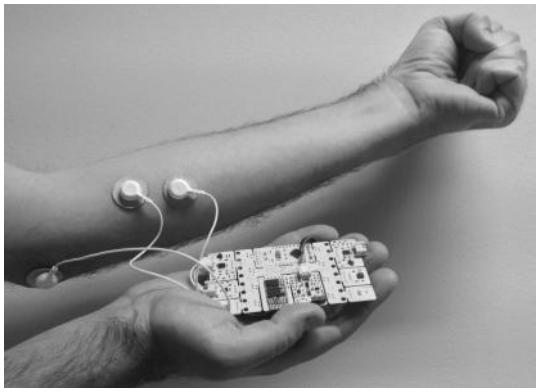

Fig. 3. Example electrode placement, with REF in a bone region (electrically neutral), and IN+ & IN- 20mm apart over the muscle belly (aligned with the muscle fibers).

PLUX – Wireless Biosignals, S.A.
Av. 5 de Outubro, n. 70 – 8.
1050-059 Lisbon, Portugal
bitalino@plux.info
http://bitalino.com/

REV A

BEWARE: DIRECT OR INDIRECT COUPLING TO THE MAINS MAY RESULT IN SHOCKING HAZARD

Electromyography (EMG)
Sensor Data Sheet

TRANSFER FUNCTION

[-1.65mV, 1.65mV]

$$EMG(V) = \frac{\left(\frac{ADC}{2^n - 1} - \frac{1}{2}\right).VCC}{G_{EMG}}$$

$$EMG(mV) = EMG(V) * 1000$$

$VCC = 3.3V$ (operating voltage)
$G_{EMG} = 1000$ (sensor gain)

$EMG(V)$ – EMG value in Volt (V)
$EMG(mV)$ – EMG value in millivolt (mV)
ADC – Value sampled from the channel
n – Number of bits of the channel[1]

[1] The number of bits for each channel depends on the resolution of the Analog-to-Digital Converter (ADC); in BITalino the first four channels are sampled using 10-bit resolution ($n = 10$), while the last two are sampled using 6-bit ($n = 6$).

Electrodermal Activity (EDA) Sensor Data Sheet

EDA 080115

SPECIFICATIONS

> **Gain:** 2
> **Range:** 0-1MOhm (with VCC = 3.3V)
> **Bandwidth:** 0-3Hz
> **Consumption:** ~2mA
> **Electrodes:** 2

FEATURES

> Skin resistance measurement
> Pre-conditioned analog output
> High signal-to-noise ratio
> Small form factor
> Raw data output
> Easy-to-use

APPLICATIONS

> Arousal detection
> Human-Computer Interaction
> Emotional cartography
> Affective computing
> Physiology studies
> Psychophysiology
> Relaxation biofeedback
> Biomedical devices prototyping

GENERAL DESCRIPTION

Sweat glands secretion is a process that allows our body to regulate its temperature, but it is also associated the sympathetic nervous system activity. Whenever we become aroused (e.g. nervous) or relaxed, that state is partially translated into the sweat production or inhibition at the glands on our hands palms and feet. This changes the resistance of our skin; Electrodermal Activity (EDA) monitoring enables the translation of these resistance changes into numerical values, allowing its use in a wide array of applications. Known uses of this sensor include emotional mapping, the polygraph test (aka lie detector), and also stress / relaxation biofeedback.

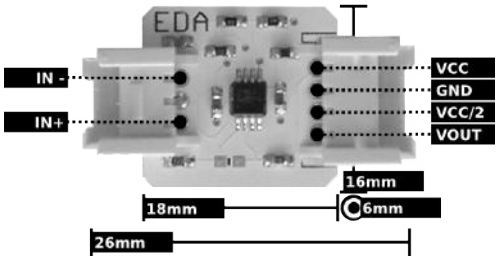

Fig. 1. Pin-out and physical dimensions.

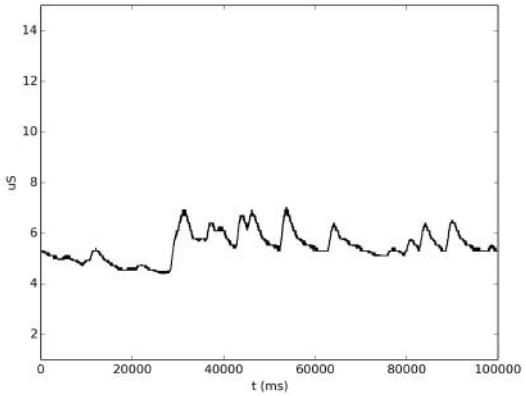

Fig. 2. Typical raw EDA data (acquired with BITalino).

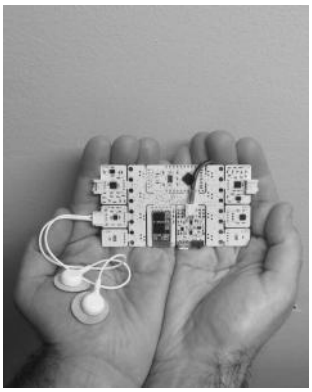

Fig. 3. Example electrode placement.

PLUX – Wireless Biosignals, S.A.
Av. 5 de Outubro, n. 70 – 8.
1050-059 Lisbon, Portugal
bitalino@plux.info
http://bitalino.com/

REV A

BEWARE: DIRECT OR INDIRECT COUPLING TO THE MAINS MAY RESULT IN SHOCKING HAZARD

Electrodermal Activity (EDA)
Sensor Data Sheet

TRANSFER FUNCTION

[$1\mu S$, $\infty\mu S$]

$$R(MOhm) = 1 - \frac{ADC}{2^n - 1}$$

$$EDA(\mu S) = \frac{1}{R(MOhm)}$$

$R(MOhm)$ – Sensor resistance value mega-Ohm ($MOhm$)
$EDA(\mu S)$ – EDA value in micro-Siemens (μS)
ADC – Value sampled from the channel
n – Number of bits of the channel[1]

[1] The number of bits for each channel depends on the resolution of the Analog-to-Digital Converter (ADC); in BITalino the first four channels are sampled using 10-bit resolution ($n = 10$), while the last two are sampled using 6-bit ($n = 6$).

2015	Filipe Rodrigues	Establishing a Framework for the development of Multimodal Virtual Reality Interfaces with Applicability in Education and Clinical Practi